Regulation of Vaccinia Virus Induced Programmed Necrosis Through Z-Form Nucleic Acid Binding Proteins

by

Heather Harrington

A Dissertation Presented in Partial Fulfillment
of the Requirements for the Degree
Doctor of Philosophy

Approved July 2016 by the
Graduate Supervisory Committee:

Bertram Jacobs, Chair
Joseph Blattman
Shelley Haydel
Jeffrey Langland
Valerie Stout

ARIZONA STATE UNIVERSITY

August 2016

ABSTRACT

The interaction between a virus and its host is a constant competition for supremacy. Both the virus and the host immune system constantly evolve mechanisms to circumvent one another. Vaccinia virus (VACV) infections are a prime example of this. VACV contains a highly conserved innate immune evasion gene, E3L, which encodes the E3 protein composed of a Z-NA-binding domain (Z-NA BD) in the N terminus and a highly characterized dsRNA binding domain in the C-terminus. Both domains of E3 have been found to be essential for the inhibition of antiviral states initiated by host type 1 IFNs. However, the mechanism by which the Z-NA-BD of E3's N-terminus confers IFN resistance has yet to be established. This is partially due to conflicting evidence showing that the Z-NA-BD is dispensable in most cell culture systems, yet essential for pathogenicity in mice. Recently it has been demonstrated that programmed necrosis is an alternative form of cell death that can be initiated by viral infections as part of the host's innate immune response to control infection. The work presented here reveals that VACV has developed a mechanism to inhibit programmed necrosis. This inhibition occurs through utilizing E3's N-terminus to prevent the initiation of programmed necrosis involving the host-encoded cellular proteins RIP3 and Z-NA-binding protein DAI. The inhibition of programmed necrosis has been shown to involve regions of both the viral and host proteins responsible for Z-NA binding through in vivo studies demonstrating that deletions of the Z-NA-BD in E3 correspond to an attenuation of pathogenicity in wild type mice that is restored in RIP3- and DAI-deficient models. Together these findings provide novel insight into the elusive function of the Z-NA-binding domain of the N-terminus and its role in preventing host recognition of viral

infections. Furthermore, it is demonstrated that a unique mechanism for resisting virally induced programmed necrosis exists. This mechanism, specific to Z-NA binding, involves the inhibition of a DAI dependent form of programmed necrosis possibly by preventing host recognition of viral infections, and hints at the possible biological role of Z-NA in regulating viral infections.

DEDICATION

To my Family.

Your unconditional love and guidance has given me the strength to become the person I am and the drive to be better. Thank you for the immeasurable support and always believing in me.

ACKNOWLEDGMENTS

Enthusiasm for science is best learned by example form those who teach it. Therefore, I would like to start by thanking my undergrad research mentor Dr. Takashi Ueda. Your leadership and teaching helped me to find my passion for research.

I need to express the greatest amount of appreciation to Dr. Jeffery Langland. You gave me the chance of a lifetime by letting me participate in your research; without your support and encouragement I would not have been able to pursue my dream of continuing my education and earning a Ph.D.

Thank you to all the current members of the Jacobs lab, I count myself very lucky to be able to come to work every day in an environment where I am surrounded by individuals who are intelligent and passionate about science. Your ideas and comments have helped shape my research into the project I am very privileged to be able to present as my dissertation thesis.

I would like to extend a special thank you to a few people. Nobuko, Hamed, and Samantha, without your support and friendship these past few months I would have not been able to accomplish all that I did. Nobuko, thank you for all you help and support in completing my assays and being a great friend throughout the years. I could always count on your help when I needed it. Hamed you have been an amazing undergrad and I know your dedication will take you anywhere you would like to go. Sam your ideas and support have helped me advance my understanding, but more important you have been an amazing lab mate and a great friend.

I need to express my appreciation to all the past members of the lab whose work has provided me with the foundation of knowledge that gave me the great opportunity to explore and learn. Specifically, I would like to thank Dr. Trung Huynh "Joe" who dedicated his time to being a leader and mentor in the lab. The skills and techniques I learned from you are invaluable.

In addition to everyone at ASU, I need to express my gratitude to our collaborators at Emory and University of Texas. Dr. Daniel Kalman, I would not have been able to complete critical components of my project without your generosity in allowing me to utilize your lab. I am especially grateful to both Dr. Jason Upton and Dr. Ed Mocarski for your wealth of knowledge and experience you have generously shared with me as I explored a new field. Additionally, I am very grateful for your willingness to collaborate and share your plasmids.

To my committee members, Dr. Joseph Blattman, Dr.Valarie Stout and Dr. Shelley Haydel, I cannot thank you enough for you willingness to participate in my graduate education. Your time, interest, and guidance have helped to develop my scientific thought process. I also need to extend an extra thank you to Dr. Karen Kibler who was very generous with her time and willingness to be a substitute for my defense.

I also need to express gratitude to both SOLS and GPSA for providing me with funding for travel and supplies to complete my projects.

Lastly I would like to thank my graduate mentor, Dr. Bertram Jacobs, "Jake." Your enthusiasm for gaining scientific insight is inspiring. The few years I have spent in your lab have shaped my future and will forever alter the way I approach scientific endeavors.

TABLE OF CONTENTS

LIST OF FIGURES

CHAPTER 1

OVERALL INTRODUCTION

Viruses and their hosts have co-evolved in a dichotomous relationship that drives development strategies employed by both organisms to circumvent the defense systems of one another. Viruses exist and propagate as obligate intracellular pathogens due to their dependency on the host's cellular machinery, which places a non-advantageous burden on the host organism. Due to this, host organisms developed multiple means of recognizing and eliminating the viral pathogens. However, due to viruses' dependence on their host's cellular machinery to replicate for survival, they have concurrently evolved strategies to subvert the host's antiviral defense mechanism to ensure continued propagation. Pathogenicity of a virus is heavily dependent on its ability to evade the host's innate defense system. This ability is heavily dependent on the host's antiviral state generated by the actions of interferon (IFN) as well as other pro-inflammatory cytokines (1).

IFNs are a group of secreted cytokines that elicit distinct antiviral effects. These cytokines have been known to alter the ability of a virus to survive and propagate (2). IFNs are systematically classified into three distinct groups. Of these three groups, type I IFNs (IFN-α/β) have been the best characterized for their role of inhibiting viral replication as a part of the innate immune system (3) (4). The innate immune response is heavily dependent on IFN-α/β as the first line of defense against viral infection (5, 6)

The generation of an antiviral state is initiated through the binding of type I IFNs to their ubiquitously expressed surface receptor proteins. This binding subsequently

results in the activation of multiple signaling cascades, which induce the transcription of hundreds of IFN-stimulated genes (ISGs) (7). These ISGs are responsible for establishing an anti-viral state within cells through a multifaceted approach involving regulation mechanisms required for viral replication, enhanced production of viral detection systems, and increased local signaling (including IFN production) in order to prime uninfected neighboring cells for the impending infection. These actions help to limit the virus from spreading further (1). In addition to their primary role involving innate anti-viral responses, type I IFNs have been demonstrated to influence elements of the adaptive immune response through priming helper T and cytotoxic T cells, and aiding in the generation of an antigen-specific response (8-10).

The production of IFN-α/β and subsequent activation of ISGs are regulated by host-encoded pattern recognition receptors (PRRs) which are capable of initiating multiple signaling cascades upon activation. These PRRs are composed of a diverse group of receptors capable of recognizing a broad range of pathogen-associated molecular patterns (PAMPs) that are distinct from host molecular patterns. This recognition allows for the sensing of a pathogen in the infected cell. During a viral infection involving viral genomic deoxy-ribose nucleic acid (DNA), single-stranded ribose nucleic acid (ssRNA), or double-stranded RNA (dsRNA) nucleic acid patterns specific to the virus act as critical PAMPs recognized by PRRs used for early detection (11). This early detection by PRRs through the detection of PAMPs is critical, as it leads to the induction of IFN-α/β, which is essential for generating a systematic antiviral state.

Following its production, IFN-α/β is secreted into the extracellular environment where it can implement both autocrine and paracrine signaling patterns through binding

to IFN-α/βRs on the cell surface to further enhance a local antiviral state. IFN-α/βRs are composed of IFNAR1 and IFNAR2 subunits (12-14). Binding of IFN to its receptor induces a signal cascade that involves Janus kinase (JAK), signal transducers, and the activation of transcription (STAT) pathways (14, 15), resulting in the formation of the IFN-stimulated gene factor 3 (ISGF3)complex (16, 17). ISGF3 then translocates into the nucleus where it binds to the IFN-stimulated response element (ISRE) and induces the transcription of ISGs (14, 18).

The ISGs that encode proteins with direct antiviral activity have a diverse range of functions including cytoskeletal remodeling, induction of apoptosis, regulation of post-transcriptional events (splicing, mRNA editing, RNA degradation and the multiple steps of protein translation) and post-translational modifications. Examples of more direct-acting ISGs that are essential for generating an antiviral state IFN-stimulated protein of 15 kDa(include ISG15), the GTPase myxovirus resistance 1(Mx1), ribonuclease L (RNaseL) and protein kinase R (PKR) (18). The majority of ISGs, however, act to prime cells for potential infection. Examples of these ISGs include PRRs that detect viral molecules and modulate signaling pathways, or transcription factors that produce an amplification loop leading to increased IFN production. Together they act to induce an antiviral state within the cell. Initiation of an antiviral state results from the complex interaction of multiple ISGs and no single gene has been shown to be absolutely essential for every virus. The substantial gap in understanding of the essential function and cooperation of ISGs in regulating the innate immune response leaves a potentially unexplored role of IFN-α/β in regulating viral infections.

The type 1 IFN system plays a pivotal role in generating a diverse variety of

antiviral responses. One such response involves the priming of cells to undergo programmed cell death during infections (19). This priming causes an antiviral effect by decreasing the time needed to eliminate infected cells (20-22). The steps involved in priming a cell for apoptosis with IFN is not limited to a single mechanism or pathway. Some of the well-characterized pathways include the induction of procaspase genes (18), PKR (10), and OAS (23, 24). The inactive pro-proteins are up-regulated and capable of inducing apoptosis upon activation by PAMPs such as dsRNA (23).

Programmed cell death in infected cells establishes an effective mechanism to contain pathogens by limiting replication to prevent the spread of the virus. Additionally, the programmed cell death simultaneously aids in the clearance of infected cells through phagocytes of the immune system. The critical role that programmed cell death plays in a host's defense against pathogens is demonstrated through the overabundance of inhibitors encoded by different pathogens in order to suppress programmed cell death (22, 25-29).

For many years, programmed cell death was synonymous with apoptosis, but recently alternative programmed cell death pathways have been identified as important regulators of the innate immune response to viral infections. These alternative forms may be essential for host inhibition of viruses that encode anti-apoptotic genes (25). The field of virally-induced, programmed cellular death is rapidly evolving with apoptosis, necrosis, and pyroptosis representing the key pathways involved in innate response to pathogens. Each mode of cell death is characterized by particular morphological changes and distinctive molecular signaling pathways. Currently, defining how a cell dies is based on three major classification criteria composed of morphology, enzymatic characteristics, and immunological characteristics (30). Apoptosis is characterized by cell shrinkage,

nuclear condensation, chromosomal fragmentation, membrane blebbing, and the formation of apoptotic bodies cleared by phagocytic cells. Apoptosis is dependent on cysteine proteases known as caspases. These caspases are induced by external stimuli, such as death receptor ligation or PRR activation, or internal stimuli that influence mitochondrial integrity. Caspases exist as zymogens within the cell and are activated in a two-stage system. The first stage involves "initiator" caspases, such as caspases-8 and -9, which are induced in response to cellular signaling. These caspases then initiate the second stage through the activation of the "executioner" caspases, caspases-7 and -3, which target cellular substrates to induce apoptotic death. Apoptosis is classified as non-immunogenic, based on retention of all the cellular content within the apoptotic bodies; this results in minimal inflammatory effects upon death. There are two known pathways leading to apoptosis: extrinsic and intrinsic pathways. Both of these pathways are known to communicate through activation of the Bcl-2 homology domain 3 (BH3)-only protein, Bid (31). The extrinsic pathway is triggered by the binding of extracellular death receptor ligands such as tumor necrosis factor (TNF), Fas ligand (FasL), and TNF-related apoptosis-inducing ligand (TRAIL) to their respective transmembrane receptors (30). The intrinsic pathway is initiated when proteins such as cytochrome c, SMAC/Diablo, and HtrA2/Omi are released from the mitochondrial intermembrane space into the cytosol in response to a variety of stresses such as chemotherapeutic drugs, UV irradiation, and microbial infection (31).

In contrast to the classical non-immunogenic apoptotic death pathway, programmed necrosis and pyroptosis are described as highly immunogenic because they release cytokines and intracellular products into the extracellular environment. This

release is a result of cell membrane integrity loss and has been associated with viral infections (30). Enzymatically, pyroptosis is classified as a caspase-1-dependent death pathway. Activation of cytoplasmic procaspase-1 results in a signal cascade leading to a loss of plasma membrane integrity and the release of cytoplasmic contents. This results in the activation of inflammatory cytokines such as IL-1β and IL-18. The activation of these cytokines causes cytoplasmic swelling and ultimately lysis resulting in the release intracellular contents (22).

Following signaling that results in induction of pyroptosis, caspase-1 undergoes auto-activation through the formation of large protein complexes known as inflammasomes. The inflammasome complex contains a member of the NOD-like receptor (NLR) family. NLRs function as sensors that detect PAMPs. Distinct inflammasomes are assembled depending on the infectious agent (32). Genetic studies in mice indicate that at least four different inflammasomes are formed in vivo: the Ipaf inflammasome, the Nlrp1b inflammasome, the Nlrp3 inflammasome, and a fourth inflammasome that is assembled upon infection with DNA viruses and some bacteria such as Francisella tularensis, or Listeria monocytogenes. This fourth inflammasome contains the cytosolic double-stranded DNA sensor Absent In Melanoma 2 (AIM2) (32).

Similar to pyroptosis, programmed necrosis is classified as an immunogenic programmed cell death that is characterized by organelle damage, cytoplasmic swelling, and the loss of plasma membrane integrity. This leads to the release of cytoplasmic contents. Unlike other pathogen-associated forms of cell death, programmed necrosis occurs independent of caspases activation. For many years, necroptosis was considered an accidental form of death that was outside the cell's

control. Only within the past decade has evidence emerged demonstrating that it is a regulated cellular death mechanism. As of recently, some of the serine/threonine kinase receptor interacting proteins (RIP) have been shown to be key regulators of necrosis signaling (25, 33) Most of the current understanding of programmed necrosis comes from the TNF-driven canonical pathway termed necroptosis which involves a RIP1 and RIP3 interaction followed by the activation of mixed-lineage kinase domain-like (MLKL). Necroptosis is initiated when tumor necrosis factor (TNF) binds to the TNF receptor 1 (TNFR1) on the cell surface. Following TNF binding, the cytoplasmic portion of TNFR1 recruits the TNF receptor-associated death domain (TRADD) which subsequently recruits a series of proteins to form the membrane-associated complex 1. This complex includes RIP1, the cellular inhibitor of apoptosis protein 1 (cIAP1), cIAP2, TNF receptor-associated factor 2 (TRAF2), and TRAF5 (34). Upon formation of complex I, RIP1 undergoes polyubiquitylation by cIAP1 and cIAP2 to generate a scaffold for docking transforming growth factor-β-activated kinase 1(TAK1); which is complexed with TAK1 binding protein 2 (TAB2) or TAB3 and the inhibitor of the NF-κB kinase(IKK) complex. Assembly of this complex activates the nuclear factor-κB (NF-κB) pathway which leads to the recruitment of the linear ubiquitin chain assembly complex (LUBAC) through the linear ubiquitin chains on RIP1. Cylindromatosis (CYLD) is then recruited to remove polyubiquitins from RIP1 leading to the destabilization of complex I. RIP1 is then able to dissociate from the membrane associated complex and interact with TRADD, FAS-associated death domain (FADD), pro-caspase 8, and FLICE-like inhibitory proteins (FLIPs) to form complex IIa. Under normal cellular conditions FLIP and pro-caspase 8 form a heterodimeric caspase that

can cleave both RIPK1 and RIPK3 to render them inactive in order to prevent necroptosis. However, in the presence of caspase inhibitors such as VACV B13R, RIP1 is not cleaved and remains active, which allows for the oligomerization and autophosphorylation of RIPK3 to occur (35). Phosphorylated RIPK3 recruits and phosphorylates the MLKL (35, 36). Upon phosphorylation, MLKL undergoes a conformational change that exposes the MLKL N-terminal domain and translocates to the membrane resulting in the loss of membrane integrity and ultimately cell death (37-42).

Even though RIP1 is critical for the activation of RIP3 through RIP homotypic interacting motif (RHIM) domain interactions in the canonical programmed necrosis pathway, RIP3 has the capacity to partner with multiple proteins that also contain RHIM domains to induce death. Upstream adaptors of RIP3 include RIP1, TIR-domain-contaning adaptor-inducing interferon-β(TRIF) which is downstream of TLR3/4 signaling pathway (29, 43-45) and DAI (26, 46) which have all been shown to contain a RHIM domain. These represent important sets of adaptor proteins in innate signaling pathways involved in the host's response to pathogens and further implicates programmed necrosis as an important host defense pathway against pathogens.

Necroptosis has been demonstrated to result from multiple pathogens including both viruses and bacteria (25, 47-50). Additionally, it has been suggested to be the default pathway when caspase activity is compromised (51, 52). Many viruses, including poxviruses and herpesviruses, inhibit caspase activity (53) and consequently have the potential to be susceptible to programmed necrosis. With the understanding that

programmed cell death is an essential component of the host defense mechanism against viral pathogens, it is not surprising that rapidly emerging evidence demonstrates that viruses have evolved mechanisms to regulate programmed necrosis in addition to apoptosis. Some of the best studied examples of this can be seen in herpesviruses. Among these viruses, murine cytomegalovirus (MCMV) encodes suppressors of apoptosis as well as a M45-encoded viral inhibitor of RIP activation (vIRA) M45, which contains an N-terminal RHIM domain that prevents the DAI recruitment of RIP3. This blocks the signal cascade leading to cell death (27, 46). Similarly, herpes simplex viruses (HSV)1 and HSV2 both utilize RHIM and Caspase-8 suppression strategies through the uses of M45 homologs; UL39-encoded ICP6 and ICP10, respectively (48). These examples demonstrate that viruses employ multiple strategies to combat diverse forms of cell death and suggests that viral regulation of programmed necrosis is a common trend that extends beyond our current understanding.

The Poxviridade family is composed of a unique cluster of large brick-shaped, enveloped viruses whose genome is composed of dsDNA. This family is noted to have a broad host range, infecting both vertebrates and invertebrates (54, 55). Of the eight genera belonging to the Poxviridade family, the Orthopoxvirus genus is the most well-characterized due to notorious members including variola virus (VARV), the causative agent of smallpox, as well as vaccinia virus (VACV), which is the prototypic poxvirus utilized to study both poxviruses and multiple facets of viral host interactions. Additionally, another significant member includes the recently emerged human pathogen monkeypox virus that caused an outbreak in the United States in 2003 (56).

Poxviruses are unique in their replication strategies, because their replication cycle occurs within the cytoplasm of their infected host, making them less reliant on host machinery (55). Poxviruses' genomes are relatively conserved, ranging from about 134kb to more than 300 kb. They have a general organization with highly conserved replication genes located within the central regions of the genome and less conserved, but critical, immune-evasion genes that likely correspond to host range specificity, in terminal regions (57). The hairpin loop of inverted terminal repetitions connects the two DNA strands (58, 59).

Viruses have evolved multiple strategies to circumvent the host's immune system. VACV is a prime example of one of these viruses and has developed numerous strategies to subvert the host's immune system, particularly with regard to the IFN system. VACV encodes virulence genes that enable the evasion of the host's immune system. Virulence genes are capable of interacting with a wide range of host proteins and pathways with diverse effects (54, 60). As a master regulator of the host's IFN system, VACV has two proteins that have been demonstrated to directly interfere with IFN signaling (61, 62). These proteins, B8R and B19R (B18R in WR VACV), are soluble IFN-binding proteins targeting IFN-γ and IFN-α/β respectively. The IFN-binding proteins are secreted from infected cells and prevent IFN from being able to initiate signaling in uninfected cells, thereby preventing the generation of an antiviral state within neighboring cells, thus allowing the virus to spread (63-65) (61, 66). Other examples of VACV virulence genes function to inhibit chemokine and cytokine signaling by preventing them from binding to their receptors IL-18 (67), TNF (68), and IL-1β (69). These virulence factors are a small

representation of the extensive list of mechanisms that viruses have developed to evade their host's immune systems and ensure survival.

VACV regulation of the IFN system is not limited to the extracellular environment. Two well studied viral proteins, K3 and E3, have been shown to interfere with the intracellular IFN-signaling pathways and aid in the IFN resistance (IFNR) phenotype to allow for an enhanced host range (70-72). The requirement for viruses to circumvent apoptosis has been well established, but more recent evidence has been emerging implicating alternative forms of programmed cell death as critical antiviral host defense mechanisms. Among the multiple immune evasion proteins encoded by VACV is B13R, which is an ortholg of the well characterized cowpox serpin inhibitor, CrmA. The serpin inhibitor functions to bind and inhibit the enzymatic activity of caspases, including caspase 8 and caspase 1 (73, 74). Specifically, the regulation of caspases has been shown to require B13R for VACV pathogenesis in mice (75); this further highlights the importance of the viral regulation of host cell death. However, the dynamic nature of programmed cell death is exemplified by the fact that VACV expresses the caspase inhibitor; B13R. The expression of B13R sensitizies infected MEFs to a RIP1-dependent TNF-induced programmed necrotic cell death (76, 77) (78). Insight into the significant role that programmed necrosis plays in host defenses during viral infections was demonstrated through infections with VACV in RIP3−/− mice, which resulted in higher viral titers and death compared to wild-type (wt) mice (25, 78). Together, this suggests that programmed cell death in viral infections is not limited to apoptosis and virus-induced programmed necrosis, but may also have other forms to restrict viral infections.

The importance of VACV regulation of the host's immune system involving IFN signaling is evident by a multidimensional approach to inhibiting it. VACV E3L is an essential virulence factor and one of the prime regulators of the viral host interactions. The significance of E3L is emphasized by the presence of a homologue in Variola that is nearly identical in sequence, as is found in every other member of the genus. The E3L gene encodes the multifunctional protein E3. Prior studies have demonstrated that E3 is essential for IFNR, host range, and pathogenesis. While VACV with wt E3 is highly IFNR, VACV deleted of E3L (VACVΔE3L) is IFN-sensitive in multiple cell lines (70, 79, 80), has a restricted host range (70, 72, 80), and is highly attenuated in mouse models (81).

It has been demonstrated in a cell culture system that E3 is required to prevent the activation of both the PKR and OAS-RNase L pathways. Infections in the absence of E3 result in the activation of PKR and subsequent phosphorylation of eIF2α leading to an arrest of translation (82). Activation of the OAS-RNase L pathway following infection with VACVΔE3L results in the degradation of ribosomal RNA (70). Additionally, it has been suggested that the restricted host range of VACVΔE3L is linked to activation of systems leading to the induction of apoptosis typically inhibited in wt VACV.

The E3L gene codes for two variants E3: a full length p25 form and a truncated p20 version. The p25 form of E3 is a 190 amino-acid-long protein and contains two highly conserved domains: an amino-terminal Z form nucleic acid-binding domain (Z-NA-BD) and a carboxyl-terminal dsRNA-binding domain (dsRNA-BD) (83, 84). The truncated p20 form of E3 occurs from leaky scanning, resulting in translation initiation

occurring at the second downstream start codon which omits the first 37 amino acids of the protein (85).

The E3 protein plays a pivotal role in the immune evasion of a host's defenses and is dependent on the presence of both domains. The dsRNA-BD located in the carboxyl-terminus(C-terminus) of E3 is highly conserved within the subfamily Chordopoxvirinae (86). The primary function of the C-terminus is to bind the dsRNA that is a byproduct of viral transcription in order to sequester it from PRRs (80, 87) (85, 88, 89) (90). The dsRNA-BD is essential for host range, IFNR, and full pathogenesis in animal models (80, 81, 87). Truncations of the last 26 amino acids from the C-terminus (VACV-E3LΔ26C) results in a highly attenuated virus that is apathogenic in the C57BL6 mouse model equivalent to VACVΔE3L (81) and induces apoptosis in HeLa cells (91).

The N-terminal Z-NA-BD of E3 is fairly well conserved among many members of the subfamily *Chordopoxvirinae* and highly conserved in the *Orthopoxvirus genus*. The Z-NA-BD shares homology with a family of IFN-inducible vertebrate proteins known to bind Z-form DNA including the DNA-dependent activator of IFN-regulatory factors (DAI) (also known as DLM-1 or ZBP-1) (92, 93) and adenosine deaminase that acts on RNA 1 (ADAR1) (94, 95). The Z-NA binding (Zα) motif was originally described in ADAR1. ADAR1 was shown to have a specificity for binding to left-handed Z-DNA (96-101) and was later identified in DAI as well as the E3 protein of VACV (96, 102). The crystal structure of the Zα of ADAR1 (103) and DAI (102) demonstrating the conserved Z-NA binding motifs found within this family.

The Zα motif is based on a common configuration composed of a winged helix-turn-helix motif (104). While this configuration is also common among B-DNA binding motifs, the crystal structures of the Zα motifs of both ADAR1 and DAI (102, 103) show that nucleic acid binding is specific to the zig-zag conformation associated with the backbone of Z-DNA. The structure of the Zα motif of the Z-NA-binding protein family are very similar despite a lack of conservation of the of amino acid sequence outside the key residues that make contact with the Z-DNA (103). A protein sequence alignment of E3 and the Zα domain of ADAR1 shows that E3 retains seven of the nine conserved residues necessary for binding to Z-DNA and is capable of binding to Z-DNA *in vitro* (105, 106).

ADAR1 is an ISG composed of 3 distinct regions, 1) two nucleic acid-binding domains, Zα and Zβ, located in the N-terminus, 2) three dsRNA-BDs located in the central region of the protein, and 3) a deaminase catalytic domain in the C-terminal (96). It plays a role in the post-translational editing of RNA by deaminating adenosine to inosine in dsRNA complexes to promote the unwinding of dsRNA (95, 107).

DAI is also an ISG that is composed of the Zα motif that is separated by an intervening linker from a second nucleic acid binding domain called Zβ, located in the N-terminus. This domain is followed by a true RIP Homotypic Interacting Motif (RHIM) domain with an overlapping B-DNA-BD and an additional two RHIM like domains located in the C-terminus. DAI has been identified to function as a cytosolic DNA sensor and an activator of innate immune responses through the activation of IRF3 and subsequent induction of IFNα/β production following stimulation with B-DNA (108) Recently, DAI was identified as an important player in the field of virally induced

programmed necrosis through utilizing the C-terminal RHIM domain to regulate programmed necrosis in MCMV.

The function of the N-terminal domain of E3 corresponds to an ability to bind Z-DNA. The Zα of both ADAR1 and DAI can complement the deletion of the N-terminal of E3 despite the lack of homology outside the Z-NA binding residues (105). Additionally, mutations that decrease affinity for Z-DNA binding within the Zα corresponds to a reduction of pathogenesis (105).

While the significance of the N-terminus of E3 can be inferred from its conservation among the *Orthopoxviruses,* understanding the biological function of the Z-NA-BD has been inhibited by the lack of a cell culture system that demonstrates a phenotype that is not redundant to that of a virus containing the C-terminus only. The initial *in vitro* studies utilizing a truncation mutant with the first 83 amino acids deleted from the N-terminus (VACV-E3LΔ83N) indicated that this domain is non-essential to host range or IFN^R with phenotypes equivalent to wt VACV (80, 109). The one variation between wt VACV and VACV-E3LΔ83N noted *in vitro* was that at late times post infection in HeLa cells, VACV-E3LΔ83N in contrast to wt VACV was able to induce the phosphorylation of eIF2α and PKR. However, unlike VACV-ΔE3L, theses phosphorylation events do not impair the virus's ability to replicate (110). *In vivo* studies conducted in C57BL6 mouse models have now confirmed suspicions that the N-terminus is in fact essential for both full pathogenesis and neurovirulance, as demonstrated by a 1000-fold reduction in pathogenisis in animals compared to wt VACV (111). The loss in pathogenicity mirrors the phenotype identified in culture showing that the N-terminus is

not required for replication but is instead associated with restricted spread beyond the site of infection (111).

Recently it has been demonstrated that the N-terminal domain of E3 is necessary for full IFN^R demonstrated by a rescue of pathogenesis to wt VACV levels in interferon-α/β receptor-knockout mice (IFNR-/-) (81, 111, 112). Additionally, through utilizing mouse embryo fibroblasts (MEFs), it was found that IFN^R corresponds to the activation of PKR in the absence of the Z-NA-BD (112). However, pathogenesis of VACV-E3LΔ83N is not restored in PKR-/- mice. Together these conflicting sets of data suggest that additional systems may be responsible for the attenuated phenotypes observed.

This study focused on the role that IFN plays in regulating programmed cell death. In Chapter 2 we investigate the function of the N-terminus of E3 in regulating a programmed necrotic death. In Chapter 3 the role of Z-NA binding by the host DAI and VACV E3 are evaluated in the role of regulating programmed necrosis.

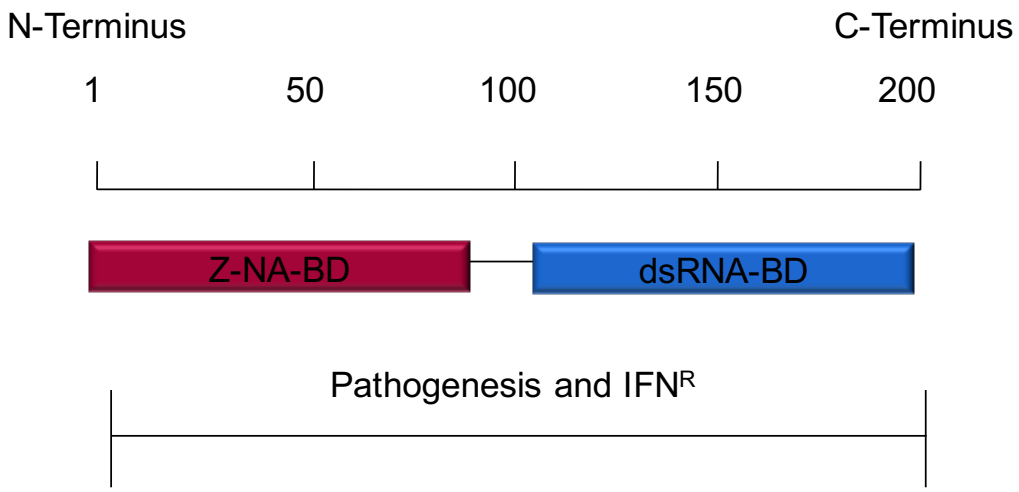

Figure 1. A basic schematic of the IFN resistance protein E3 in wt VACV. E3 is a 25 kDa protein that has two domains. In the N terminal is the Z-NA-binding domain that can bind to Z-form nucleic acid including Z-DNA or Z-RNA. In the C-terminal is the dsRNA-binding domain that is responsible for the sequestering of dsRNA done by VACV in the infected cells. Both domains have been shown to be responsible for full pathogenesis in mice, for full inhibition of PKR in both mice and in cells in culture, and for full IFN resistance in mice. The two main forms of E3 that wt VACV generates is depicted with full length E3 at the top followed by the truncated p20 E3 naturally produced.

Figure 2. E3 sequence homology in the orthopox family N-terminal domain. Yellow indicates highly conserved amino acids. Green indicates 100% conserved residues. Orange star symbolizes residues that interact with Z-form nucleic acids and blue circles are residues that interact with PKR. Reference sequences used for alignment include: Vaccina virus WR gb|AAO89338.1 ,Variola virus gb|ABG45643.1, Ectromelia virus ref|NP_671561.1, Cowpox virus emb|CRL86821.1, Raccoonpox ref|YP_009143366.1, Horsepox gb|ABH08163.1, Camelpox gb|ABH08163.1, Swinepox ref|NP_570192.1, Sheeppox ref|NP_659606.1, Deerpox ref|YP_002302383.1.

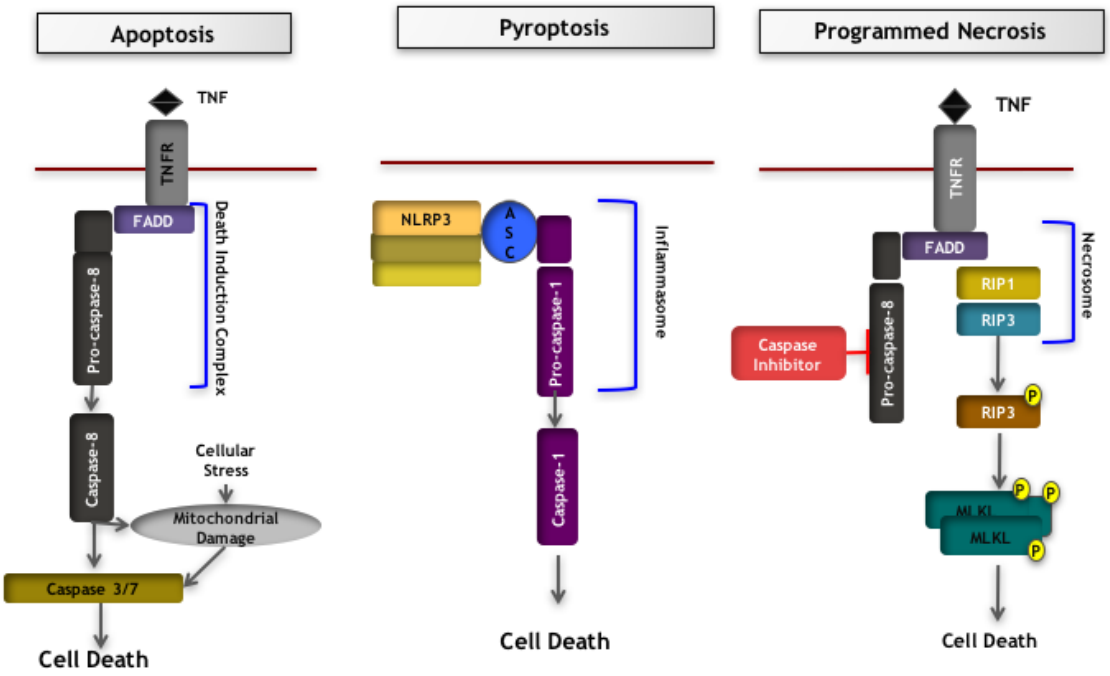

Figure 3. A schematic depicting the three major programmed cell death pathways. Apoptosis is shown on the left followed by necroptosis in the middle and pyroptosis on the right. Apoptosis signals through both intrinsic and extrinsic signaling cascades and is enzymatically dependent on a series of initiator and executioner caspases. Classical necroptosis signals through the TFN death receptor and functions independently of caspases through the use of RIP 1 and RIP3 leading to the activation of MLKL. Pyroptosis utilizes non-classical caspases activated through the formation of an inflammasome.

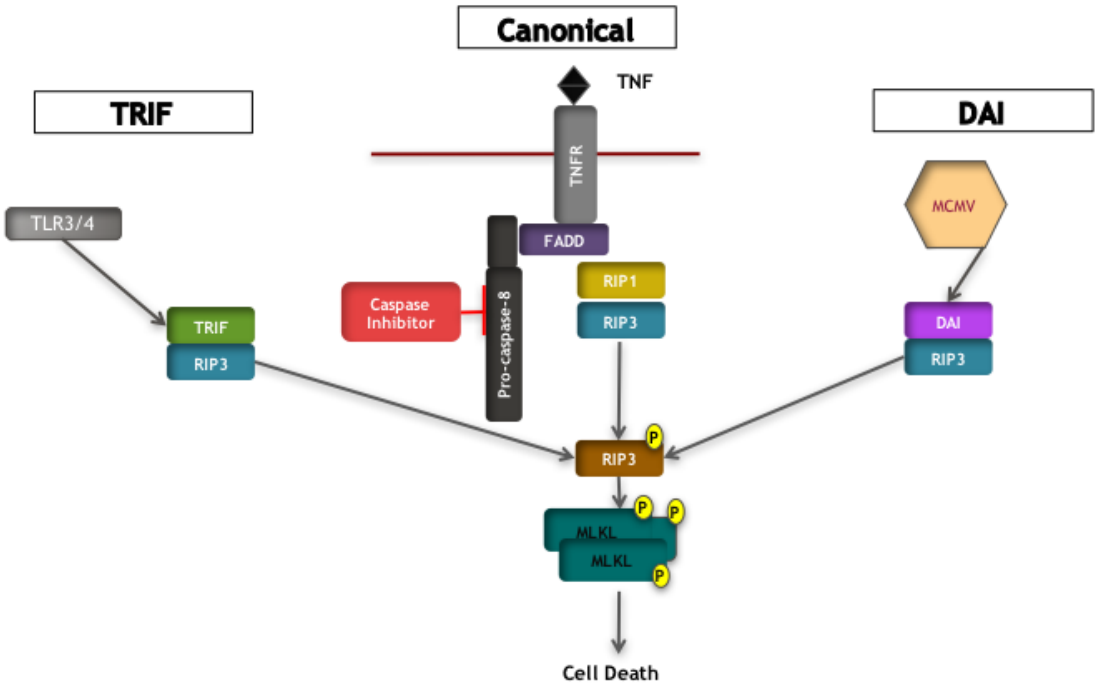

Figure 4. Canonical and noncanonical programmed necrosis pathway. Canonical activation of necroptosis uses RIP1 as an adaptor protein for the recruitment and activation RIP3 downstream of TNF family death receptors (TNFR1, Fas, TRAIL). Noncanonical activation of programmed necrosis via DAI was previously demonstrated in MCMV infection or via TRIF, which is downstream of TLR3 and TLR4 activation, driving recruitment and activation of RIP3. In all forms of RHIM-dependent activation of RIP3, RIP3 activation through phosphorylation results in RIP3-dependent recruitment and phosphorylation of MLKL leading to plasma membrane leakage and other features of programmed necrosis.

CHAPTER 2

THE E3 AMINO TERMINUS OF VACCINIA VIRUS IS REQUIRED TO INHIBIT INTERFERON REGULATED PROGRAMMED NECROSIS

ABSTRACT

Programmed necrosis is an alternative form of programmed cell death that functions as part of the innate immune response initiated by viral infections. It occurs when caspase activity is inhibited and aids in the immune response's clearance of virus-infected host cells. Vaccinia virus (VACV) encodes both a caspase inhibitor and the essential IFN resistance (IFN^R) gene, E3L. This gene encodes the protein, E3, which contains a Z-NA-binding domain (Z-NA-BD) in the N-terminus and a dsRNA-binding domain in the C-terminus. The protein is responsible for inhibiting the host type I interferon (IFN) pathway and is required for full pathogenesis. In the past, the Z-NA-BD of the protein has been shown to be dispensable for replication and IFN^R in most culture cells, yet critical for pathogenicity in mice models. In addition to being essential for *in vivo* models, the N-terminus containing the Z-NA-BD has been found to be highly conserved within poxviruses, indicating that it has has an essential function needed by the virus. Characterization at a molecular level has been limited due to lack of evidence demonstrating a specific molecular or biochemical function of the N-terminus. In this study we identify a cell culture system using L929 cells that demonstrated type I IFN sensitivity of VACV lacking the N-terminus of the E3 protein mirroring the previously *in vivo* studies. IFN sensitivity of VACV lacking the N-terminus of E3 is demonstrated

by a reduction of plaquing efficiency and the rapid induction of cell death. Furthermore, our research indicates that the N-terminus is required to inhibit IFN-primed, RIP3-dependent cell death through the phosphorylation of MLKL, independent of RIP1. *In vivo*, the highly attenuated phenotype VACV which encode for E3 deleted of the N-terminus in wild type (wt) mice is is reversed in a RIP3-deficient mouse model. Overall this work demonstrates that the N-terminal domain of E3 is required to inhibit type I IFN-primed, virally-induced, non-canonical, programmed necrosis.

INTRODUCTION

Type I interferons (IFNs) (IFN-α/β) are potent cytokines that function as a major component of the innate immune system and prohibit viral replication and spread. In response to viral infections, most cells are able to rapidly induce the synthesis of IFN and generate an antiviral state (105). IFN-α/β induce an antiviral state by binding to their IFN-α/β receptor located on the surfaces of cells. Binding results in the initiation of a signal cascade utilizing the JAK/STAT pathway, ultimately resulting in the upregulation of IFN-stimulated genes (ISGs) (18, 113). Hundreds of ISGs are upregulated in response to IFN, some of which function to prime the cells into an antiviral state including multiple Pattern Recognition Receptors (PRRs).

VACV is an IFN-resistant dsDNA virus that is unique in its ability to replicate in the cytoplasm of its infected host. Due to its unique mechanism of replication, it has evolved to evade the host immune response with approximately one third of its genome dedicated to virulence factors. VACV depends on its ability to circumvent the host's IFN system. A major contributor to the VACV IFN-resistant phenotype is the dsRNA binding protein E3. VACV deleted of E3L (VACVΔE3L) is IFN sensitive in cells typically noted for their permissive nature, including rabbit kidney RK-13 cells and human Huh7 cells (70, 79, 80).

The IFN-resistant phenotype has primarily been attributed to inhibition of Protein Kinase R (PKR). Previous studies demonstrated that RNA interference against PKR in

Huh7 cells reversed the IFN-sensitive phenotype of VACVΔE3L. The ability to inhibit PKR primarily maps to the C-terminus of E3, which encodes a ds-RNA-binding domain (dsRBD) (80) .

Characterizing the function of E3's second highly conserved domain located in the N-terminus of E3 has been problematic. *In vitro*, the N-terminus is completely dispensable for IFN resistance and replicationin most cells (80, 114), but is necessary for full pathogenesis in mice (81, 111). In mouse models, the N-terminus is required for spread of infection (81) and neurovirulence (111). Recently, the highly attenuated phenotype of VACV deleted of the N-terminus (VACVE3LΔ83N) seen in mouse models was demonstrated to be due to IFN sensitivity as seen by a restoration of pathogenesis in mice deleted of the type I IFN receptors (IFN-α/βR$^{-/-}$ mice) (112).

Using 129MEFs, IFN sensitivity was found to correspond to VACV-E3LΔ83N signal induction of antiviral pathways by PKR, which is an IFN-inducible PRR that recognizes dsRNA. 129 MEFs infected with VACVE3LΔ83N induced the phosphorylation of the translation initiation factor eIF2α leading to protein synthesis shutdown. IFN resistance was restored in PKR$^{-/-}$ MEFs by knockdown of PKR in MEFs (112). However, Pathogenesis of VACV-E3LΔ83N was not restored in PKR-/- mice, suggesting that PKR was not essential for inhibiting VACV-E3LΔ83N pathogenesis in mice.

Despite significant evidence that the N-terminus is required for IFN resistance, the molecular function unique to this domain remains elusive, as a system has not been

established that is consistent with the IFN-sensitive phenotype in mouse models. The lack of a consistent phenotype between *in vivo* and *in vitro* models suggests that cells may be utilizing an alternative IFN-regulated cell mechanism to inhibit replication of VACV-E3LΔ83N.

The type 1 IFN system plays a huge role in generating a large variety of antiviral responses. One such response is the priming of programmed cell death during infections. In the current generalized model of programmed cell death, apoptosis represents the predominate cell death pathway with other distinct death pathways acting in a cooperative or substitutive fashion. Recently, alternative cellular death mechanisms have come into focus with regard to viral infections: necroptosis and pyroptosis. New studies has shown that alternative death pathways may be essential for inhibition of viruses that encode anti-apoptotic genes such those seen in VACV(25).

Programmed necrosis has recently been demonstrated to function as an alternate host defense pathway initiated during the course of a viral infection, specifically, when caspase function is inhibited in susceptible cells (51, 52). Alternative programmed death is required during many viral infections because many viruses encode caspase inhibitors, including poxviruses and herpesviruses (53). These inhibitors prevent the cell from signaling through caspase-dependent pathways to induce death. In infections that inhibit caspase functions, programmed necrosis is initiated in a caspase-independent manor in order to bypass the pathogen regulation of cell death. Initiation of programmed necrosis has been demonstrated to play a significant role in antiviral host defense by reducing viral replication and clearing virally infected cells (25, 27).

Programmed necrosis is an inflammatory form of programmed cell death. Activation leads to the induction of a signal transduction pathway involving RIP3 and the downstream pseudokinase known as mixed lineage kinase-like (MLKL). Activation of MLKL leads to defects in membrane integrity (40, 42). The classical programmed necrosis pathway induces death following TNF binding toclassical death receptors (DRs), under caspase-inhibited conditions, and results in the formation of a RIP1-RIP3 complex called a necrosome. The necrosome then interacts through RIP homotypic interaction motif (RHIM) domains and employs the kinase function of both proteins (25, 27, 53, 115, 116). The role of RIP3 in programmed necrosis is not limited to the classical pathway but is also required for programmed necrosis initiation through non-classical pathways such as IFN-regulated PRR activation (43, 115, 116).

As with most host defense mechanisms, viruses have adapted to regulate the programmed necrosis to bypass the host and allow for the infection to continue. An example of this has been demonstrated in Murine Cytomegalovirus (MCMV) (27, 46). In MCMV infections, RIP3 can complex with DAI, through their RHIM domains, in the signaling cascade to induce programmed necrosis. To prevent the induction of programmed necrosis, MCMV encodes an M45 protein which acts as a viral inhibitor of RIP activation (vIRA). M45 functions by sequestering RIP3, impeding the signal transduction that induces cytokine activation and programmed necrosis (28, 44, 117, 118).BecauseVACV has the capacity to produce a caspase inhibitor, it is likely that it must also have the capacity to inhibit the induction of programmed necrosis. In this study, the role of the N-terminus of E3 on the inhibition of a virally-induced necroptosis that is regulated by type I IFN is investigated.

MATERIALS AND METHODS

Cells and viruses. L929 cells were maintained in minimum essential medium (MEM) supplemented with 5% fetal bovine serum (FBS) (HyClone) and not allowed to exceed 7 passages. HEK293T cells were maintained in Dulbecco's modified minimum essential medium (D-MEM) supplemented with 10% FBS. The Western Reserve (WR) strain of wt VACV and virus mutants deleted of the full E3L gene (VACVΔE3L), the coding for the N-terminal 83 amino acids of E3 (VACVE3LΔ83N), or the coding for the N-terminal 37amino acids of E3 (VACVE3LΔ37N) were generated previously (81). All virus stocks were generated in BHK cells. Crude lysates were purified by pelleting through a 36% sucrose pad.

Interferon Resistance Evaluation by Plaque Reduction. 6-well plates of subconfluent L929 cell monolayers were treated with 0-300 U/mL of mouse IFN-α (Calbiochem) 18 h prior to infection. Cells were then infected with $1x10^2$ PFU of either WR strain of wt VACV or VACVE3LΔ83N virus diluted in MEM containing 2% FBS. Cell monolayers were infected with 100 µL of virus after aspirating the media off the dishes. Cells were incubated at 37°C, 5% CO_2 for 1 hour, with rocking every 10 minutes. After 1 hour cells were overlaid with MEM containing 5% FBS, and incubated at 37ºC. 48-72 hours post infection (hpi), upon formation of plaques, the monolayers were stained with crystal violet (0.5 % in 20% ethanol) and plaques were counted. The reduction in the number of plaques was recorded as a percentage of plaques in the absence of interferon and was plotted against increasing units of interferon.

Protein synthesis shut off and protein loss assay. 50% confluent L929 cell monolayers in 60 mm dishes were infected with WR strains of wt VACV or VACVΔE3L or E3L N-terminal mutants (VACVE3LΔ83N or VACVE3LΔ37N) at an MOI of 5. At 30 minutes prior to indicated time of radiolabeling, cells were washed twice with PBS to remove all media containing methionine and were subsequently overlaid with methionine free DMEM (CellGro) for 30 minutes at 37°C. Following starvation of methionine, the cells were incubated for 30 min at 37°C with labeling media containing 50 μCi [35S]methionine/ml (800 Ci/mmol, Perkin Elmer) to label newly synthesized proteins. Cells were washed twice with pre-warmed PBS, then pelleted and lysed in 100 μL of 1X SDS [62.5 mM Tris-Cl, 10% glycerol, 2% SDS, 0.0005% bromophenol blue, 0.1% 2-mercaptoethanol, 1X Halt Protease and Phosphotase Inhibitor Cocktail (Pierce Thermo Scientific)]. Protein lysates were isolated utilizing QIAshredder columns (Qiagen) by spinning lysates in columns at 16,000xg for 2 minutes at 4°C. Samples were stored at -80°C. The samples were boiled for 5 minutes and separated on denaturing 10% SDS-PAGE gels. The gels were stained for total protein levels with Coomassie staining solution (0.1% Coomassie Brilliant Blue R-250, 40% methanol and 10% glacial acetic acid) for 30 minutes.The gels were then destained with destaining solution (40% methanol and 10% glacial acetic acid) three times, each 20 minutes, and were incubated overnight in 10% glacial acetic acid to remove any residual stain. Radiolabeled proteins were visualized by autoradiography with a 24-hour film exposure at -20°C.

Live imaging of L929 infected cells. L929 cells were plates in 12 well CytoOne tissue culture treated plates(USA Scientific) and pre-treated with 100 U/mL of mouse

IFN-α (Calbiochem) for 18 h prior to infection. A live nuclear stain was applied using Hoechst 33342 (2'-[4-ethoxyphenyl]-5-[4-methyl-1-piperazinyl]-2,5'-bi-1H-benzimidazole) and incubated 15 minutes prior to infection. Cells were infected with an MOI of 5 with either wt VACV or VACVE3LΔ83N as described above. For images used to evaluate alterations in morphology, infected cells were incubated for an additional 5 hours and imaged with an EVOS™ FL Auto Imaging System (Invitrogen™). For time-lapse imaging, cells were overlaid with MEM media containing 1μM SYTOX® Green nucleic acid stain (Thermo Fisher Scientific). Cells were incubated at 37°C with 5% CO2-supplemented air on an EVOS™ FL Auto Imaging System(Invitrogen™) with onstage incubator system and an image was taken every 2 minutes for 5 hours.

L929 Viability Assay. Viability was assessed with a SYTOX® nuclear stain uptake assay or by a *CellTiter-Glo*® Luminescent Cell Viability Assay(Promega). For SYTOX® nuclear stain uptake assay L929 cells were plates in 12 well CytoOne tissue culture treated plates(USA Scientific) and pre-treated with 100 U/mL of mouse IFN-α (Calbiochem), for 18 h, prior to infection. A live nuclear stain was applied using Hoechst 33342 and incubated 15 minutes prior to infection. Cells were infected with an MOI of 5 with either wt VACV or VACVE3LΔ83N as described above. At 5 hpi, SYTOX® Green nucleic acid stain (Thermo Fisher Scientific) was added to the media at a concentration of 1μM and allowed to incubate for 15 minutes. Cells were then evaluated for viability by imaging a total of 10 fields with a 20X objective, using EVOS™ FL Auto Imaging System (Invitrogen™) to evaluate. Percent viability was determined by comparing the number of cells that had SYTOX® incorporation to total

number of cells. For *CellTiter-Glo*® Luminescent Cell Viability Assay, L929 cells were plated in a 96-well plate and pre-treated with 100 U/mL of mouse IFN-α (Calbiochem) for 18 hours, then infected at an MOI of 5. At 12 hpi, *CellTiter-Glo* reagent was added according to manufacturer's recommendations and incubated at room temperature for 30 minutes. Results were read on a GloMax® 96 Microplate Luminometer(Promega) as relative luminesce units (RLU).

Inhibitors and Treatment of cells: All inhibitor treatments were applied for 1 hour prior to infections. Inhibitors were also added to the media used to infect and overlay cells. Mock treatments consisted of the addition of DMSO (Sigma) at the volume used in corresponding treatments. Requirement for caspase involvement in cell death was evaluated by treating cells with the pan-caspase inhibitor Z VAD-FMK (ZVD) (ApexBio) at 100μM. Evaluation of the requirement of RIP proteins were evaluated with the use of GSK inhibitors at 3μM. N-(6-(Isopropylsulfonyl)quinolin-4-yl)benzo[d]thiazol-5-amine (GSK872, GlaxoSmithKline) was used to inhibit RIP3 activity. 3-Benzothiazol-5-yl-7-(2,5-dimethyl-2H-pyrazol-3-yl)-thieno[3,2-c]pyridin-4-ylamine (GSK 843GlaxoSmithKline) was used to evaluate the requirement for kinase activity of RIP3. 2,2-Dimethyl-1-(5(S)-phenyl-4,5-dihydro-pyrazol-1-yl)-propan-1-one (GSK963, GlaxoSmithKline) was used to determine the requirement of RIP1 activity. Cells used as a positive control for programmed necrosis were treated with mouse TNF-α (Sigma) at 20ng/ml following a 1-hour pretreatment with 100μM of ZVD (ApexBio).

Protein Extraction and Western immunoblot analysis. L929 cells were pre-treated with 100 U/mL of mouse IFN-α (Calbiochem) for 18 hours, prior to infection, and were infected with viruses at an MOI of 5. At 4 HPI, cells were scraped into the medium

and subsequently pelleted by centrifugation at 500 × g for 10 minutes at 4°C. The supernatant was removed and the cells were washed, pelleted, and washed a second time with ice-cold PBS. Cell extracts were then obtained by lysing the cells in complete Triton X lysis buffer (20 mM Tris-HCl, pH 7.4, 150 mM NaCl, 1 mM Na_2EDTA, 1 mM EGTA, 1% Triton X-100, 2.5 mM sodium pyrophosphate, 1 mM β-glycerophosphate, 1 mM Na_3VO_4, and 1X Halt Protease and Phosphotase Inhibitor Cocktail, Pierce Thermo Scientific) and incubated on ice for 5 minutes. Samples were centrifuged at 15,000 × g for 20 minutes at 4°C. Supernatant was collected and SDS protein loading dye (3X) was added. For samples used for MLKL aggregation, cells were scraped and pelleted as described above but lysed in100 μL of 1X SDS (62.5 mM Tris-Cl, 10% glycerol, 2% SDS, 0.0005% bromphenol blue, 1X Halt Protease and Phosphotase Inhibitor Cocktail, Pierce Thermo Scientific) without 2-mercaptoethanol. Lysates were transferred into QIAshredder columns (Qiagen), spun at 16,000xg for 2 minutes at 4°C. All samples were stored at -80°C. Samples were boiled for 5 minutes, separated on a denaturing 10% SDS-PAGE gel, and then transferred onto a nitrocellulose membrane at 100 volts for 75 minutes in 10 mM CAPS, pH 11 with 20% methanol. Following transfer, the membrane was incubated in blocking buffer (140 mM NaCl, 3 mM KCl, 20 mM Tris [pH 7.8], 0.05% Tween 20, 3% nonfat milk) for 1 hour at room temperature. Rabbit polyclonal antibodies were used to detect P-MLKL (Abcam 1:2000) and total MLKL (Abcam 1:1000), and mouse monoclonal antibodies were used to detect glyceraldehyde-3-phosphate dehydrogenase (GAPDH). Primary antibodies were diluted in blocking buffer and blots were exposed to antibodies overnight. Secondary goat anti-rabbit IgG conjugated to horseradish peroxidase (1:5000, Santa Cruz) or anti-mouse IgG conjugated

to horseradish peroxidase (1:5000, Santa Cruz) were incubated at room temperature for 1 hour. Immunoreactive bands were visualized by chemiluminescent development using SuperSignal West Dura Duration substrate (Pierce Biotechnology).

Intranasal infections of mice. Anesthesia and infections were carried out as previously described (112). Briefly, wt C57BL/6 and RIP3−/− mice were anesthetized with a ketamine cocktail containing 37.5 mg/ml ketamine (Lloyd Laboratories, Shenandoah, IA), 7.5 mg/ml xylazine (Vedco, St. Joseph, MO), and 2.5 mg/ml acepromazine maleate (Fort Dodge Laboratories, Fort Dodge, IA) at the age of 8 to 10 weeks. Intraperitoneal injection (IP) of anesthesia was given at a dose of 1 µl per gram of body weight. Anesthetized mice were infected with 5 µl containing 10^6 PFU of either WR strain of wt VACV or VACVE3LΔ83N virus intranasally. Mice were monitored daily for clinical signs and given a clinical score based on weight loss, lethargy, respiratory distress, declines in general appearance (scuffed), and eye infections. Each clinical sign was given a score of 1 to 5 with 5 representing severe symptomology. Weight loss score was determined by the percent of their original weight with 100% of original weight receiving a score of 0; 93.7 to 99.9% given a score of 1; 86.2 to 93.2% given a score of 2; 78.6 to 86.1% given a score of 3;71.0 to 78.5% given a score of 4; 70% and below was given a score of 5 (81, 111). All mice were euthanized by asphyxiation using CO2 when any mouse dropped below 30% of their initial weight or reached a clinical score above 25.

Statistics. Statistical analysis was done by using a two-tailed, unpaired T test. P values of $p<0.001$ were represented as ***, $p<0.01$ were represented as **, $p<0.05$ were represented as * and no significance (N.S.) was used to represent $p>0.05$. In order to

determine the model of regression for cell viability, relative viability was transformed logarithmically,then subjected to a linear regression analysis. Statistical significance in this analysis meant that regression was occurring in a logarithmic manner.

RESULTS

E3, the multifunctional protein encoded by VACV, plays an essential role in counteracting the host innate immune system. One of its primary functions involves inhibition of the downstream type I IFN effects. While E3's C-terminus has been extensively characterized for its role as a dsRNA-binding molecule, the same level of characterization for the N-terminal Z-NA-binding domain has not been possible. Limitations in characterizing the biological role of the N-terminus are primarily due to a lack of viable cell culture systems in which any significant function of the protein can be observed. Specifically, no systems have been able to identify a biological role for the protein in inhibiting interferon responses, which are essential in mouse models (112). In an attempt to further evaluate the function of the N-terminus, our lab has discovered a cell culture system that mirrors the need for a functional N-terminus in inhibiting the interferon response, previously observed in mouse models, through the use of a murine fibroblast cell line (L929).

The N-terminus is required for type I IFN resistance in L929 cells. L929 cells were pretreated with increasing amounts of mouse IFN-α prior to infection. Subsequently, cells were infected with equivalent plaque forming units (PFUs) of wtVACV or VACV expressing E3 with a truncated N-terminus (VACV-E3LΔ83N) (111). As seen in figure 6, plaque formation by wtVACV is resistant to IFN-α pretreatment, but the plaque formation ofVACV-E3LΔ83N was IFN-α sensitivity. This increased sensitivity caused the percent of original PFUs to decrease in a with increasing IFN-α U/mL treatments until a treatment of just over 100 U/mL, where no plaque formation was observed. This demonstrated that the N-terminus of E3 is, in fact, essential

for VACV circumvention of the antiviral state induced by type 1 IFNs, similar to the results observed in mouse models.

Global reduction of protein in VACV-E3LΔ83N-infected L929 cells in an IFN-dependent manner. One of the most common ways that IFN inhibits virus replication is by inhibiting viral protein synthesis. In an attempt to evaluate the relationship between protein synthesis in L929 cells pretreated with mouse IFN-α and VACV E3 N-terminal mutants, newly synthesized proteins were labelled with a pulse of [^{35}S]methionine at various times post-infection. These proteins were then separated by SDS-PAGE and visualized by autoradiograph (Fig.7A). As expected, wtVACV is able to circumvent the inhibition viral protein sysnthesis the E3 sequestering dsRNA and VACVΔE3L resulted in rapid protein synthesis shutdown due to the absence of E3(110, 112). Inhibition of new protein synthesis is demonstrated by the lack of isotope incorporation with the retention of total cellular proteins visualized by Coomassie staining (Fig.7B). The autoradiographs also show that, at later times post-infection, the lanes with lysates of cells pretreated with IFN-α and infected VACV-E3LΔ83N did not have isotope-labeled protein present. However, the lack of labeled protein within these lanes does not necessarily indicate protein synthesis shutdown due to the corresponding failure to recover proteins from IFN-treated, VACV-E3LΔ83N -infected L929 cells (Fig.7B), as visualized in the stained gels. This absence of total protein on the stained gels does not fit the classical pattern of protein synthesis shutdown through eIF2-α. The loss of total viral and cellular proteins suggests that there is an alternative cellular process occurring. More significant, this process is primed by IFN-α treatment, and occurs only in the absence of a functional N-terminus on VACV's E3.

Type I interferon sensitivity in N-terminal mutants result in alterations of cell morphology. In order to gain insight into the IFN-α-dependent process that leads to total protein loss following infections with VACV expressing E3 N-terminal mutants, live imaging was conducted. L929 cells were pretreated with mouse IFN-α and infected with wt or with VACV expressing E3 N-terminal mutants. Observations captured through live imaging showed that L929 cells pretreated with IFN and infected with VACV-E3LΔ83N undergo unique morphological changes not seen in the other conditions (Fig. 8). Starting at approximately 4HPI, pretreated L929 cells infected with E3LΔ83N progressively underwent cytoplasmic enlargement and cytoplasmic membrane disruption, not seen in cells infected with wtVACV, irrespective of IFN treatment. The cellular swelling and cytoplasmic membrane disruption suggests that an IFN-α dependent alternative process of programmed cell death that does not fit the classical morphology of apoptosis may occur in cells infected with E3L N-terminal mutants. This loss of cellular membrane integrity and cytoplasmic enlargement may represent the cellular process responsible for the global loss of recovery of proteins shown earlier.

IFN-α sensitivity results in a rapid death characterized by membrane permeability. L929 cells that were pretreated with IFN-α and infected with E3 N-terminal mutants suggests that total protein loss is due to rapid activation of programmed cell death that results in loss of membrane integrity. In order to evaluate if the morphology results from a cellular death mechanism, a cell viability assay was performed using a membrane-impermeable nuclear stain. This assay demonstrated that L929 cells pretreated with IFN-α and infected with VACV expressing the N-terminal mutant results in increased cellular death compared to an uninfected control and cells infected with wt

VACV (Fig. 9). These results are apparent from SYTOX dye uptake, which indicates membrane permeability. Combining these results with the live imaging results suggests that the morphological changes correlate with programmed cell death.

IFN-α primed death is dependent on RIP3 and is caspase independent. Programmed cell death pathways can be broadly separated into those that are caspase dependent (apoptosis and pyroptosis) and those that are caspase independent (necroptosis, or programmed necrosis). To determine if del83N-induced death was caspase dependent, we asked if cell death was sensitive to a membrane permeable, pan-caspase inhibitor, Z-VAD-FMK (ZVD). ZVD globally inhibits all known caspases (ref) (46). ZVD, however, had no effect on IFN-sensitivity of E3LΔ83N. This suggests that del83N induced cell death is caspase independent. The most well characterized caspase independent cell death is programmed necrosis. Programmed necrosis is dependent on the protein kinase, RIP3. Thus, we asked if a RIP3 specific inhibitor, GSK872, could reverse the IFN-sensitivity of E3LΔ83N. The incorporation of this inhibitor fully rescued plaquing efficiency of E3LΔ83N in IFN-treated L929 cells. This indicated that the IFN-α dependent reduction of plaquing efficiency corresponds to a RIP3 dependent mechanism.

Global protein loss is dependent on RIP3 and occurs independently of caspase activity. In observing GSK872's ability to recover plaquing efficiency, we wanted to determine if it would also rescue the failure to recover protein from E3LΔ83N-infected cells, previously observed. As seen in Fig. 11, the addition of GSK872 fully restored recovery of proteins from IFN-α treated, E3LΔ83N-infected cells. ZVD had no effect on the failure to recover proteins from IFN-treated, E3LΔ83N-infected cells. These results correlated with the plaque reduction assay results and demonstrated that the

IFN-α sensitive failure to recover proteins was dependent on RIP3 and independent of caspases.

Alterations in cellular morphologies involving cytoplasmic enlargement and membrane disruption dependent on RIP3 occurs independently of caspases. After demonstrating that the IFN-α-associated phenotypes could be rescued with the addition of GSK872, signifying the system's dependence on RIP3, we wanted to observe through live imaging if GSK872 had an effect on rescuing cell morphology. Live imaging was conducted on untreated VACV-E3LΔ83N-infected control cells, IFN-α-treated VACV-E3LΔ83N-infected cells with the addition of GSK872, and IFN-α-treated VACV-E3LΔ83N-infected cells with the addition of ZVD (Fig. 12). The results of this imaging showed that cell morphology was in fact conserved in both untreated VACV-E3LΔ83N-infected control cells and IFN-α-treated VACV-E3LΔ83N-infected cells with the addition of GSK872. IFN-α-treated VACV-E3LΔ83N-infected cells with the addition of ZVD, on the other hand, resulted in cell morphologies as previously observed that were characterized by membrane disruption and cytoplasmic enlargment.

Inhibition of RIP3 rescues cell viability. The compiled results of the plaque reduction assays, Coomassie-blue staining, and live imaging led us to repeat the SYTOX© green dye up-take assays. This time we wanted to include VACV-Δ83N + GSK872 and VACV-E3LΔ83N + ZVD to confirm our prior results (Fig. 13). The results of these assays demonstrated that VACV-E3LΔ83N and VACV-E3LΔ83N + ZVD resulted in decreased cell viability when treated with IFN-α. This confirmed that the cell death occuring was indeed not dependent on caspases. In contrast, the presence of GSK872 in VACV-E3LΔ83N-infected cells, rescued cell viability to levels consistent

with the MOCK and wtVACV assays performed. This provided further evidence to support the hypothesis that we were observing a form of programmed cell death that was dependent on RIP3.

VACVs that produce E3L-encoded proteins with truncated N-termini result in MLKL activation. In order to confirm that the cell death was due to a form of programed necrosis, the status of MLKL was examined in MOCK, wt VACV, E3LΔ83N VACV, and TNF cells. It has been well documented that one of the final steps in programmed necrosis involves the aggregation and phosphorylation of MLKL(52). Western blots were performed in order to assay for the presence and phosphorylation of MLKL (Fig. 14). TNF+zVAD treatment was used as a positive control(52). Phosphorylation of MLKL was demonstrated to occur in L929 cells pretreated with IFN-α and infected with E3L N-terminal mutants (Fig.14). Phosphorylation of MLKL was specific to IFN-α treated and E3LΔ83N infected cells and the positive control (Fig. 14C). Phosphorylation of MLKL in L929 cells pretreated with IFN-α and infected with VACV E3LΔ83N occurred at very early times post infection (3 hpi**,** Fig. 14B). MLKL also ran as an aggregate under non-reducing conditions, in extracts from IFN-treated, E3LΔ83N infected cells (Fig. 14A). These results indicate that programed necrosis, involving the aggregation and phosphorylation of MLKL, was occurring in IFN-treated E3LΔ83N infected L929 cells.

RIP3 activity is required for IFN-α-sensitive plaque reduction but reduction is independent of RIP1. In confirming that cell death was a caspase-independent programmed necrosis based on the requirement for RIP3, we also wanted to determine if what we were observing was a classical form of necroptosis involving both RIP3 and

RIP1 that had been previously described with VACV(25). We therefore evaluated the requirements for both RIP1 and RIP3.. To accomplish this, we utilized a RIP1 inhibitor known as GSK963 in multiple assays: plaque reduction assay, total protein staining, cell viability assay, and MLKL activation. GSK963 was unable to rescue plaquing efficiency (Fig. 15), global protein loss (Fig. 16), cell viability (Fig. 17), or MLKL activation (Fig. 18) in L929 cells pretreated with IFN-α and infected with VACV-E3LΔ83N. Treatment with the RIP3 inhibitor, GSK872, restored IFN-α resistance in all assays. These results suggested that we were observing a novel form of programmed necrosis in VACV-infected cells that is dependent on RIP3 and independent of RIP1.

The kinase domain of RIP3 is required for loss of viability. As a further measure to evaluate the requirement of a functional RIP3, we conducted a cell viability assay utilizing an additional small molecule inhibitor specific to the kinase activity of RIP3 (GSK843). Once again, rescue of viability in L929 cells pretreated with IFN-α was achieved by treatment with the RIP3 inhibitor GSK872 but not the RIP1 inhibitor GSK963, while partial rescue of viability was observed following treatment with the RIP3 kinase-specific inhibitor (GSK843) (FIG 19).

Deficiency of RIP3 rescues VACV-E3LΔ83N pathogenesis in mice. Finally, the *in vitro* results were confirmed *in vivo* using mouse pathogenesis studies utilizing wt C57BL/6 and RIP3 genetically deficient (RIP3-/-) mice. Mice were intranasaly infected with 10^6 PFU of either wt VACV or VACV-E3LΔ83N and monitored for clinical symptomology. Wt VACV infections resulted in significant pathology in both types of mice. As expected, VACV-E3LΔ83N was apathogenic in wt C57BL/6 mice.

Pathogenesis of VACV-E3LΔ83N was restored in RIP3-/- mice to levels equivalent to that of wt VACV (Fig. 20).

DISCUSSION

In this chapter the role of the N-terminal domain of the product of VACV's essential immune evasion gene, E3L, was evaluated. There is overwhelming evidence that in VACV, E3 is a potent virulence factor with primary functions involving conferring IFN resistance. While the C-terminus of this gene product has been well characterized, the function of the N-terminus has remained elusive. While the highly conserved nature of this gene product amongst poxviruses implies it provides an essential function, for many years no replication phenotype in cells could be identified (Langland and Jacobs 2004). To date, the most significant biological phenotype associated with deletions of the N-terminus was a 3-4 log loss of virulence in both the intranasal (IN) and intracranial (IC) mouse models (81, 111). In both IN and IC models, pathogenesis of VACV-E3LΔ83N is fully restored in IFNAR-/- mice, clearly demonstrating that the N-terminus is required for IFN resistance *in vivo* (112). The IFN sensitivity of VACV-E3LΔ83N was found to be mediated by PKR and reproducible in 129 MEFs. Surprisingly, this PKR-mediated IFN sensitivity in primary cells did not correspond to prior mouse pathogenesis studies, as VACV-E3LΔ83N had maintained a highly attenuated phenotype in mice that were genetically deficient in PKR. These findings indicated that there is an alternative IFN-regulated programmed cellular death mechanism that VACV utilizes the N-terminus of E3 to circumvent. This process is able to regulate *in vivo* virulence in the absence of the N-terminus of E3.

Attempting to gain insight into the function that the N-terminus of E3 plays in inhibiting IFN signaling led us to screen murine cell lines for an IFN-sensitive phenotype

that could be used to determine the molecular role of the terminus, mimicking previous *in vivo* experiments. A breakthrough came when the murine fibroblast L929 cell line was screened. In L929s, VACV expressing E3 protein with truncated N-termini (VACV-E3LΔ83N) were highly IFN-sensitive and VACV expressing full length E3 was able to replicate in the presence of high doses of IFN. The IFN sensitivity of VACV-E3LΔ83N was demonstrated through a plaque reduction assay. L929 cells were pretreated with increasing amounts of mouse IFN-α to promote an antiviral state and were subsequently infected with VACV-E3LΔ83N or wt VACV. VACV-E3LΔ83N-infected cells that were pretreated with IFN-α were unable to form plaques in a logarithmic, IFN-α dose-dependent manner with a 50% reduction in plaquing efficiency seen at an IFN-α concentration between 3 and 10 U/ml. Wt VACV retained an IFN-resistant phenotype, shown by its ability to form plaques even at the highest dose of IFN-α. The IFN-sensitive phenotype observed in VACV-E3LΔ83N-infected L929 cells indicated that they may be a viable system for evaluating the biochemical function of the N-terminus of E3.

Regulation of translation is a common antiviral mechanism that can be influenced by IFN signaling. During viral infections, the activation of PKR leads to phosphorylation of the alpha subunit of translation initiation factor eIF2. This phosphorylation results in protein synthesis shut off, thereby preventing virus replication (119, 120). VACV-E3LΔ83N has been shown to lead to late activation of PKR in some cells in culture, demonstrating that the N-terminal domain is necessary for full initiation of PKR. However, unlike what is seen following classical PKR activation, this late activation does not inhibit late viral protein synthesis or inhibit viral replication (110).

To gain further insight into whether translational regulation was contributing to IFN sensitivity, protein synthesis was evaluated by radiolabeling proteins with [^{35}S]methionine at multiple times post infection. This evaluation demonstrated that when VACV is deleted of E3L (VACVΔE3L), infections result in the loss of [^{35}S]methionine incorporation, regardless of IFN treatment. This was seen by 6 HPI and signified early recognition of viral infection. The loss of [^{35}S]methionine incorporation in VACVΔE3L corresponded to a pattern of protein synthesis termination demonstrated through Coomassie staining. Cells that were treated with IFN-α and infected with VACVE3LΔ83N also demonstrated a reduction of [^{35}S]methionine incorporation. Unexpectedly, there was a corresponding global protein reduction that was not previously noted in VACVΔE3L-infected cells. Additionally, this reduction was IFN-dependent and inhibited by wt VACV infections. This phenomenon demonstrated a novel phenotype that was potentially an unexplored IFN-regulated mechanism to control viral infections.

The newly observed phenotype involving a global protein loss in an IFN-dependent manner over the course of infections with VACVE3LΔ83N in L929 cells caused us to question the structural modifications that could account for this loss of total cellular protein. Live imaging of L929 cells that were pretreated with IFN-α and infected with VACV expressing E3 N-terminus mutants suggests that total protein loss may be attributed to a loss of membrane integrity. L929 infected with VACVE3LΔ83N following treatment of IFN-α demonstrated dramatic alterations in morphology; most notable of these changes were membrane blebbing and cytoplasmic enlargement occurring at early time points post infection. These early alterations in morphology suggested that the cells might be induced to undergo rapid programmed cell death through mechanisms not

typically seen in apoptosis. To evaluate if the morphology observed was due to a cellular death mechanism, a cell viability assay was performed. Morphology changes observed did correlate to cellular death. This further suggested that the N-terminus of E3 functions to inhibit an IFN-primed programmed cell death.

While the apoptosis form of programmed cell death has long been recognized as a host strategy to restrict viral infections, alternative forms have been recently identified through the study of cell-intrinsic mechanisms to regulate viral infections. To determine whether the IFN-primed cell death induced in the absence of the E3 N-terminus was apoptosis or another characterized mechanism of programmed cell death, a series of inhibitors were employed to target critical proteins in apoptosis, pyroptosis, and programmed necrosis. Through the use of a pan-caspase inhibitor we demonstrated that the IFN-sensitive phenotype of VACV-E3LΔ83N in L929 cells was not due to caspase-dependent mechanisms of programmed cell death, which excluded both pyroptosis and apoptosis as the cause of death. The inhibition of caspases was not able to rescue plaquing efficiency, global protein loss, alterations in morphology or cell viability. Instead, cell death seemed to be attributed to a programmed necrotic death, as an inhibitor targeting RIP3, an essential protein in the programmed necrosis pathway, was able to restore IFN resistance. In the presence of the RIP3 inhibitor, assays with VACV-E3LΔ83N infections demonstrated results that were equivalent to results with wt VACV infections. Induction of programmed necrosis was subsequently confirmed through the demonstration of MLKL activation and through the utilization of an additional inhibitor specific to the kinase activity of RIP3, which prevented the reduction in cell viability.

These results are consistent with necrotic death, as both MLKL activation and the utilization of RIP3 are hallmarks of this form of programmed cell death.

A pivotal moment for uncovering programmed necrosis as a host defense mechanism came with the discovery that VACV-infected cells treated with TNF were able to undergo a RIP3 kinase-dependent programmed necrosis. More important, mice lacking RIP3 were unable to utilize programmed necrosis, making them more susceptible to VACV infections (25). Induction of programmed necrosis was demonstrated to be dependent on a functioning VACV-encoded caspase inhibitor and to signal through canonical necroptosis, which involves RIP1:RIP3 interactions utilizing RHIM domains after TNF induces death receptor activation (25).

Previous studies have shown that VACV is capable of inducing programmed necrosis in the presence of TNF; this induction, however, is dependent on both RIP1 and RIP3, although other RHIM-containing proteins have also emerged as adaptor proteins for RIP3 activation (27, 44, 46, 117). In follow-up to these studies, we decided to evaluate the requirement of RIP1 in the VACVE3LΔ83N-induced programmed necrosis to gain better insight into how the E3 N-terminus may function to prohibit cell death. Utilizing a small molecule inhibitor specific to RIP1, we demonstrated that VACVE3LΔ83N-infected L929 cells treated with IFN-α are able to undergo programmed necrosis independently of RIP1 activity. This represents a unique pathway of programmed necrosis induction by VACV that implicates a regulatory mechanism beyond the previously described function of a caspase inhibitor.

It has been suggested that programmed necrosis may represent the default cell

death pathway utilized when caspases inhibitors are encoded by pathogens (29). However, in addition to the requirement for a pathogen-encoded caspase inhibitor, the infected cells must also express sufficient levels of RIP3 (51, 52). Consequently, the biological significance of RIP3-dependent programmed necrosis induced by VACV-E3LΔ83N required us to examine *in vivo* models. Mice genetically deficient in RIP3 were used to demonstrate that the IFN-regulated programmed necrotic death in VACV-E3LΔ83N-infected L929 cells corresponded to biological significance *in vivo*. In C57B6 mice ,VACV-E3LΔ83N infections were apathogenic. In RIP3-deficient mice, however, pathogenesis was equivalent to that of wt VACV.

This study has provided significant insight into the biological role that the N-terminus of E3 plays in evading the host IFN system. It can be concluded from these results that the N-terminus of E3 is required to prevent the initiation of an IFN-primed, virally induced programmed necrosis. Additionally, the induction of programmed necrosis represents a unique pathway not previously described in VACV infections, as it occurs independently of RIP1. This shows that with the rapidly evolving field of pathogen-associated programmed necrosis, VACV could offer a valuable tool to investigate non-canonical pathways and mechanisms for pathogen regulation.

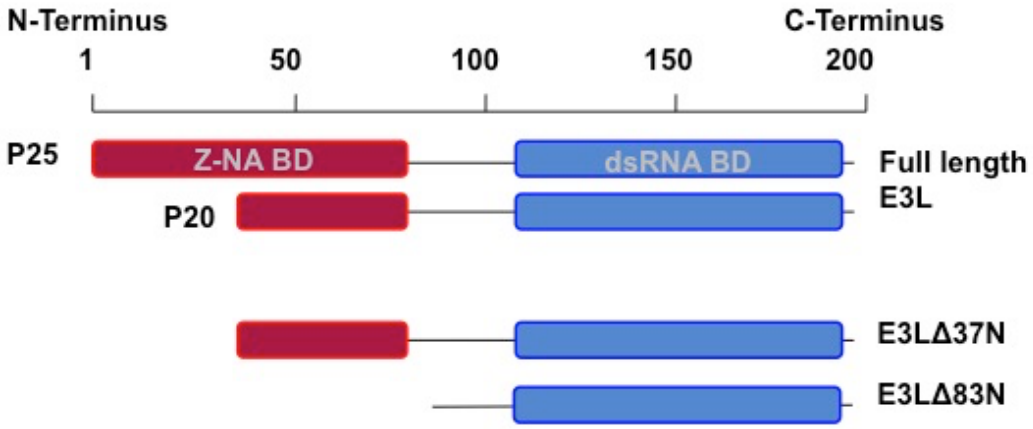

Figure 5. Schematic of E3 N-terminal truncation mutants. The two main forms of E3 that wt VACV generates is depicted with full length E3 at the top followed by the truncated P20 E3 naturally produced during infection. Below the wt versions of E3 are truncation mutants generated by deleting the first 37 (E3LΔ37N) or the first 83 amino acids (E3LΔ83N).

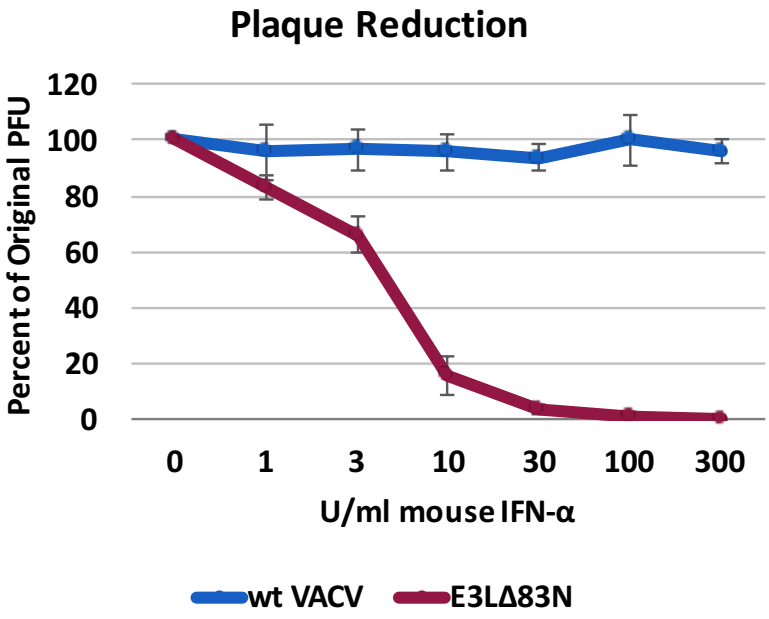

Figure 6. IFN-sensitivity plaque reduction assay. Assay was preformed by pretreating a monolayer of L929 cells with increasing concentrations of mouse IFN-α for 18 hours prior to infection. VACV with wtE3 was IFN resistant but truncation of the E3 N-terminus (VACV-E3LΔ83N) resulted in an IFN-sensitive virus, with a 50% reduction occurring between 3 and 10 units/ml. The percent of original plaque forming units (PFUs) is plotted against the dosage of IFN-α Units (U)/mL utilizing both wt VACV (blue) and mutated VACV producing E3 proteins with truncated N-termini (red).

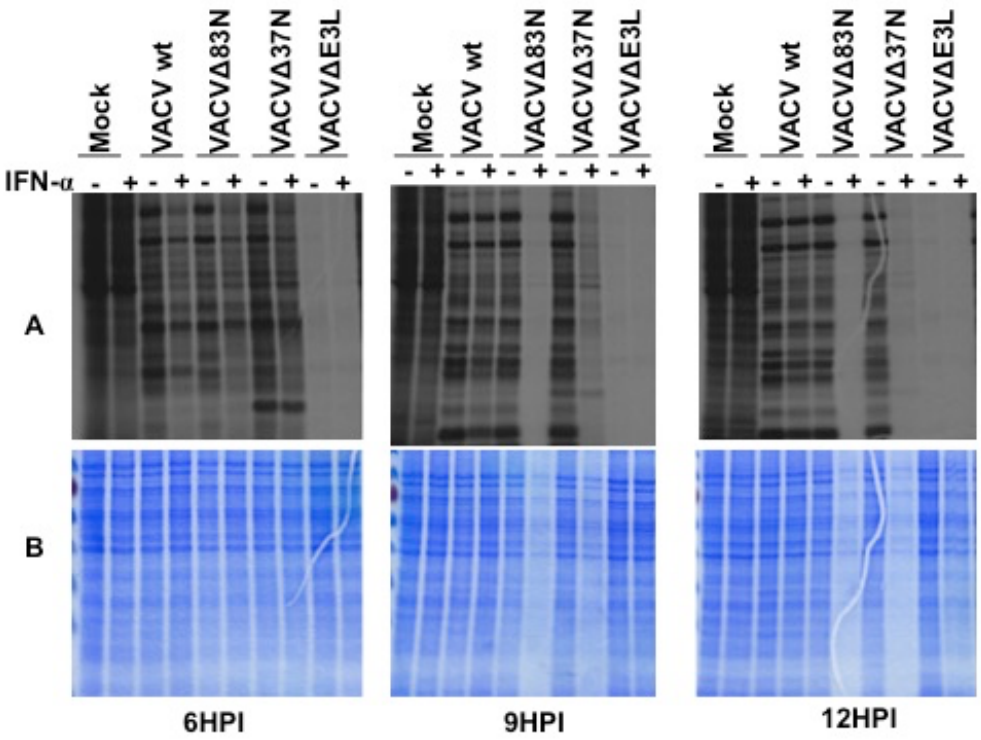

Figure 7. Evaluation of protein synthesis and total cellular proteins L929 cells were pretreated with 100U/ml of mouse IFN-α (based on previously determined inhibitory concentration) for 18 hours prior to infection. Cells were then infected with Mock, wt, and VACV expressing E3L mutants at an MOI of 5. Infected cells were then starved at for 1 hr, pulsed with [^{35}S]methionine for 30 min and then harvested. Proteins from equal cell volumes were separated on 10% SDS-PAGE gels. **(A)** Radiolabeled proteins were analysed by autoradiography; **(B)** Total protein was evaluated by Coomassie blue staining. Samples pretreated with IFN and infected with VACV-E3LΔ83N demonstrated a significant global reduction in protein**.**

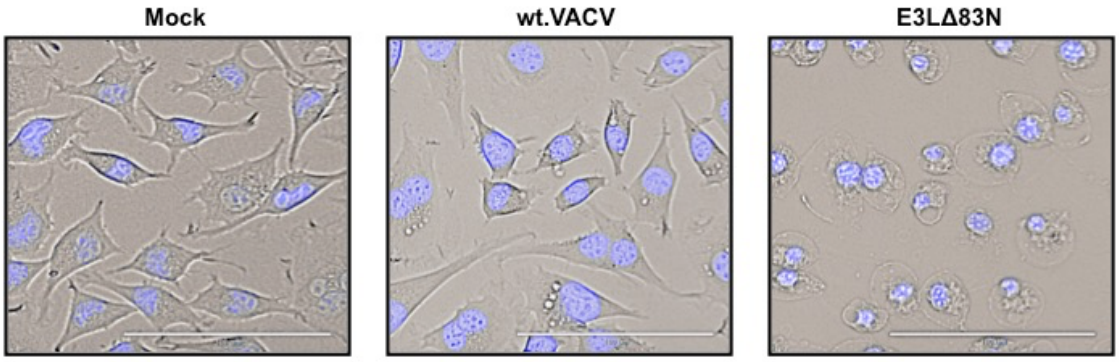

F**igure 8. Morphological changes in L929 cells following infection.** Transmitted live imaging at 6 HPI of L929 cells pretreated with 100U/ml of mouse IFN-α and then infected with an MOI of 5 of mock, wt VACV, or VACV-E3LΔ83N. IFN-treated cells infected with VACV-E3LΔ83N underwent drastic changes in morphology that is atypical for classical cytopathic effect (CPE) or apoptosis.

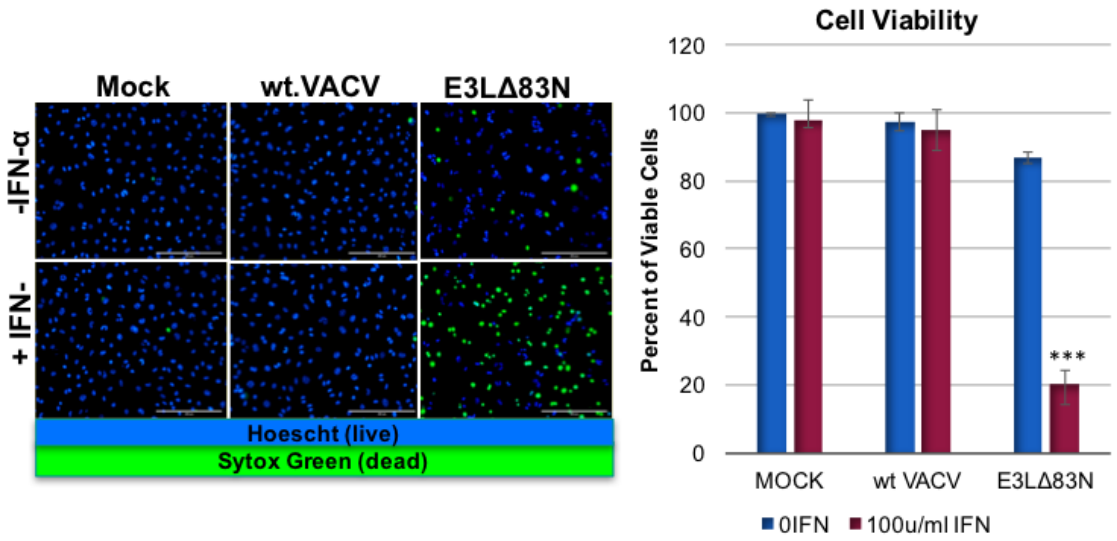

Figure 9. Loss of viability in IFN-sensitive N-terminal truncation mutants: Cell viability was determined using SYTOX© green dye uptake assays utilizing the average viable cells observed in 10 fields 5 HPI . **(A)** Loss of membrane integrity and cell death is indicated by the uptake of both dyes (green). **(B)** The percent of viable cells 5 hpi are compiled from the SYTOX© green dye uptake assays performed. These percentages are plotted for each cell group (wt VACV, VACV-E3LΔ83N, and MOCK) for 0 U/mL IFN-α pretreatments (blue) and 100 U/mL IFN-α pretreatments (red). IFN-sensitive VACV expressing N-terminal E3 mutants undergo a rapid loss of membrane integrity and cellular death.

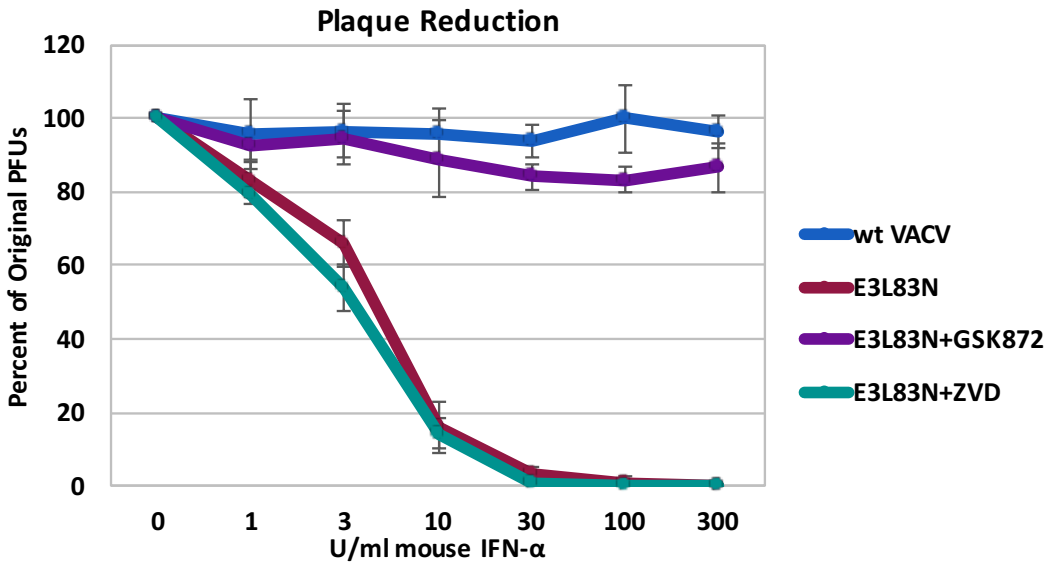

Figure 10. Rescue of plaguing efficiency by inhibiting RIP3. Plaque reduction assay was performed by pretreating L929 cells with increasing amounts of mouse IFN-α for 18 hours prior to infection. Cells were then treated with 100μM of a RIP3 inhibitor (GKS872), or 50μM of a pan-caspase inhibitor (ZVD) or mock-treated (DMSO) for 1 hour prior to infection. Cells were then infected with equivalent PFU of wt VACV or VACV-E3LΔ83N and plaques were allowed to form and the percent of PFU reduction was calculated. IFN resistance was not restored in cells treated with ZVD but was restored by treatment with GKS872.

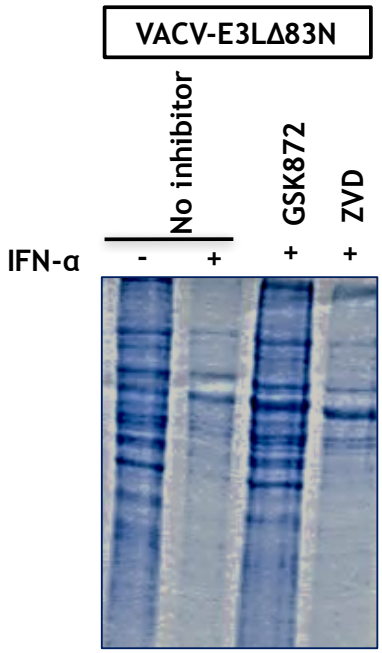

Figure 11. Rescue of global protein loss by inhibiting RIP3. Coomassie blue staining of total protein lysates following pretreatment of L929 cells treated with 100U/ml and infected with control VACV-E3LΔ83N at an MOI of 5. Evaluation for reduction of total protein for untreated control VACV-E3LΔ83N cells, IFN-α-treated VACV-E3LΔ83N-infected cells, IFN-α-treated VACV-E3LΔ83N-infected cells with the addition of GSK872, and IFN-α-treated VACV-E3LΔ83N-infected cells with the addition of ZVD. Lower amounts of Commassie staining correlate to higher global protein loss.

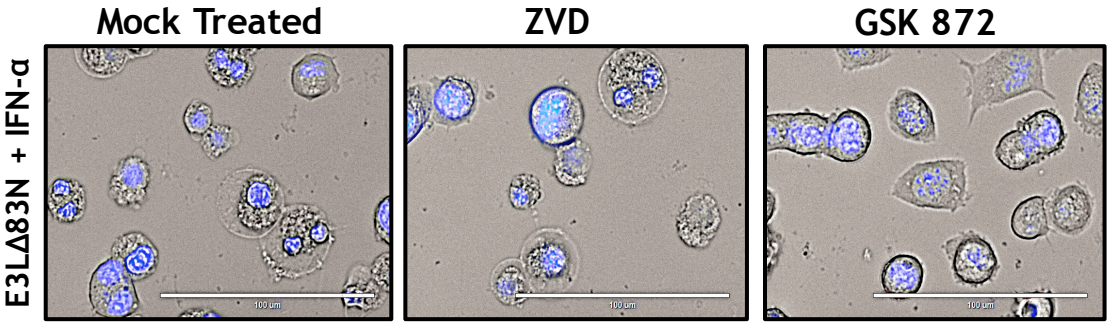

Figure 12. Rescue of morphological changes by inhibiting RIP3. Transmitted live Imaging at 6 HPIof L929 cells pretreated with 100U/ml of mouse IFN-α for 18 hours and for one hour with either mock, ZVD-FMK or GKS872 prior to infection and then infected with VACV-E3LΔ83N at an MOI of 5. Ghost cell morphology is inhibited by the treatment of GKS872 but not ZVD.

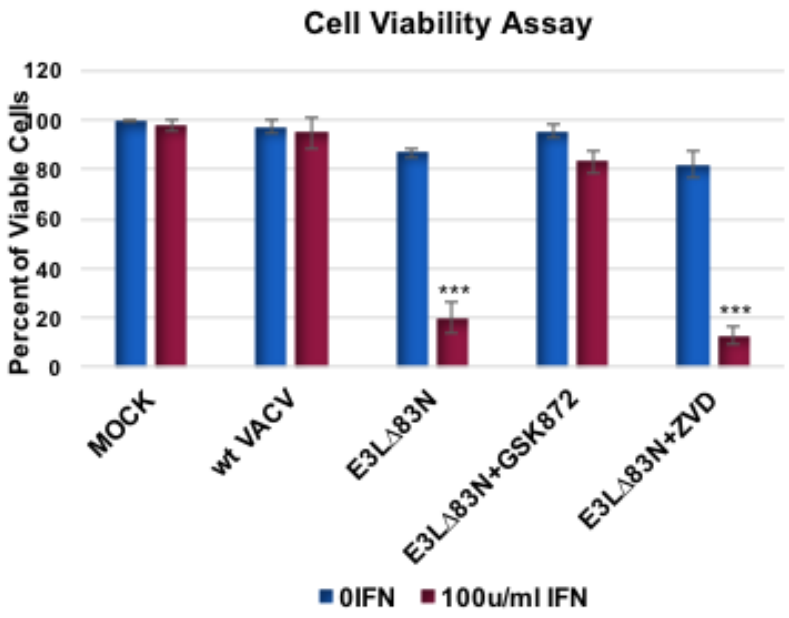

Figure 13. Rescue of cell viability by inhibiting RIP3. The percent of viable cells was evaluated at 5 hpi SYTOX© green dye uptake assay. Values are based on the average of 10 fields of view at 20X magnification. These percentages are plotted for each cell group (MOCK, wt VACV, VACV-E3LΔ83N, VACV-E3LΔ83N+GSK872, and VACV-E3LΔ83N+ZVD) for 0 U/mL IFN-α pretreatments (blue) and 100 U/mL IFN-α pretreatments (red).

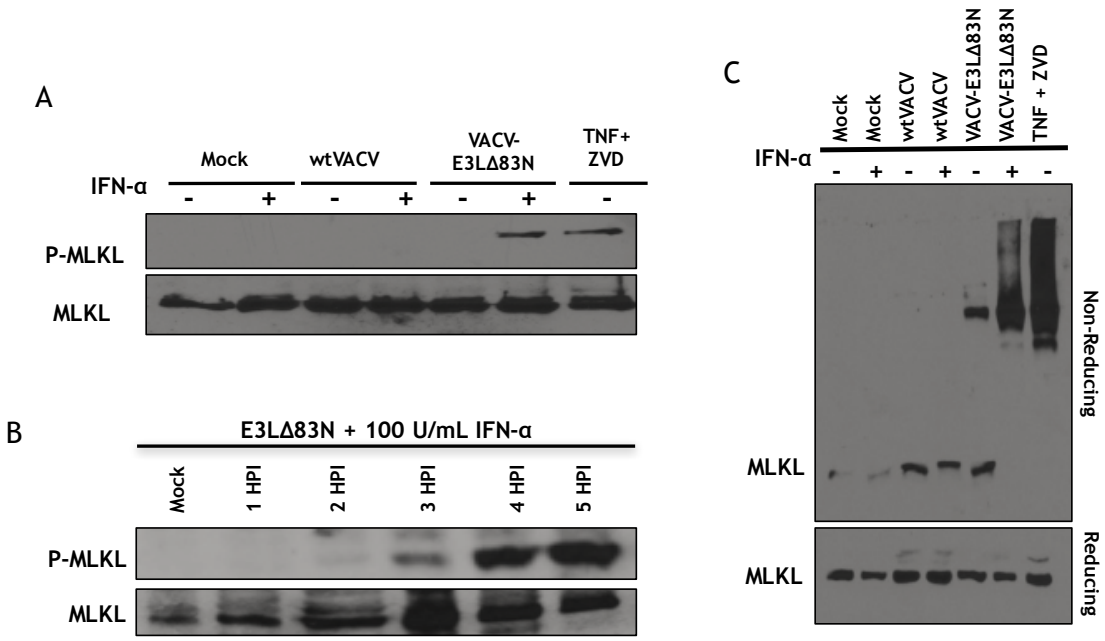

Figure 14. Western blot detection of MLKL phosphorylation. Western blots were performed for the detection of MLKL and its phosphorylation. **(A)** MLKL and phosphorylated MLKL expressions are shown for MOCK, wt VACV, VACV-E3LΔ83N, and TNF positive control samples under both untreated and 100 U/mL IFN-α-treated conditions. Phosphorylation of MLKL is specific to VACV-E3LΔ83N in IFN-α-treated cells. **(B)** The MLKL and phosphorylated MLKL expressions are shown for VACV-E3LΔ83N from 1-5 hours post infection. MLKL activation is observed as early as 3 hpi. **(C)** Aggregated total MLKL expression levels are shown under non-reducing conditions, demonstrating activation by oligomerization as seen by a shift. MLKL aggregation is specific to VACV-E3LΔ83N in IFN-α-treated cells.

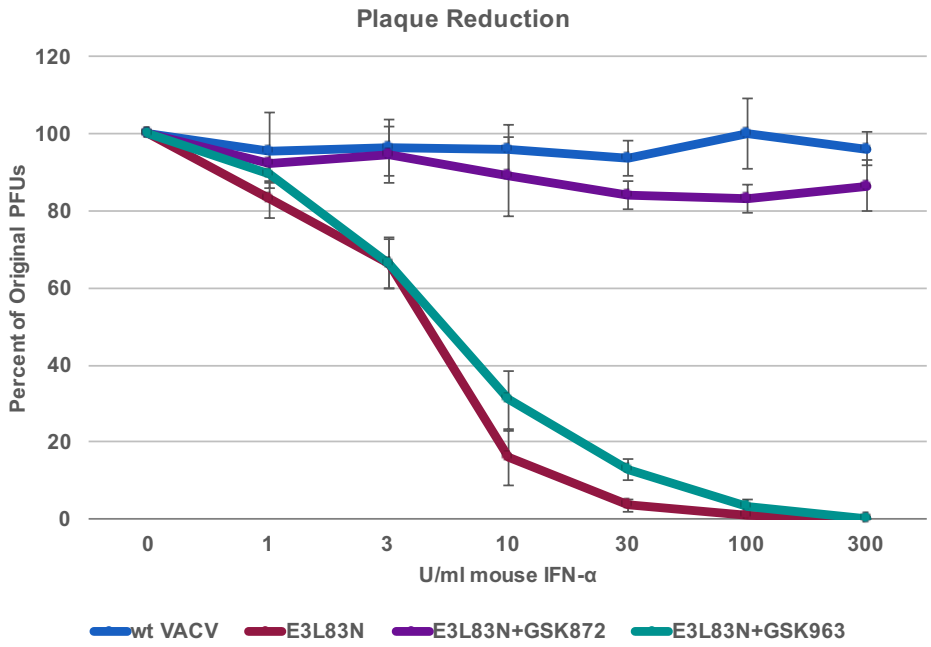

Figure 15. Rescue of plaquing efficiency is rescued by inhibiting RIP3 but not RIP1. The percent of original plaque forming units (PFUs) is plotted against the dosage of IFN-α Units (U)/mL utilizing wt VACV (blue), VACV-E3LΔ83N(red), VACV-E3LΔ83Nwith GSK872 (green), and VACV-E3LΔ83N with GSK963 (purple).

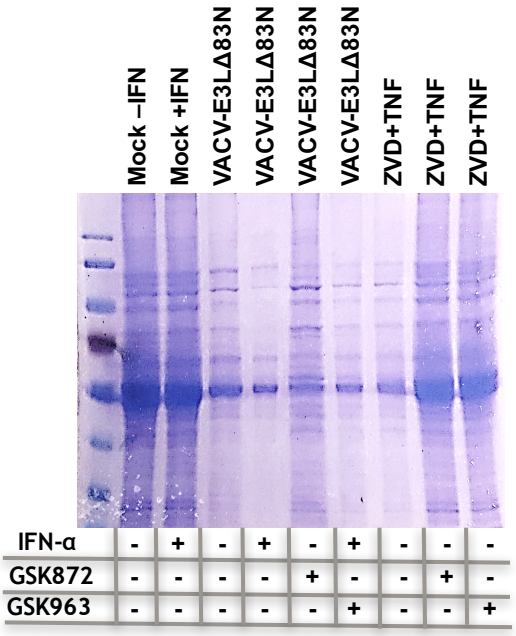

Figure 16. Rescue of total protein loss by inhibition of RIP3 but not RIP1. Cells were either treated with or without IFN and either mock-infected , infected with VACV-E3LΔ83N or were treated with ZVD plus TNFα . For lanes 5 and 8, cells were treated with a RIP3 inhibitor, GSK872, while for lanes 6 and 9, cells were treated with a RIP1 inhibitor, GSK963. Only the RIP3-specific inhibitor prevents protein release in VACV-E3LΔ83N-infected cells, while both inhibitors prevent protein release in cells treated with ZVD and TNFα.

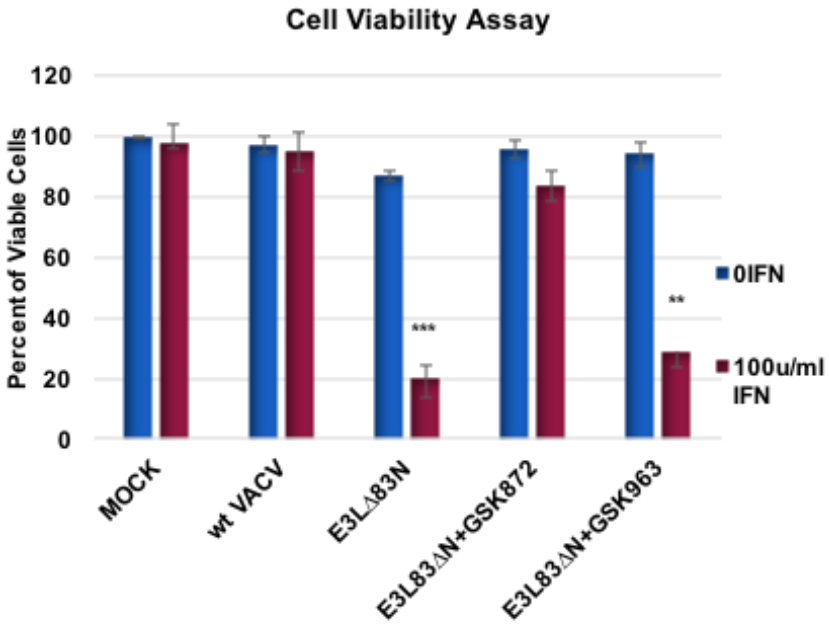

Figure 17. Cell viability rescue by inhibiting RIP3 but not RIP1. The percent of viable cells 5 hours post transfection (make consistent) are compiled from the SYTOX© green dye uptake assays performed. These percentages are plotted for each cell group (MOCK, wt VACV, VACV-E3LΔ83N, VACV-E3LΔ83N+GSK872, and VACV-E3LΔ83N+GSK963) for 0 U/mL IFN-α pretreatments (blue) and 100 U/mL IFN-α pretreatments (red).

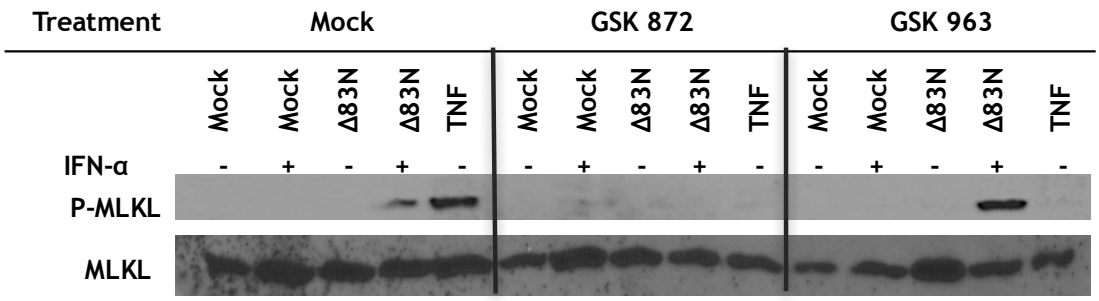

Figure 18. Phosphorylation of MLKL is prevented by inhibiting RIP3. A Western blot was performed to check for MLKL and phosphorylated MLKL expression. The blot was performed for both untreated and IFN-treated MOCK and VACV-E3LΔ83N-infected cells in addition to TNF treated cells with additional MOCK, GSK 872, and GSK 963 treatments.

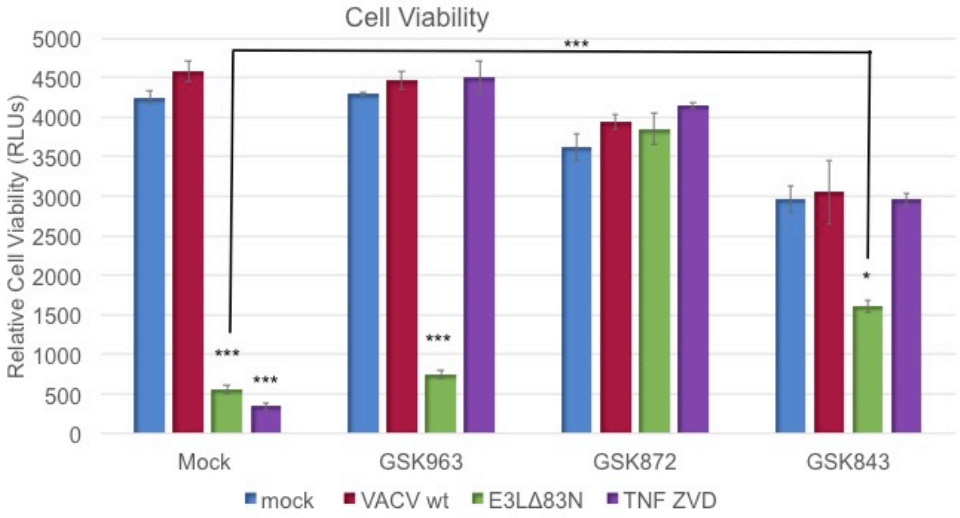

Figure 19. Rescue of cell viability by inhibiting RIP3 but not RIP1. A cell viability assay was performed using a cell titer glow cell viability assay in L929 cells pretreated for 18 hours with IFN-α. Cells were then treated with DMSO (mock), GSK963 (RIP1 inhibitor), GSK872 (RIP3 inhibitor), or GSK843 (RIP3 kinase-specific inhibitor). Cells were infected with mock, wt VACV, VACV-E3LΔ83N, or TNF ZVD (positive control for RIP1-, RIP3-dependent death). Relative cell viability is measured in relative luminescence units (RLUs) at 12 hours post-infection/treatment.

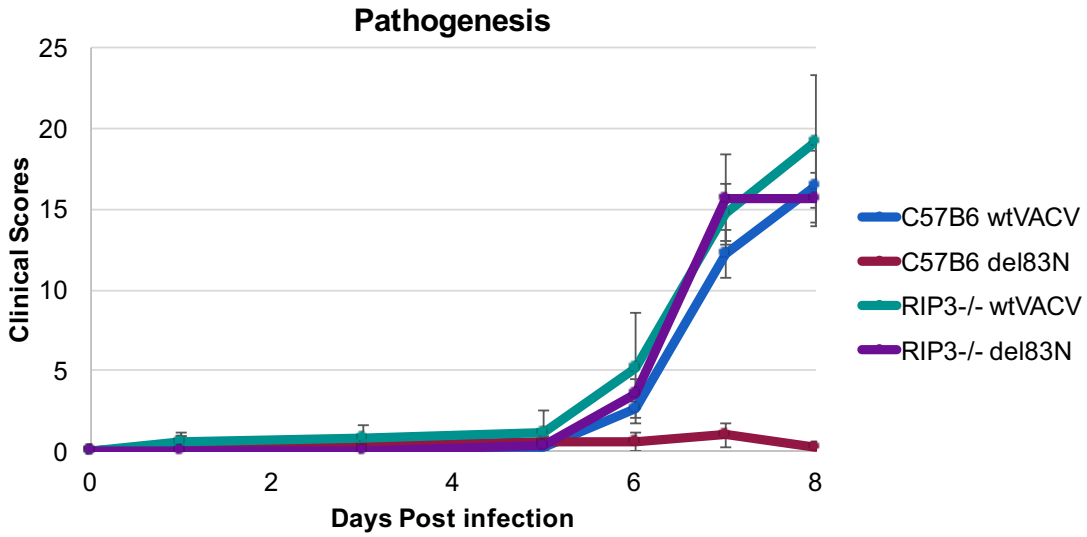

Figure 20. RIP3 deficiency restores pathogenesis of VACV-E3LΔ83N. 8-10-week-old C57BL/6 mice were infected by intranasal route with 10^6 PFU of the indicated viruses. Clinical scores (based on multiple symptoms) indicate that wt VACV is pathogenic in the mice, beginning at 6 days post-infection (DPI) while VACV-E3LΔ83N remains non-pathogenic throughout the experiment. However, in mice with homozygous disruption of the RIP3 gene, the pathogenesis of VACV-E3LΔ83N parallels that of wt VACV.

CHAPTER 3

VACCINIA VIRUS-INDUCED PROGRAMMED NECROSIS IS REGULATED BY Z-NA BINDING PROTEINS

ABSTRACT

The N-terminus of E3 encoded by VACV has been demonstrated to be essential for inhibiting a RIP1-independent programmed necrosis that is regulated by type I interferons. The N-terminus shares homology to the family of Z-DNA binding proteins that includes ADAR-1 and DAI. Prior studies have demonstrated substitution of the N-terminus of E3 with distantly related Z-DNA binding domains fully complements pathogenesis of VACV. Additionally, point mutations that decrease the affinity of Z-DNA binding also correlate to a decrease in VACV pathogenesis in mice. Together, these results suggest that a functional Z-DNA binding domain of E3 is necessary for full pathogenesis. In this study the cytosolic DNA sensor, DAI, is implicated as the adaptor protein for RIP3 activation in programmed necrosis resulting from infections with VACV lacking a functional E3 Z-DNA binding domain. Expression of both RIP3 and DAI are required to induce programmed necrosis *in vitro.* The highly attenuated phenotype of VACV with E3 Z-DNA binding domain mutations is reversed in mice genetically deficient of DAI. Furthermore, induction of programmed necrosis was dependent on the presence of a functional Z-DNA binding domain in DAI and the absence of a functional Z-DNA binding domain in E3. These results grant novel insight into the elusive functions of the E3L Z-DNA-binding domain. Together, they suggest that Z-NA may be recognized as a PAMP by DAI and is sequestered from recognition by the VACV-encoded Z-DNA-binding domain of E3.

INTRODUCTION

In investigating the role the N-terminus of E3 plays in inhibiting an IFN-primed programmed necrosis, indications of its function can be inferred by the homology between E3 and a family of Z-form nucleic acid (Z-NA) binding proteins. Several prior studies have indicated that Z-NA binding plays a role in the induction of the IFN pathway. Both mammalian proteins ADAR1 and DNA-induced activator of interferon (DAI) are regulated by IFN and contain Z-NA-binding domains (Z-NA-BD) (96, 102). In mammalian systems, DAI has been identified as a cytosolic sensor capable of recognizing dsDNA and activates the IFN pathway (108, 121). The Z-NA-BD of E3 is highly conserved among orthopoxviruses, and shares structural homology to a family of Z-DNA-binding proteins, such as IFN-inducible ADAR-1 and DAI (108, 121). However, the presence of Z-NA-BD is not restricted to mammalian cultures. Fish encode PKZ, a PKR-like protein that contains a Z-NA-BD in place of the dsRNA binding domains found in human PKR (122). The PKZ protein has been implicated in host pathogen defense mechanisms. PKZ can be upregulated following immune stimulation resulting in the phosphorylation of eIF2α. Together, these findings suggest that Z-NA binding has a role in the host response to viral infections.

Since the identification of Z-NA-BDs, there has been significant interest in uncovering their role in binding nucleic acids in the left-handed configuration (Z-NA). An even more confounding question is if the presence of Z-NA in a cell contributes to host immune responses to pathogens such as VACV. Recent studies of VACV E3 demonstrated that deletion of the Z-NA-BD results in significant loss of viral

pathogenicity (105). Additionally, site-directed mutagenesis of key Z-NA binding residues that decreased binding affinity for Z-NA corresponded to a decrease in neurovirulance (105). The Z-NA-BD and, more specifically, the regions required for Z-NA binding are essential for virulence.

Further evidence to support the role the N-terminus has as a Z-NA-BD and its significance in pathogenesis was provided by domain-swapping studies where the Z-NA-BD of E3 was replaced with a Z-NA-BD from one of two distantly related Z-DNA binding proteins, ADAR-1 and DAI. Despite having very limited sequence homology outside of amino acid residues that make contact with Z-NA, Z-NA-BD chimeric viruses fully complemented the pathogenesis and retained lethality in intracranial infections (105). Furthermore, point mutations that diminish Z-NA binding in chimeras decrease the pathogenicity of the virus equivalent to the attenuation seen in the Z-NA-BD point mutations in E3 (105).

During viral infections, early detection is essential for initiating an innate immune response and protecting the host organism. Viral nucleic acids recognized as an essential PAMP are also recognized by PRR for the activation of the innate immune response (123). DAI has been demonstrated to act as a cytosolic DNA sensor that can initiate an innate immune response independent of the well-established endosomic DNA sensor, TLR 9 (108, 121). DAI has been shown to recognize foreign DNA and upregulate type I IFN in addition to the initiating other immune responses.

DAI is a multifunctional protein that can be IFN-upregulated or constitutively expressed depending on tissue type. It is composed of 3 nucleic acid-binding domains: a RHIM domain and two additional RHIM-like repeats (28, 117). Consistent with the other

members of the Z-NA-binding protein family, the Z-NA-BDs are located within the N-terminus. DAI contains tandem Z-NA-BDs termed $Z\alpha_{DAI}$ and $Z\beta_{DAI}$. The third nucleic acid binding domain (D3) is located next to the $Z\beta_{DAI}$, and is unique from the first two binding domains; D3 is reported to bind right-handed B-DNA (108). The N-terminal region, including D3, is thought to be essential for sensing multiple forms of DNA. DAI has been shown to be able to bind both Z and synthetic B forms of DNA (108). Binding of DNA activates DAI, inducing the C-terminus to bind to the serine/threonine kinase, Tank binding kinase 1 (TBK1), and the transcription factor, IFN regulatory factor 3 (IRF3) (108). Evidence has established that all three nucleic acid binding domains are essential for full activation of the DNA-dependent immune response (121). Additionally, DAI induction of the innate immune responses may require that DAI dimerizes (121). Interestingly, the Z-NA-BDs of DAI contribute to stress granule localization similarly to that of E3 (124).

DAI belongs to a family of Z-NA-binding proteins that are found in a diverse array of organisms. Some of the best studied examples include the vertebrate ADAR1, the fish protein kinase containing Z-DNA-binding domains (PKZ) and the viral E3 of poxviruses. Biochemically, they can all tightly and specifically bind to Z-DNA. Based on the orientation of the binding residues, many of them also have the capacity to convert B-DNA to Z-DNA (123). Despite a lack of sequence homology, a common binding mode to the left-handed orientation is achieved through a consistent structure paired with a few highly conserved residues that are involved in DNA binding. The conserved positively charged or polar residues confer specificity to the unique zig-zag conformation of the Z-DNA backbone. This conservation of binding residues can be seen with a protein

sequence alignment of the Z-NA-BD of E3 and the $Z\alpha_{mDAI}$. E3 contains seven out of the nine conserved residues necessary for binding to Z-DNA. While there are many water-mediated hydrogen-bonds supporting Z-DNA interactions with the binding pocket, the interactions between tyrosine and the C8 of guanine oriented in a SYN conformation is essential for conferring the specificity to Z-DNA binding (97). The structural homology found within the Z-NA-BD consists of 3 β-strands and 3 α-helices (123). Z-NA-BDs recognize Z-DNA with conformational specificity through the α helix (α3) and the wing, which is made up mostly of an antiparallel β-sheet involving β2 and β3 and a β-loop (123). The $Z\alpha_{DAI}$ is considered a canonical Z-NA-BD and maintains high specificity to Z-DNA. The $Z\beta_{DAI}$ domain has also been shown to bind Z-NA; however, it also has the ability to bind and convert B-DNA to Z-DNA (123).

In Chapter One we demonstrated that the Z-NA-BD located in the N-terminus of E3 is required to inhibit an IFN-regulated programmed necrosis. This form of VACV-induced programmed necrosis occurred in a RIP1-independent fashion in contrast to findings that originally implicated necrotic death as an alternate host defense pathway against VACV (25). In classical programmed necrosis, RIP3 utilizes RIP1 as an adaptor protein to initiate the signal transduction cascade leading to MLKL phosphorylation and subsequent cell death. The formation of the RIP3, RIP1 complex is achieved through the interaction of RHIM domains found on both proteins. Additional RHIM-containing proteins have been implicated to function as adaptor proteins of RIP3 in the induction of non-classical programmed necrosis. DAI, and TIR-domain-containing adapter-inducing interferon β (TRIF) both contain RHIM domains and can interact with RIP3 to initiate programmed necrosis. In particular, DAI has been shown to be a sensor of multiple

members of the herpes virus family infection used in the induction of programmed necrosis (4).

Until the recent discovery that the Z-NA-BD of E3 is required to inhibit an IFN-regulated programmed necrosis, the molecular mechanism by which it conferred IFN resistance was unknown. However, due to the homology between the ZαDAI and the Z-NA-BD of E3, both having the capacity to bind Z-NA, it was hypothesized that E3 may act as a competitive inhibitor of the host-encoded Z-NA binding proteins (23). Additionally, it has been proposed that DNA-mediated oligomerization of DAI contributes to the activation of the innate immune response (5). It is possible that VACV E3 competes with DAI for the binding to Z-NA, thereby preventing activation of the innate immune response or induction of programmed necrosis.

In this chapter we investigate DAI as an alternative adaptor protein of RIP3 in the induction of VACV-induced programmed necrosis. Additionally, we investigate the requirement for a functional Z-NA-BD of both E3 and DAI.

RT-PCR Methods. RNA was isolated from mock or IFN-treated cells at 18 hours post-treatment using Qiagen's Rneasy Mini Kit (74104) with the optional on-column DNase digestion (79254). 500ng of RNA was then reverse transcribed into cDNA using PrimeScript™ RT reagent Kit (Takara, RR037A). Samples were amplified using PrimeTime® Gene Expression Master Mix (IDT, 1055772) on a CFX Connect™ Real-Time PCR Detection System (BioRad, 1855201). Predesigned primer sets were purchased from IDT; order numbers are as follows: DAI (Mm.PT.58.21951435), RIP1 (Mm.Pt.58.9721411), RIP3 (Mm.PT.58.33227794), MLKL (Mm.PT.58.16870825), GAPDH (Mm.PT.39a.1). Fold induction of genes was determined using the ΔΔCq method with GAPDH as the control gene and untreated cells as mock.

Immunoblotting: Protein extraction and Western immunoblot analysis. L929 cells were pretreated with 100 U/mL of mouse IFN-α (Calbiochem) for 18 hours. If indicated as infected, cells were infected with viruses at an MOI of 5. L929 infected cells were harvested at 4 HPI. Cells were scraped into medium and subsequently pelleted by centrifugation at 500 × g for 10 min at 4°C to extract lysates. The supernatant was removed, and the cells were washed, pelleted, and washed a second time with ice-cold PBS. Cells lysates were then obtained by lysing the cells in complete Triton X lysis buffer (20 mM Tris-HCl, pH 7.4, 150 mM NaCl, 1 mM Na2EDTA, 1 mM EGTA, 1% Triton X-100, 2.5 mM sodium pyrophosphate, 1 mM β-glycerophosphate, 1 mM Na3VO4, and 1X Halt Protease and Phosphotase Inhibitor Cocktail, Pierce Thermo Scientific) and incubated on ice for 5 min. Samples were centrifuged at 15,000 × g for 20

min at 4°C. Supernatant was collected and SDS protein loading dye (3X) was added. All samples were stored at -80°C. Samples were boiled for 5 min, separated on a denaturing 10% SDS-PAGE gel, and then transferred onto a nitrocellulose membrane at 100 volts for 60 min in 10 mM CAPS, pH 11 with 20% methanol. Following transfer, the membrane was incubated in blocking buffer (140 mM NaCl, 3 mM KCl, 20 mM Tris [pH 7.8], 0.05% Tween 20, 3% nonfat milk) for 1 hour at room temperature. Rabbit polyclonal antibodies were used to detect P-MLKL (Abcam, 1:2000) and total MLKL (Abcam, 1:1000), Z DNA binding protein 1(DAI) (Abcam, 1:1000), RIP3 (Abcam, 1:2000), RIP1 (BD, 1:1000) and mouse monoclonal antibodies were used to detect glyceraldehyde-3-phosphate dehydrogenase (GAPDH). Primary antibodies were diluted in blocking buffer and blots were exposed to antibodies overnight at ratios specified. Secondary goat anti-rabbit IgG conjugated to horseradish peroxidase (1:10,000, Santa Cruz) or anti-mouse IgG conjugated to horseradish peroxidase (1:10,000, Santa Cruz) were incubated at room temperature for 1 hour. Immunoreactive bands were visualized by chemiluminescent development using SuperSignal West Dura Duration substrate (Pierce Biotechnology).

Cells and viruses and Treatments. L929 cells were maintained in minimum essential medium (MEM) supplemented with 5% fetal bovine serum (FBS, HyClone) and not allowed to exceed 7 passages. L929 cells were treated with indicated concentrations of mouse IFN-α (Calbiochem) for 18 h prior to infection. HEK293T cells were maintained in Dulbecco's modified minimum essential medium (D-MEM) supplemented with 10% HI FBS. Cells used as a positive control for programmed necrosis were treated with TNF-α (Sigma) (L929: mouse TNF-α at 20ng/ml; HEK293T: human TNF-α at

50ng/ml) following a 1-hour pretreatment with 100μM of ZVD (ApexBio).Viruses were previously generated using the WR strain of VACV by methods previously described (81). E3 N-terminal mutations include an N-terminal truncation (VACV-E3LΔ83N). Point mutation viruses include a loss of Z-NA binding mutant (VACV-E3L-P63A) and a negative control (VACV-E3L-E42A) that retains the Z-NA binding capacity. Chimeric viruses were generated as previously described by replacing the Z-NA-BD of E3 (Nucleotides 61-261, representing amino acids 1 to 67 of the vaccinia virus E3L gene product (S64006) with either the Zα domain of DAI (VACV-E3L-ZαmDAI, nucleotides 116-316 of AF136520) or ADAR1 (VACV-E3L-ZαhADAR1, nucleotides 554-742 of U10439). All virus stocks were grown in BHK cells. Crude virus stocks were purified by pelleting through a 36% sucrose pad and confirmed by sequencing.

Expression of DAI and RIP3 in HEK 293T . The human RIP3 and DAI or mutant versions of the proteins were expressed from plasmid expression systems in HEK 293T cells that inherently lack both proteins. The following plasmids were generously donated by Ed Mocarski (Emory University) and Jason Upton (University of Texas): p3XFLAG-CMV-10 (empty vector), p3XFLAG-CMV-10 (Hs) WT RIP3, p3XFLAG-CMV-10 (Hs), wt DAI, p3XFLAG-CMV-10, MutRHIM-A (Hs,DAI(I206QIG209→A206AAA209))(Sac2), p3XFLAG-CMV-10 DAI ΔZα(Hs DAI(78-429), p3XFLAG-CMV-10 DAI ΔZαβ (Hs DAI(170-449)), p3XFLAG-CMV-10 mutZα (Hs DAI N46D/Y50A) (BcII), p3XFLAG-CMV-10 mutZβ (Hs DAI N141D/Y145A) (Mscl). Plasmids were constructed using p3XFLAG-CMV-10 with cut sites of BgIII and Xbal. Sequences were confirmed using the N-CMV-30 primer (5'-AAT-GTC-GTA-ATA-ACC-CCG-CCC-CGT-TGA-CGC-3') and C-CMV-24 (5'-

TAT-TAG-GAC-AAG-GCT-GGT-GGG-CAC-3'). Plasmids were transformed into One Shot® TOP 10 chemically competent E. coli (Invitrogen) according to manufacturer's instructions and incubated on ampicillin-LB agar plates at 37^{o}C overnight. Transformed bacteria were cultured in Terrific Broth (TB) containing ampicillin. Plasmids were isolated using a Maxi Prep Kit (Qiagen). Plasmids were transfected into HEK 293T cells using X-treme GENE™ HP DNA Transfection Reagent (Sigma) according to manufacturer's instructions. At 48 hours post transfection, if indicated, the cells were treated as described below and infected at an MOI of 5 with the indicatedvirus.

Mouse Intranasal Infections of Mice. Anesthesia and infections were carried out as previously described (81). Briefly, wt C57B6 and mice genetically deficient of DAI (ZBP-1 -/-) mice were anesthetized with a ketamine cocktail containing 37.5 mg/ml ketamine (Lloyd Laboratories, Shenandoah, IA), 7.5 mg/ml xylazine (Vedco, St. Joseph, MO), and 2.5 mg/ml acepromazine maleate (Fort Dodge Laboratories, Fort Dodge, IA) at the age of 8 to 10 weeks. Intraperitoneal injection (IP) of anesthesia was given at a dose of 1 µl per gram of body weight. Anesthetized mice were infected with 5 µl containing 10^6 PFU of either WR strain of wt VACV or VACV-E3LΔ83N virus intranasally. Mice were monitored daily for clinical signs and given a clinical score based on weight loss, lethargy, respiratory distress, decline in general appearance (scruffed), and eye infections. Each clinical sign was given a score of 1 to 5 with 5 representing sever symptomology. Weight loss score was determined by the percent of their original weigh with 100% of original weight receiving a score of 0; 93.7 to 99.9% given a score of 1; 86.2 to 93.2% given a score of 2; 78.6 to 86.1% given a score of 3; 71.0 to 78.5% given a score of 4; and 70% and below was given a score of 5 (81, 111). All mice were euthanized by

asphyxiation using CO2 when any mouse dropped below 30% of their initial weight or reached a clinical score above 25. **Generation of DAI point mutant**. Generation of point mutations were constructed by whole plasmid PCR mutagenesis using overlapping primers as previously described (92). Briefly, 100ng p3XFLAG-CMV-10 (Hs) WT DAI was then used as a DNA template in whole plasmid PCR. 500 μM hDAI ZαP63A F primer (5'- GTCTCCCTCACATCCGCAGCCACCTGGTGCTT -3'), 500 μM hDAI ZαP63A R primer (5' -AAGCACCAGGTGGCTGCGGATGTGAGGGAGAC-3'), 500 μM dNTPs, 2 mM $MgSO_4$, 1X Pfx buffer, 1X Enhancer and *Platinum pfx* polymerase enzyme (Invitrogen) were mixed in a 25 μL reaction volume. PCR amplifications were performed with 95ºC for 3 minutes, followed by 18 cycles of amplification (95ºC for 15 seconds, 52ºC for 1 minute, 72ºC for 12 minutes). Primers were designed to generate p3XFLAG-CMV-10 hDAI ZαP63A containing a site specific point mutation in the DAI Zα domain of the Z-NA binding residue corresponding to the point mutation found in VACV E3L-P63A. Samples were subject to restriction digests overnight at 37 ºC by DPN1 using Cutsmart buffer (NEB) and DPN1 (NEB). Following digest, sample was ethanol precipitated with 2.5 volumes of 95% ethanol, 0.1 volume of 7.5M ammonium acetate, and 10μL glycogen (Fermentas). The DNA was washed in 70% ethanol, dried and resuspended in 10μL of distilled water. One Shot® TOP 10 chemically competent E. coli (Invitrogen) cells were transformed with p3XFLAG-CMV-10 hDAI ZαP63A according to manufacturer's instructions and incubated on ampicillin-LB agar plates at 37^oC overnight. Isolated colonies were selected; plasmid DNA was extracted using the PureYield TM Plasmid MiniPrep System (Promega) and the DNA was resuspended in 50 μL nuclease free water (Invitrogen). Mutation was confirmed by sequencing.

Interferon resistance evaluation by plaque reduction. 6-well plates of subconfluent L929 cell monolayers were treated with 0-300 U/mL of mouse IFN-α (Calbiochem) 18 hours prior to infection. Cells were then infected with approximately 100 PFU of the indicated virus diluted in MEM containing 2% FBS in a volume of 100 µL. Cells were incubated at 37°C, 5% CO_2 for 1 hour, with rocking every 10 minutes. After 1 hour, cells were overlaid with of MEM containing 5% FBS, and incubated at 37ºC. Following the formation of plaques, approximately 48-72 hpi, the monolayers were stained with crystal violet (0.5 % in 20% ethanol) and plaques were counted. The reduction in the number of plaques was recorded as a percentage of plaques in the absence of interferon and was plotted against increasing units of interferon.

SYTOX® nuclear stain uptake viability assay. L929 cells were plated in 12-well CytoOne tissue culture treated plates (USA Scientific) at a confluency of 35% and pretreated with 100 U/mL of mouse IFN-α (Calbiochem) for 18 hours prior to infection. Cells were incubated with Hoechst 33342 dye for 15 minutes prior to infection. If indicated, cells were pretreated for 1 hour prior to infection and subsequently infected with an MOI of 5 with the indicated virus. At 5 , SYTOX® Green nucleic acid stain (Thermo Fisher Scientific) was added to the medium at a concentration of 1 µM and allowed to incubate for 15 minutes. Percent of viable cells was determined by calculating the average number of cells that were double-stained for Hoechst and SYTOX compared to the total number of cells present in each field. The average viability was calculated from a total of 10 fields using a 20X objective of 20X on an EVOS™ FL Auto Imaging System (Invitrogen™).

***CellTiter-Glo*® Luminescent Cell Viability Assay (Promega).** HEK293T cells were plated in a 96-well plate and transfected and treated as described above. Cells were infected with the indicated virus as described above at an MOI of 5. At 12 HPI, *CellTiter-Glo* reagent was according to manufacture's recommendations and incubated at room temperature for 30 minutes. Results were read on a GloMax® 96 Microplate Luminometer (Promega) as relative luminesce units (RLU).

Protein staining. 50% confluent L929 cell monolayers in 60 mm dishes were infected with WR strains of wt VACV or with VACV expressing the indicated E3 N-terminal mutants at a MOI of 5. At 12 HPI, cells were washed twice with pre-warmed PBS, then pelleted and lysed in 100 μL of 1X SDS (62.5 mM Tris-Cl, 10% glycerol, 2% SDS, 0.0005% bromophenol blue, 0.1% 2-mercaptoethanol, 1X Halt Protease and Phosphotase Inhibitor Cocktail, Pierce Thermo Scientific). Protein lysates were isolated utilizing QIA Shredder columns (Qiagen) by spinning lysates in columns at 16,000xg for 2 minutes at 4^{o}C. Samples were stored at -80°C. The samples were boiled for 5 minutes and separated on denaturing 10% SDS-PAGE gels. The gels were stained for total protein levels with Coomassie staining solution (0.1% Coomassie Brilliant Blue R-250, 40% methanol and 10% glacial acetic acid) for 30 minutes, then were destained with destaining solution (40% methanol and 10% glacial acetic acid) three times, each 20 minutes, and incubated overnight in 10% glacial acetic acid to remove any residual stain.

Sequencing of the E3L recombinant virus mutants. Virus DNA was extracted by treating an aliquot of the virus stock with a 1:1 ratio of virus and phenol equilibrated with 10 mM Tris HCl, pH 8.0, 1 mM EDTA (Sigma). Subsequently the aqueous phase of

the sample was re-extracted with equal volumes of phenol:isoamylalcohol:chloroform (25:24:1) (Sigma). The aqueous phase from the above step was re-extracted once again with an equal volume of chloroform:isoamylalcohol (24:1) (Sigma), followed by precipitation as described above.

Gene amplification was preformed using PCR with E3L flanking primers to amplify the gene for sequencing. Briefly, 100 ng of virus DNA template, 500 μM of E3L F, 500 μM of E3L R, 500 μM dNTPs, 2 mM $MgSO_4$, 1X Pfx buffer, 1X Enhancer and *Platinum pfx* polymerase enzyme (Invitrogen) were mixed in a 50 μL reaction volume. PCR amplifications were performed with 95ºC for 5 minutes, followed by 30 cycles of amplification (95ºC for 1 minute, 55ºC for 1 minute, 68ºC for 5 minutes). PCR product was separated by agarose gel electrophoresis (0.8%, GTG grade). DNA was extracted from the gel using Wizard® SV Gel and PCR Clean up Kit (Promega) according to the manufacturer's instructions, and sequenced.

Statistics. Statistical analysis was done by using a two-tailed, unpaired T test. *P* values of $p<0.001$ were represented as ***, $p<0.01$ were represented as **, $p<0.05$ were represented as * and no significance (N.S.) was used to represent $p>0.05$

RESULTS

DAI is upregulated in L929 cells following IFN-α treatment. The IFN-α-sensitive phenotype of VACV-E3LΔ83N in L929 cells is due to the induction of programmed necrosis. Under these conditions, programmed necrosis occurs independently of RIP1. RIP1 functions as the adaptor protein for RIP3 activation in the classical programmed necrosis pathway; but because we had determined that RIP1 is not involved in the induction of death in this system, we sought to identify the adaptor protein being utilized in its place. Several other RHIM-containing proteins have been shown to interact with RIP3 to induce programmed necrosis. Upon review of other known RIP3 adaptor proteins, DAI emerged as a potential candidate because it contains a homologous Z-NA-BD to the one deleted in VACV-E3LΔ83N. Induction of programmed necrosis in L929 cells by VACV-E3LΔ83N requires the treatment of IFN-α. Therefore, we decided to evaluate if DAI expression was induced following IFN-α treatment. In addition to DAI, other important proteins in the programmed necrosis signaling pathway were examined including RIP1, RIP3, and MLKL. Alterations in transcript levels were evaluated by qPCR normalized to GAPDH. No significant changes of transcript levels were observed in RIP1, RIP3, or MLKL following IFN-α treatment. Treatment of L929 cells with IFN-α resulted in a significant induction of DAI with greater than a 3-log induction (Fig21A). Protein levels of RIP1, RIP3, MLKL, and DAI were also evaluated for changes corresponding to IFN-α treatment of L929 cells by Western blotting. An increase in the

protein level of DAI was observed in IFN-α-treated L929 cells (Fig. 21B). No substantial changes were noted in the other three proteins that were evaluated.

DAI is required for the induction of programmed necrosis by VACV-E3LΔ83N. Expression of DAI was demonstrated to be significantly increased in L929 cells following IFN-α treatment. Due to the diversity of ISGs we wanted to determine if DAI expression, in the absence of IFN stimulation, was sufficient to induce susceptibility to programmed necrosis in cells infected with VACVE3LΔ83N. HEK293T cells express RIP1 but are deficient in both RIP3 and DAI. Utilizing a plasmid expression system, we induced the expression of either RIP3 alone or in combinations with DAI in HEK293T cells. Following transfections, cells were either treated with TNF-α and a caspase inhibitor(ZVD) or infected with wt VACV or VACVE3LΔ83N. In the presence ZVD, TNF-α activates the classical programmed necrosis signaling cascade involving RIP1 and RIP3. Expression of RIP3 was sufficient to sensitize the HEK293T cells to programmed necrosis following treatment with TNF-α and ZVD. Expression of RIP3 alone was not sufficient to sensitize the cells to VACVE3LΔ83N induced death. The expression of both RIP3 and DAI was required for the induction of programmed necrosis in VACVE3LΔ83N infected cells(Fig. 22). Wt VACV was unable to induce death in any condition tested. This implicated DAI as the adaptor protein for RIP3 in programmed necrosis induced by VACVE3LΔ83N.

Deficiency of DAI(ZBP1-/-) rescues pathogenesis of VACV E3LΔ83N in mice. The initial indication that the N-terminus of E3L is essential and conferred IFN resistance was demonstrated by a 3 log reduction in pathogenesis in mice. VACVE3LΔ83N is

apathogenic in wt C57BL/6 mice but has equivalent pathogenesis to wt VACV in IFNRα/β-/- mice. Evidence thus far suggests that the IFN sensitive phenotype of VACVE3LΔ83N is due to the induction of an IFN primed programmed necrosis. We have shown that in the absence of RIP3 VACVE3LΔ83N is as pathogenic as wt VACV implicating programmed necrosis as a host defense mechanism in VACVE3LΔ83N infections. In order to further evaluate DAI as the candidate adaptor protein required for RIP3 activation we conducted an *in vivo* pathogenesis study. IN infections were done in C57BL/6 and mice genetically deficient for DAI(ZBP1-/-) mice with VACVE3LΔ83N or wt VACV. As expected VACVE3LΔ83N was highly attenuated in C57BL/6 mice. VACVE3LΔ83N pathogenesis was restored in in ZBP1-/- mice(Fig.23).

The Zα domain of DAI is required for the induction of programmed necrosis by VACV E3LΔ83N. The presence of homologous Z-NA-BD found both in the full length E3L and in DAI lead to the hypothesis that the Z-NA-BD found in the N-terminus my function to bind to and sequester a PAMP form being sensed by the Z-NA-BD($Z\alpha_{DAI}$) of DAI. However, DAI is a multidimensional protein with numerous interaction domains. The $Z\alpha_{DAI}$ domain of DAI shares the greatest homology to the E3L Z-NA-BD and is specific for binding left handed DNA(102, 123). The $Z\beta_{DAI}$ is also able to bind Z-NA but with less specificity as it is also known to bind right handed(B-DNA). The D domain binds B-DNA exclusively. Lastly DAI contains three RHIM domains in the C-terminus with RHIM-A predicted to be the most important for the induction of programmed necrosis through its interaction with RIP3(125). Therefore we wanted to evaluate which binding domain was utilized in VACVE3LΔ83N induced programmed necrosis. In order

to accomplish this, we once again utilized an expression system in HEK293T cells with plasmids containing domain specific mutations. Cells were transfected with RIP3 and DAI mutants and then infected with VACVE3LΔ83N. Any cells expressing mutations in the $Z\alpha_{DAI}$ were resistant to VACVE3LΔ83N induced death. Expression of mutations $Z\beta_{DAI}$ were susceptible to VACVE3LΔ83N induced death(Fig.24). Additionally it was shown that VACVE3LΔ83N induced death was dependent on a functional RIP3 RHIM and the RHIM-A of DAI(Fig24). This RHIM dependent pattern is consistent with the previous studies of herpesvirus family induced programmed necrosis. Together these results indicate that functional RHIM domains in both RIP3 and DAI and the $Z\alpha_{DAI}$ are required for VACVE3LΔ83N induced programmed necrosis.

IFN-α sensitivity and programmed necrosis is due to the loss of Z-NA binding domain function in E3L. Programmed necrosis in VACV infections appears to be competitively regulated by two distantly related proteins that both encode a Z-NA-BD in their N-terminus. Our data suggest that the Z-NA-BD of E3L is required to suppress programmed necrosis while the $Z\alpha_{DAI}$ is necessary for its induction. Although both Z-NA-BD are structurally similar, very little sequence homology is present. The exception to the absence of sequence homology is the presence of a few highly conserved residues. The conserved residues found in both Z-NA-BD are responsible and necessary for conferring binding specificity to Z-NA(105). Our data thus far suggests that a competitive regulation of VACV induced programmed necrosis between the $Z\alpha_{DAI}$ and the E3L Z-NA-BD. We therefore hypothesize that the regulation of VACV induced programmed necrosis maps to the conserved Z-NA binding residues. In order to evaluate

VACV E3L mutants were generated containing site specific point mutations. VACVE3L-P63A contains a point mutation required for Z-NA binding and is therefore a loss of function mutant. VACV E3L-E42A was generated as a control point mutant. In VACVE3L-E42A the mutated residue is located outside of the binding pocket and does not make contact with Z-NA therefore it retains its binding function. We sought to evaluate if a disruption in Z-NA binding is responsible for the original phenotypes observed in VACVE3LΔ83N induced programmed necrosis. In order to evaluate this L929 cells were pretreated with IFN-α to induce the expression of DAI and infected with the VACV E3L point mutates. The loss of Z-NA binding function point mutant had phenotypes consistent with a full truncation of the E3L N-terminus. In L929 cells pretreated with IFN-α, the loss of function point mutant resulted in a dose dependent reduction of plaquing efficiency (Fig26), cytoplasmic enlargement and membrane blebbing(Fig.27), global protein loss(Fig. 28), reduction in viability(Fig29) and phosphorylation of MLKL(Fig. 30). The control point mutant that retained the Z-NA binding mirrored the phenotype of wt VACV. Together these findings indicate that the IFN-α primed programmed necrosis in VACV infections is due to the loss of the ability to bind to Z-NA.

Z-NA-BD chimeric viruses rescue IFN sensitivity and prevent programmed necrosis. Domain swapping experiments were conducted to confirm that the IFN-α primed programmed necrosis induced by VACV mutants corresponds to Z-NA binding function. Chimera viruses were generated by exchanging the Z-NA-BD of E3L with the Zα domains of two distantly related Z-NA binding proteins including the human ADAR1(VACVE3L-$Z\alpha_{hADAR1}$) and mouse DAI(VACVE3L-$Z\alpha_{mDAI}$). Z-NA-BD

swapping fully compensated for the Z-NA-BD of E3L and was able to inhibit the induction of programmed necrosis equivalent to wt VACV. Chimeric viruses retained their plaquing efficiency indicating IFN-α resistance (Fig31). There was no significant loss of viability at early times post infection(Fig32). Finally, chimera viruses did not induce MLKL phosphorylation in IFN-α treated L929 cells(Fig33). Once again this data suggest that the capacity to bind to Z-NA is required to inhibit the IFN-α primed programmed necrosis in VACV infected cells.

DISCUSSION

In this study we investigated the role of the Z-NA-BD of E3L in regulating an IFN-primed programmed necrosis. Our previous work demonstrated that VACV encoding for a E3L protein lacking the Z-NA-BD(VACV E3LΔ83N) was highly attenuated as a result of a rapid induction of a RIP3-dependent programmed necrotic death following infection in IFN-treated cells. However, this death occurred independently of RIP1, which is required as the adaptor protein in the classical necroptosis pathway. To gain insight into both the function of the E3 Z-NA-BD and the alternative pathway used in VACV-induced programmed necrosis we turned our attention back to the highly conserved Z-NA-BD motif.

E3 is an essential innate immune evasion protein that confers IFN resistance. While the C-terminus has been well characterized in its role of binding and sequestering dsRNA, the function of the conserved N-terminus has remained elusive. The N-terminal half of E3 is a member of the Zα family of Z-NA binding proteins (106). Other members of this family include the Zα domains of ADAR1 (96) and DAI (93). These three Z-NA-BDs have a conserved structure consisting of a helix-turn-helix motif with an additional β-sheet. The structures of $Z\alpha_{ADAR1,}$ $Z\alpha_{DAI}$ and Z-NA-BD of E3 are very similar; however, the amino acid sequence is not conserved outside of the residues that make contact with Z-NA (105). Seven of the nine residues found in the other members of this family that are involved in the interaction with Z-DNA are conserved in the N-terminus of E3 (105).

The functional and structural homology between the Z-NA-BD of E3 and the Zα domain of DAI led us to investigate the possibility of DAI as an alternative RIP3 adaptor protein in VACV-induced programmed necrosis. DAI has previously been demonstrated to initiate a RIP1-independent programmed necrosis in several herpesvirus infections. In these herpesvirus models of programmed necrosis, DAI utilizes its C-terminal RHIM domain to interact and activate RIP3, thereby inducing the signal cascade leading to death (29, 46).

Induction of programmed necrosis in VACV lacking a Z-NA-BD in the E3 protein was dependent on IFN stimulations prior to infection. The requirement for IFN stimulation signifies that the mechanisms involved with the induction of death utilizes an ISG. Therefore, we sought to determine if our primary candidate, DAI, was upregulated in response to IFN stimulation in L929 cells. Our results demonstrated that DAI is upregulated in L292 cells (Fig. 21). Furthermore, we demonstrated that ectopic expression of RIP3 and DAI was sufficient to evoke susceptibility to VACV-E3LΔ83N-induced programmed necrosis in the absence of IFN stimulation (Fig. 22).

Confirmation of the significant role that DAI plays in the highly attenuated and IFN-sensitive phenotype of VACV-E3LΔ83N was further established by pathogenesis studies. IN infections demonstrated that VACV-E3LΔ83N is apathogenic in mice expressing DAI in contrast to the highly pathogenic wt VACV. However, pathogenesis was fully restored in mice genetically deficient in DAI (Fig.23) and mirrored the rescue of pathogenesis seen in RIP3-/- mice previously shown in chapter 1 (Fig. 20). Together this data implicated DAI as the RIP3 adaptor protein used in VACV-E3LΔ83N induced programmed necrosis.

The requirement of DAI in programmed necrosis induced by VACV lacking a Z-NA-BD was highly suggestive that the Z-NA binding may have a significant biological role in the viral host interaction. Because DAI and the Z-NA-BD of E3 are both members of the Zα family of Z-NA-binding proteins, our investigation turned to evaluating the role that Z-NA-binding ability plays in the induction of programmed necrosis. While DAI is a member of the Zα family, it also consists of multiple domains that are not involved with the Z-NA-binding function. Therefore, we wanted to determine if the domains specific to Z-NA binding in DAI were required for its role in VACV induced programmed necrosis. Through the use of ectopic expression of DAI containing mutations or deletions of various domains we demonstrated that a functional Zα domain was required for death to be induced (Fig. 24). The Zα domain of DAI is specific to Z-NA binding and its requirement confirmed that the Z-NA-binding ability plays an important role in VACV-induced programmed necrosis.

VACV expressing a full length E3 is resistant to DAI-regulated programmed necrosis, but deletion of the Z-NA-BD of E3L sensitized it death induction. Since the ability of DAI to bind Z-NA is required for VACV-E3LΔ83N-induced programmed necrosis we then sought to evaluate if the inhibition of death by full length E3 was a function of its ability to bind Z-NA. Z-NA binding by E3 is predicted to require seven highly conserved residues (16-mat). A VACV E3 point mutant that lacks the ability to bind to Z-NA was generated to evaluate the requirement of a functional Z-NA-BD for the inhibition of programmed necrosis. The disruption of Z-NA binding in E3 induced by a single residue change resulted in a phenotype and propensity to induce an IFN-primed programmed necrosis equivalent to that of VACV-E3LΔE3L. Thus, the function of the

N-terminus of E3 to inhibit a DAI-driven programmed necrosis corresponds specifically to its ability to bind to Z-NA.

As a final measure to evaluate Z-NA-binding function to regulate VACV-induced programmed necrosis, we asked if Z-NA-BD of distantly related members of the Zα protein family could functionally replace the one found in E3. While the general Z-NA-BD structure is conserved, the amino acid sequences have very little homology within the Zα family outside of the residues used to contact Z-NA. VACV E3L chimera viruses were generated by replacing the coding for the Z-NA-BD of E3 with either that of the Zα domain from mouse DAI or human ADAR1. E3 Zα chimera viruses were as efficient as wt VACV in inhibiting programmed necrosis. The uses of these viruses confirmed that the ability to inhibit programmed necrosis in VACV-infected cells was specific to the ability to bind Z-NA.

This work demonstrated that the N-terminal Z-NA-BD of E3 functions to inhibit a DAI-driven programmed necrosis. The ability of E3- to inhibit programmed necrosis depends on its ability to bind to Z-NA. Additionally, the induction of VACV-induced programmed necrosis in the absence of the Z-NA-BD of E3 requires a functional Zα domain of DAI, which has specificity for binding Z-NA. This dynamic interplay between two Z-NA binding proteins in the regulation of VACV-induced programmed necrosis suggests they work in a competitive fashion. This regulation of VACV-induced programmed necrosis by two opposing, competing Z-NA-binding proteins illuminates the possibility that Z-NA may play a biologically significant role as a PAMP during VACV infections, with E3 functioning to sequester it to prevent sensing by DAI.

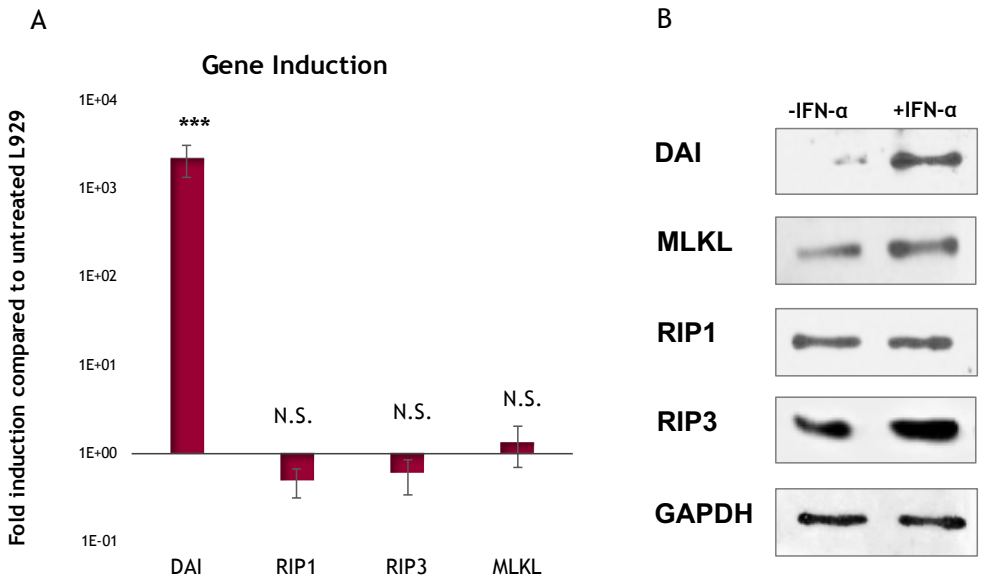

Figure 21. IFN-α regulation of DAI expression in L929 cells. The expression of DAI, RIP1, RIP3, and MLKL is determined after 100 U/mL IFN-α treatments for 18 hours in L929 cells. **(A)** Transcript levels are measured using qPCR. **(B)** Protein expression levels are measured byWestern blot analysis.

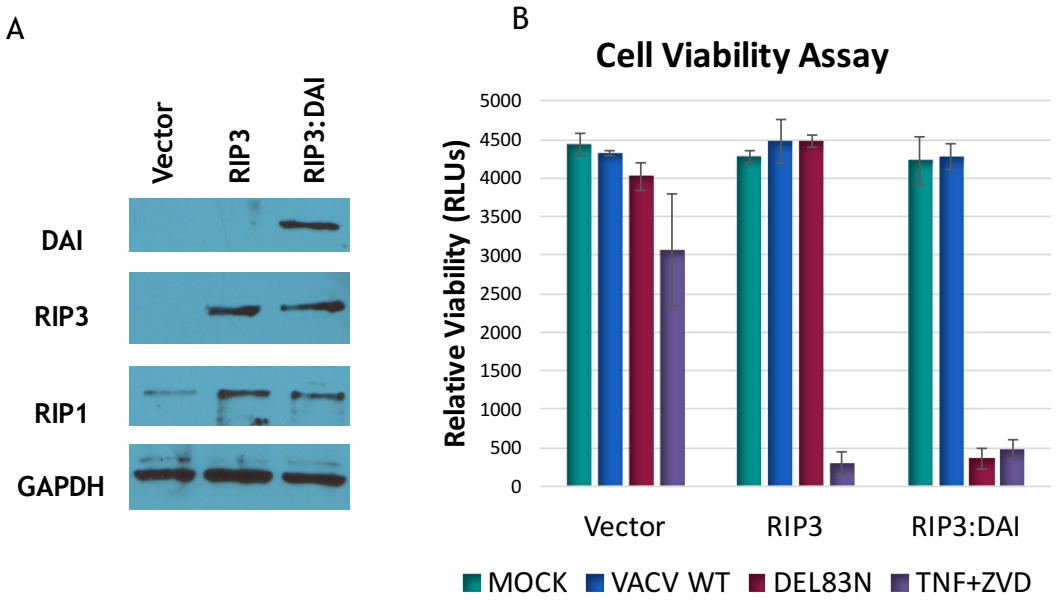

Figure 22. VACV-induced programmed necrosis requires both RIP3 and DAI. Viability of human 293T cells under indicated conditions was measured by Cell Titer-Glo Assay at 12 hours post infection/treatment. 293T cells are deficient in RIP3 and DAI. Ectopic expression of RIP3 sensitizes cells to TNF+ZVD treatment, but not VACV-E3LΔ83N infection. Ectopic expression of RIP3 and DAI sensitizes cells to VACV-E3LΔ83N infection. The viability of cells infected with either MOCK, wt VACV, or VACV-E3LΔ83N, or treated with TNF+ZVD is measured in relative luminescence units under RIP3- and DAI-deficient conditions, RIP3-expressing and DAI-deficient conditions or and RIP3- and DAI-expressing conditions.

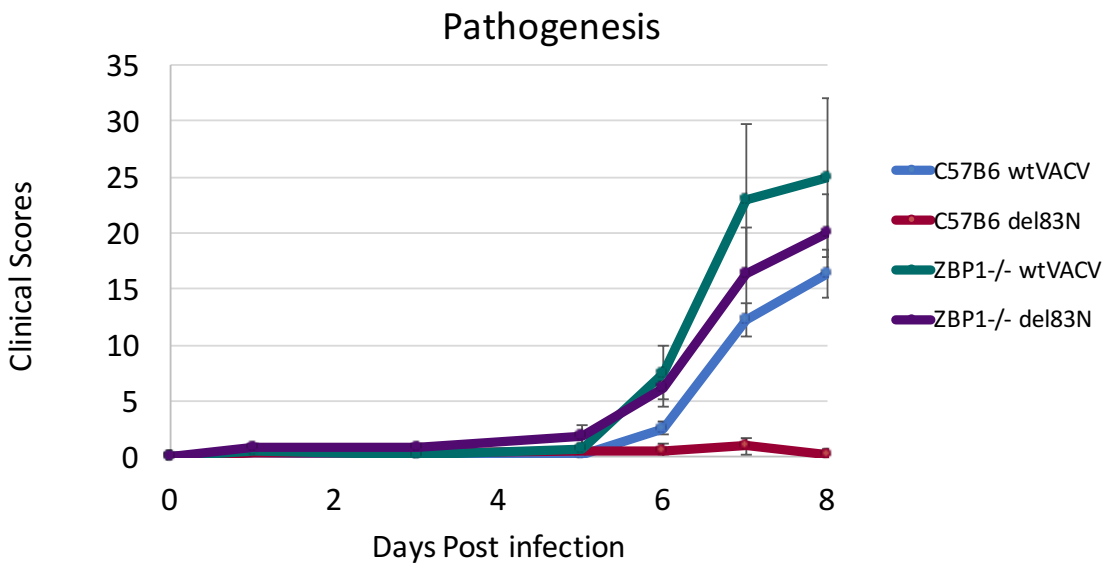

Figure 23. Rescue of VACV-E3LΔ83N pathogenesis in ZBP1-/- mice. 8-10-week-old C57BL/6 mice were infected by intranasal route with 10^6 PFU of the indicated viruses. Clinical scores (based on multiple symptoms) indicated that wt VACV is pathogenic in the C57BL/6mice, while VACV-E3LΔ83N was not. However, in mice with a homozygous disruption of the ZBP-1 (DAI/DLM) gene, VACV-E3LΔ83N becomes pathogenic.

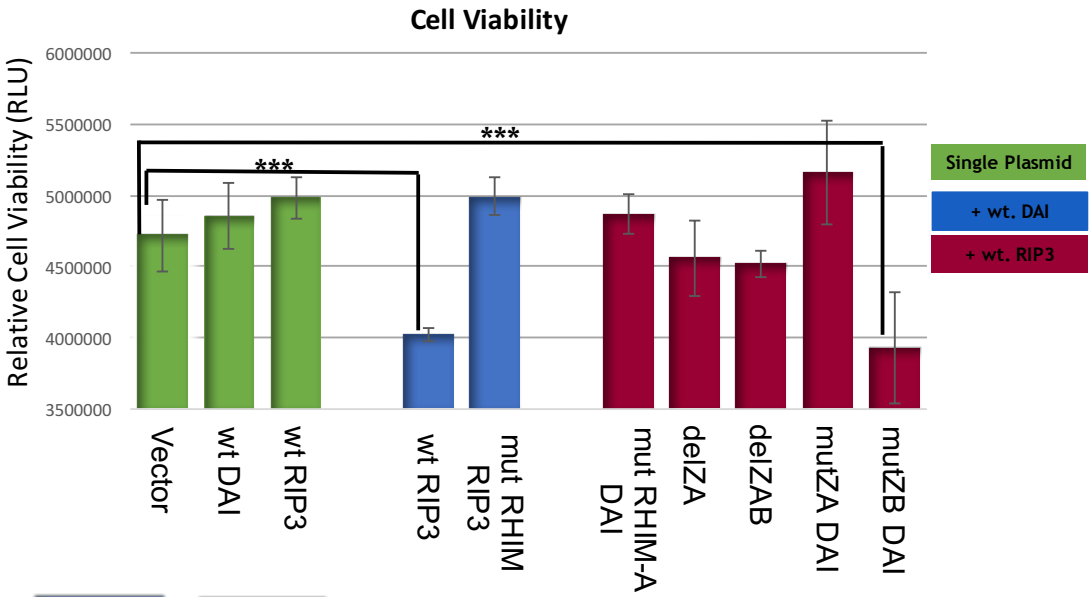

Figure 24. Mutations of the Za domain of DAI rescues viability. Cell viability assays were performed utilizing a plasmid expression system in HEK293T cells. Control transfection (single) vector, DAI, or RIP3 (green). Cell viability assays were then performed utilizing DAI in combination with RIP3 and DAI in combination with RIP3 with a mutated RHIM domain (blue). Lastly, viability assays are performed using RIP3 in combination with DAI with a mutated RHIM-A domain, deleted Zα domain, deleted Zα and Zβ domains, mutated Zα domains, and mutated Zβ domains. Viability was assed using a Cell Titer Glow Assay following a 12-hour infection with VACV-E3LΔ83N.

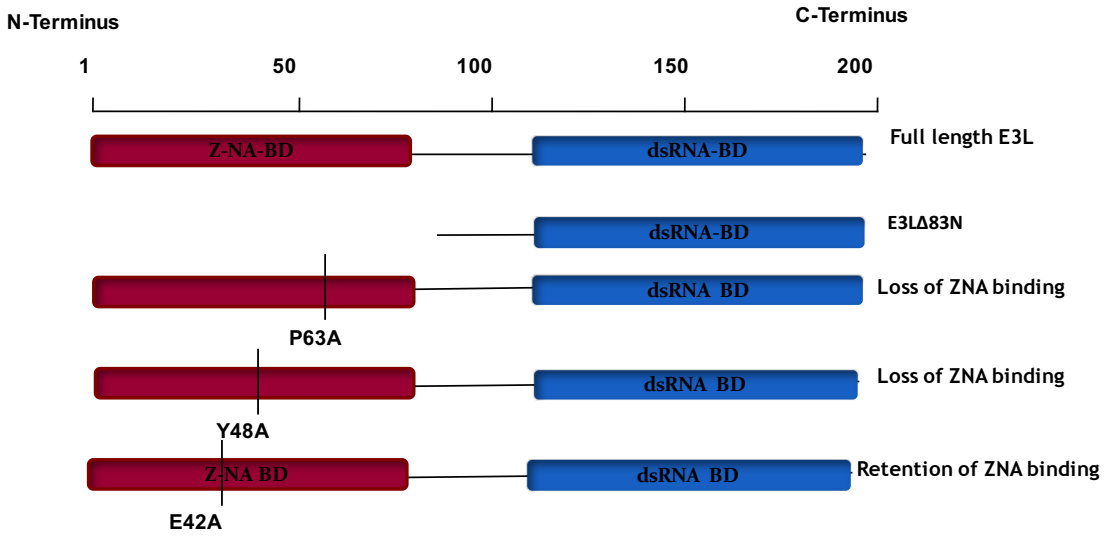

Figure 25. Schematic of E3 Z-NA binding domain and generated mutants. (A) E3 is a 25 kDa protein. In the N-terminus is the Z-NA-binding domain that has several distinct residues that can bind to Z-form nucleic acid including Z-DNA or Z-RNA. **(B)** To insure the phenotypes observed are specific to the loss of Z-NA binding, a point mutation was generated of a predicted key Z-NA-binding residue (E3L_P63A). Additionally a control point mutant was generated that has a mutated residue outside the predicted interacting regions of the domain (E3L_E42A).

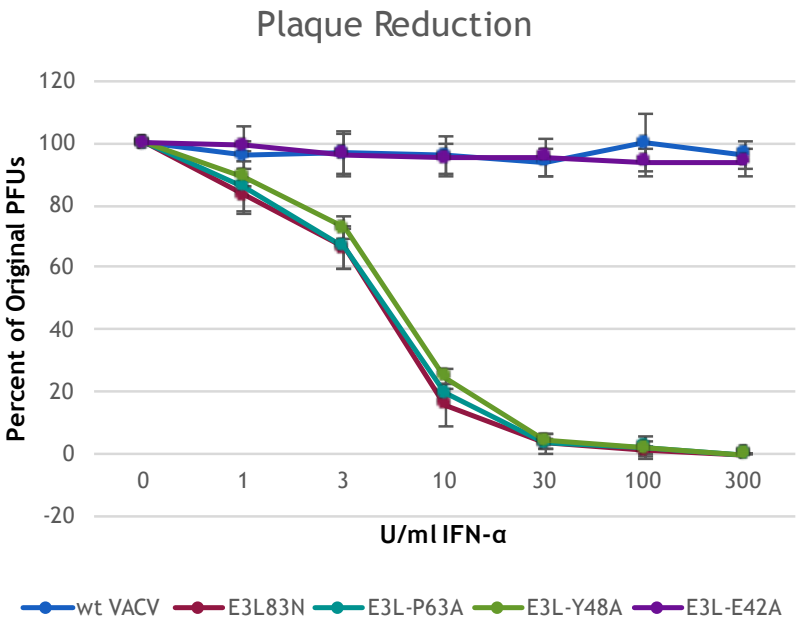

Figure 26. Disruption of E3 Z-NA binding results in IFN sensitivity in L929 cells. Plaque reduction assay using Z-NA-binding domain point mutants was performed by pretreating L929 cells with increasing amounts of mouse IFN-α for 18 hours prior to infection. The P63A and Y48A point mutations in the Z-NA-binding domain of E3 results in disruption of binding. E42A is a negative control point mutation located outside the binding domain. Loss of Z-NA-binding function resulted in equivalent IFN sensitivity as that of VACV-E3LΔ83N, while the control point mutant retained IFN resistance equivalent to wt.

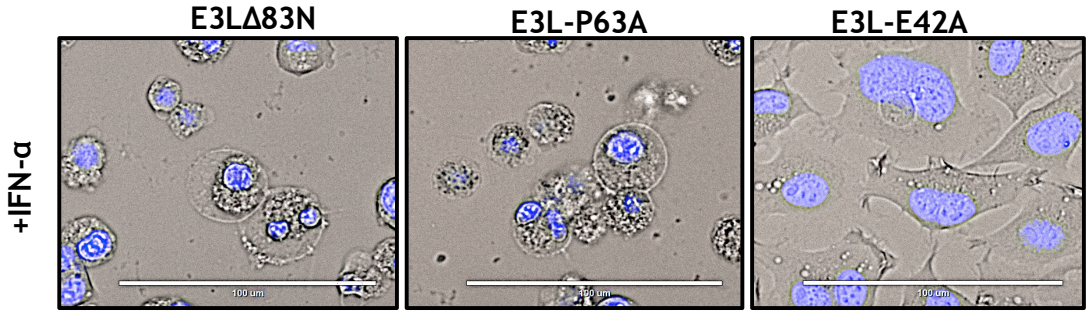

Figure 27. Alterations in morphology is specific to loss of Z-NA binding function in E3. Transmitted live imaging at 6 HPI of L929 cells pretreated for 18 hours with 100U/ml of mouse IFN-α followed by infection with E3LΔ83N, E3L-P63, or E3L-E42A at an MOI of 5. Ghost cell morphology is specific to IFN-treated cells and the loss of a functional Z-NA binding domain.

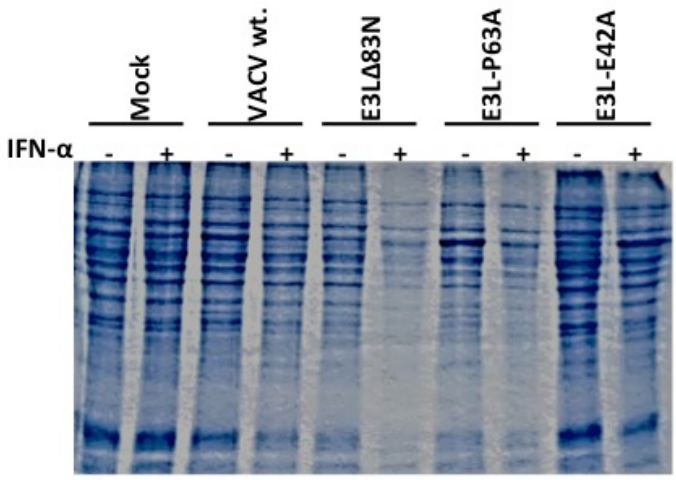

Figure 28. Global protein loss is due to loss of Z-NA binding. L929 cells were pretreated with 100 U/ml of mouse IFN-α for 18 hours prior to infection. Cells were then infected with mock, wt VACV, E3LΔ83N, E3L-P63A, and E3L-E42A at an MOI of 5. A total protein gel was utilized to demonstrate the global cellular proteins in both IFN-α treated and untreated cells. Samples pretreated with IFN and infected with E3 mutants with a loss of Z-NA-binding ability demonstrated a significant global reduction in protein.

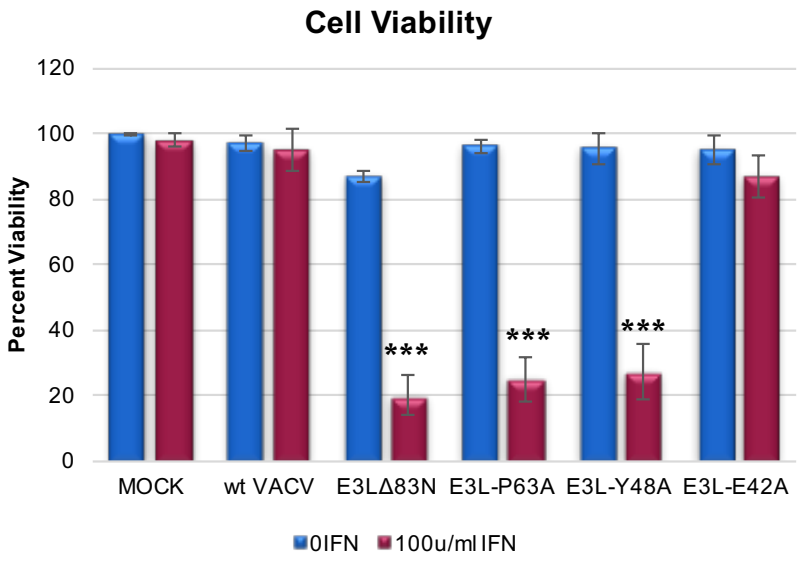

Figure 29. Loss of viability corresponds to the loss of the ability of E3 to bind Z-NA . The percent of viable cells 5 hours post transfection are compiled from the SYTOX© green dye up-take assays performed. Cell viability was determined using an average of viable cells in 10 fields These percentages were plotted for each infected cell group (MOCK, wt VACV,VACV- E3LΔ83N, VACV-VACVE3L-P63A, and VACV-E3L-E42A) for 0 U/mL IFN-α pretreatments (blue) and 100 U/mL IFN-α pretreatments (red). Induction of rapid cell death is consistent with the loss of Z-NA binding and IFN sensitivity. N-terminal mutants with disrupted Z-NA binding capacity consistently induce a rapid loss of membrane integrity and cellular death.

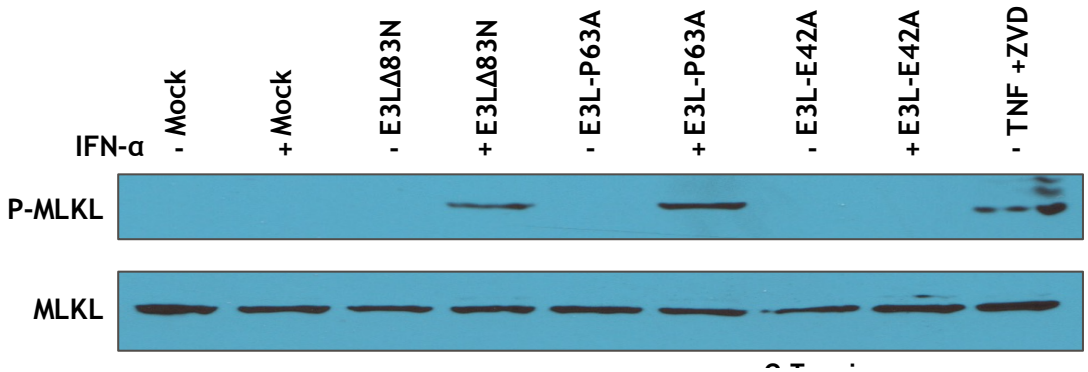

Figure 30. Inhibition of MLKL activation requires E3 Z-NA binding. A Western blot was performed to check for MLKL and phosphorylated MLKL expression. The blot was performed for both untreated and IFN-treated MOCK, VACV-E3LΔ83N, VACV-E3L-P63A, and VACV-E3L-E42A cells infected cells. TNF+ZVD-treated cells were added as a positive control. MLKL phosphorylation corresponds to the loss of Z-NA binding.

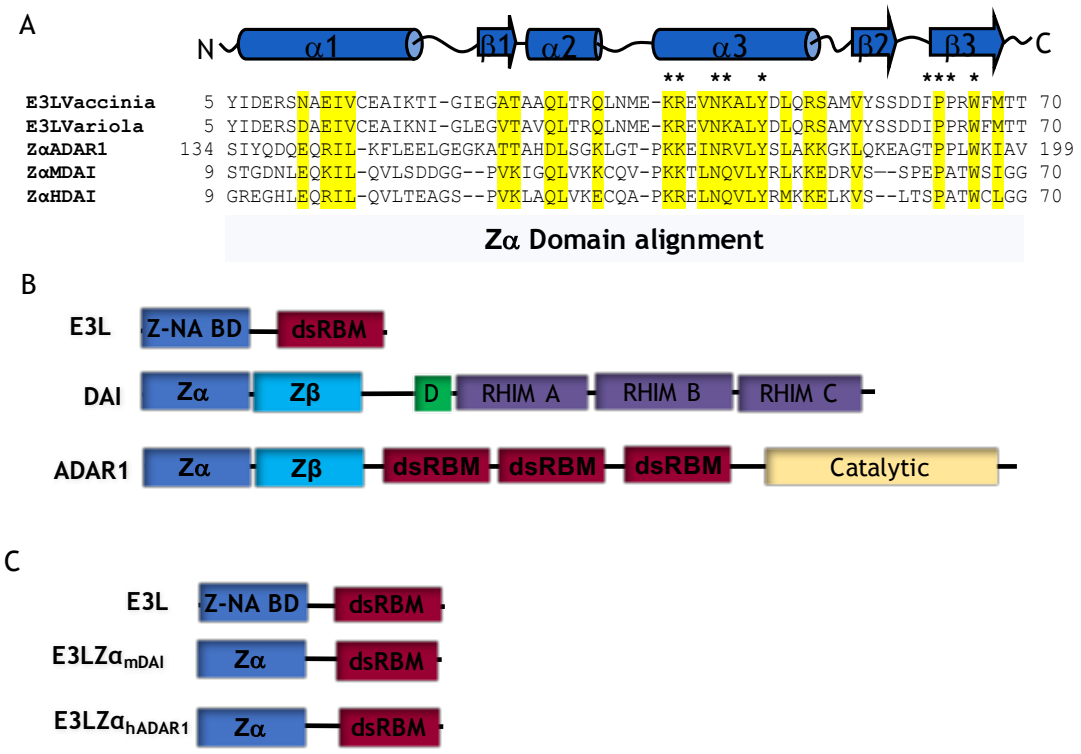

Figure 31. E3 Z-NA binding residues are conserved in the Zα domain of DAI. **(A)** Sequence alignment of the Z-NA-BD of E3, mouse and human DAI normalized by length. Green signifies 70% conservation and corresponds to residues required for Z-NA binding. **(B)** A schematic of the organization of the protein domains for E3, DAI, ADAR1 (p150). **(C)** A schematic of VACV domain-swapping chimera viruses generated by replacing the N-terminus of E3 with the Zα domains of either human ADAR1 (E3LZα$_{hADAR1}$) or mouse DAI (E3LZα $_{mDAI}$).

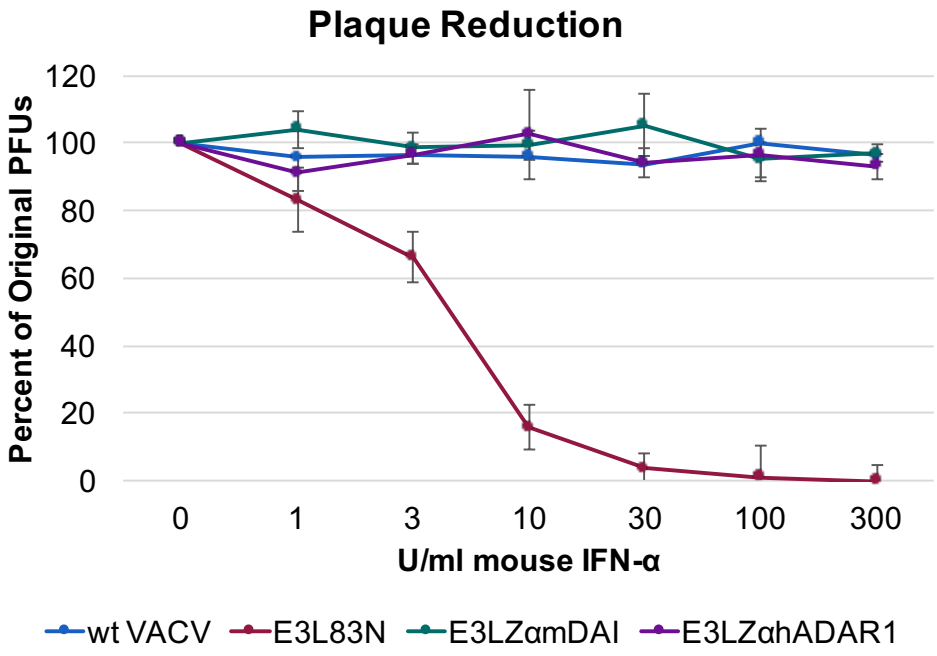

Figure 32. Zα functionally replaces the E3 Z-NA-BD for plaquing efficiency. Plaque reduction assay was performed by pretreating L929 cells with increasing amounts of mouse IFN-α for 18 hours prior to infection. Cells were infected with equivalent PFUs and allowed to form plaques. The percent of original plaque forming units (PFUs) is plotted against the dosage of IFN-α Units (U)/mL utilizing wt VACV (blue), VACV-E3LΔ83N (brown), VACV-E3LZα$_{mDAI}$ (purple), and VACV-E3LZα$_{hADAR1}$ (green). Viruses expressing any version of a functional Z-NA-BDZ-NA-BD are IFN-α resistant.

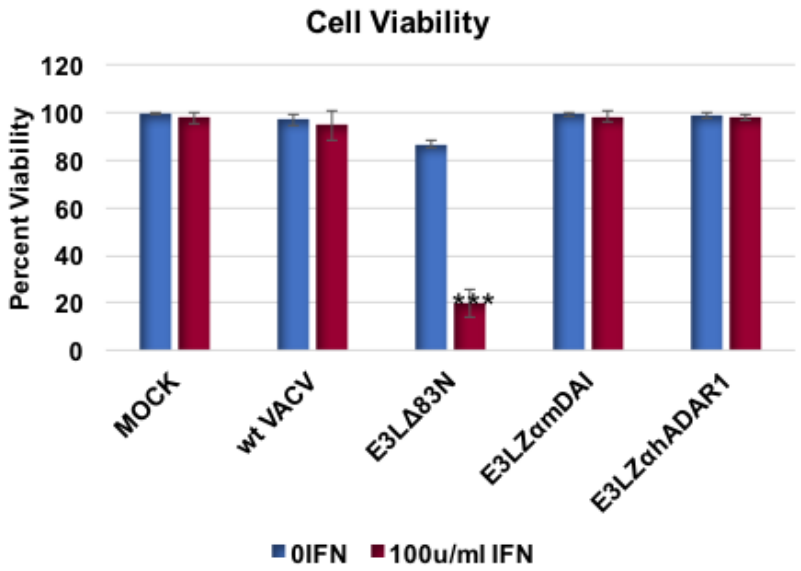

Figure 33. The *Zα* of DAI or ADAR1 functionally replaces the E3 Z-NA-BD to inhibit loss of cell viability. The percent of viable cells 5 hours post transfection were compiled from the SYTOX© green dye uptake assays performed. These percentages were plotted for each infected cell group (MOCK, wt VACV, VACV-E3LΔ83N, VACV-E3LZα$_{mDAI}$, and VACV-E3LZα$_{hADAR1}$) for 0 U/mL IFN-α pretreatments (blue) and 100 U/mL IFN-α pretreatments (red). Presence of a functional Z-NA-BD prevents induction of cell death.

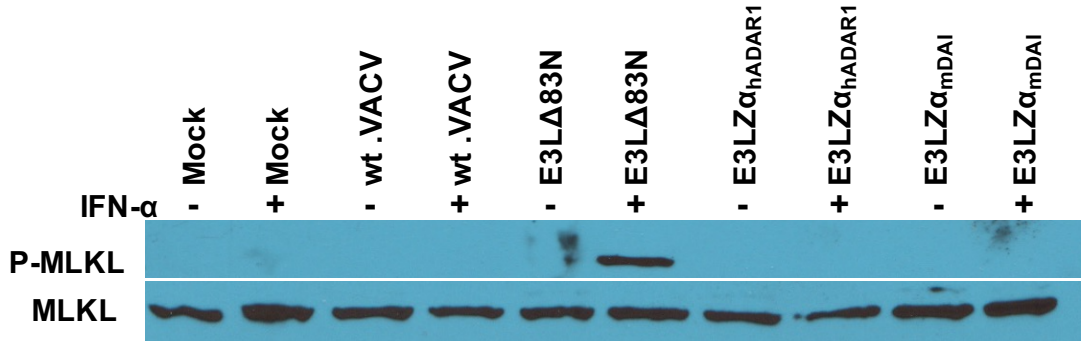

Figure 34. E3 Z-NA-BD chimera viruses do not induce MLKL phosphorylation
A Western blot was performed to check for MLKL and phosphorylated MLKL expression. The blot was performed for both untreated and IFN-treated MOCK, wt VACV, VACV-E3LΔ83N, VACV-E3LZα$_{hADAR1}$, and VACV-E3LZα$_{mDAI}$ infected cells. Presence of a functional Z-NA-BD inhibits programmed necrosis.

CHAPTER 4

OVERALL DISCUSSION

In this study, the role of the Z-NA-binding domain located in the N-terminus of E3 on type I IFN-primed programmed necrosis inhibition was investigated. This was done through initially studying L929 cells. It was found that wt VACV was IFNresistant and could effectively replicate in the presence or absence of IFN. However, when VACV was modified to produce E3 proteins with truncated N-termini, a rapid IFN-primed cell death was induced. These results led us to question the role of both the N-terminus of E3 and the mechanisms involved in the induction of programmed cell death.

Programmed necrosis was identified as a method of cell death to investigate further. Because previous work had also demonstrated that RIP3 is an essential protein for inducing programmed necrosis, we decided to inhibit RIP3 activity through the RIP3 kinase inhibitor GSK872. Inhibition of the RIP3 activity in cells infected with the previously attenuated mutant VACV restored viral replication, even in the presence of interferon.The rescue of IFN sensitivity supported the hypothesis that the cell death previously examined was indeed programmed necrosis. To confirm this hypothesis, MLKL activation, which takes place in the last step of programmed necrosis, was confirmed in IFN+ cultures infected with the modified VACV. Phosphorylation levels in the assay were sufficient to establish that MLKL activation was occurring. This result in combination with the results of RIP3 inhibition on cell cultures confirmed that the previous cell death observed was in fact due to programmed necrosis.

In order to determine which host proteins have roles integral to programmed

necrosis, we researched the literature to identify candidates that have been known to initiate the process. Through this research, the protein DAI came up as the prime candidate for a RIP3 adaptor protein. Consequently, we analyzed DAI levels in both IFN^+ and IFN^- cultures through qPCR and Western blots. The results of these characterization experiments showed that DAI was absent in IFN^- cells, but upregulated in IFN^+ cells. This led us to investigate HEK293T cells, which were known to be deficient of both RIP3 and DAI. No cell death was observed in these cells through either TNF treatment (the classical necroptosis pathway) or through infection with the modified VACV However, expression of RIP3 through transfection, recover the formation of RIP1-RIP3 complexes, which then induced cell death. On the other hand, addition of RIP3 to the cells was not sufficient to recover VACV-E3LΔ83N-induced programmed necrosis; this induction required the addition of DAI in conjunction with RIP3 to cultures. These results demonstrated that cell death through programmed necrosis is heavily dependent on both RIP3 and DAI. Confirmation of the biological relevance of RIP3 and DAI in VACV infections was demonstrated through pathogenesis studies. Intranasal infection with VACV containing E3 N-terminal mutations are apathogenic; however, in mice genetically deficient of either RIP3 or DAI (ZBP1-/-), the pathogenesis was rescued to wt VACV levels.

Since both E3 and DAI are members of the same Zα family, we wanted to determine if the Z-NA-binding function was required on both proteins. A previous domain swapping study of the Z-NA binding domain of the N-terminus of E3 with other Z-NA-binding domains (Zα DAI or ZαADAR1) demonstrated that despite having less than 20% sequence homology to the E3 Z-NA-BD, the Zα domains functionally replace

the Z-NA-BD of E3(105, 106, 126). The results of this study demonstrated that replacing Z-NA binding domains in E3 had no significant effect on the performance of VACV. Additionally, further evidence to support the requirements of a functional Z-NA-BD in E3 is seen by a loss of pathogenesis corresponding to any disruption of the Z-NA binding (105).

These results led us to further investigate the effect of a potential Z-NA-binding domain in E3 on programmed necrosis. By utilizing the HEK293T system, the domains of DAI required to initiate programmed necrosis were evaluated. It was found that the Zα domain confers specificity to Z-NA binding, and along with RHIM domain A, was required for the induction of death. In order to investigate the Z-NA-binding role of E3, we artificially induced point mutations in key residues of E3 responsible for coding the possible Z-NA-BD on E3. Incorporation of these point mutations resulted in a substantial attenuation of the modified VACV phenotype in IFN^+ cultures that was not observed in wild type. This result demonstrated that the previous cell loss observed in IFN^+ cells infected with the E3 N-terminus mutant of VACV was due to the missing Z-NA-binding domain that resulted from truncation. From this finding, we were able to determine that the Z-NA-binding domain of E3 has a significant effect on the inhibition of programmed necrosis for VACV.

A compilation of this data shows that the N-terminus of E3 plays a critical role in inhibiting the IFN-primed and virally-induced programmed necrosis that is dependent on both the RIP3 kinase domain and the Z-DNA-binding host protein DAI. Since the N-terminus contains a Zα domain that is functionally replaceable by the Zα domain of DAI

and the ability to bind to Z-NA is required by both proteins in this system, we hypothesize that the N-terminus of E3 functions in inhibition of necroptosis by inhibiting DAI. Induction of necroptosis correlates with loss of Z-NA binding of the N-terminus, suggesting that the N-terminus of E3 may compete with DAI for binding to a viral or host macromolecule that DAI senses to induce necroptosis. Viral inhibition of DAI has previously been demonstrated in the herpesvirus system through the use of a competitive RHIM inhibitor. However, E3 inhibition is likely a novel mechanism of inhibition as it does not contain an identifiable RHIM domain.

Further characterization of the E3 and DAI function during VACV infection could provide significant insight into signaling events leading to RIP3-dependent necrosis. It will also provide a greater understanding of the use of programmed necrosis as an innate host defense mechanism. The rapid induction of this highly inflammatory death occurs prior to late viral protein synthesis stages and therefore may provide valuable insight into adaptive immune responses and insight into safer vaccine development.

Since our results suggest that the Z-nucleic acid-binding function of the N-terminus of E3 is important for inhibition of induction of necroptosis, and since the Zα-containing protein DAI has been implicated in sensing virus infection, this work may have the potential to evaluate Z-NA as a possible PAMP. Enhanced understanding of the role of the Z-NA-BD in E3 can provide insight into the pathogenesis of monkeypox virus, as it contains a natural truncation in the N-terminal Zα domain of its E3 homologue (80, 109).

Recently, programmed necrosis has been identified as an important pathway in the field of oncology. Many cancers have been shown to have low RIP3 expression, thereby reducing their susceptibility to programmed necrosis (127). Currently myxomavirus, which lacks a Zα domain on its E3 homologue, is in testing in humans as an oncolytic virus. Investigating how the presence or absence of Zα domains in relationship to RIP3 level could provide significant insight into the engineering of effective oncolytic viruses.

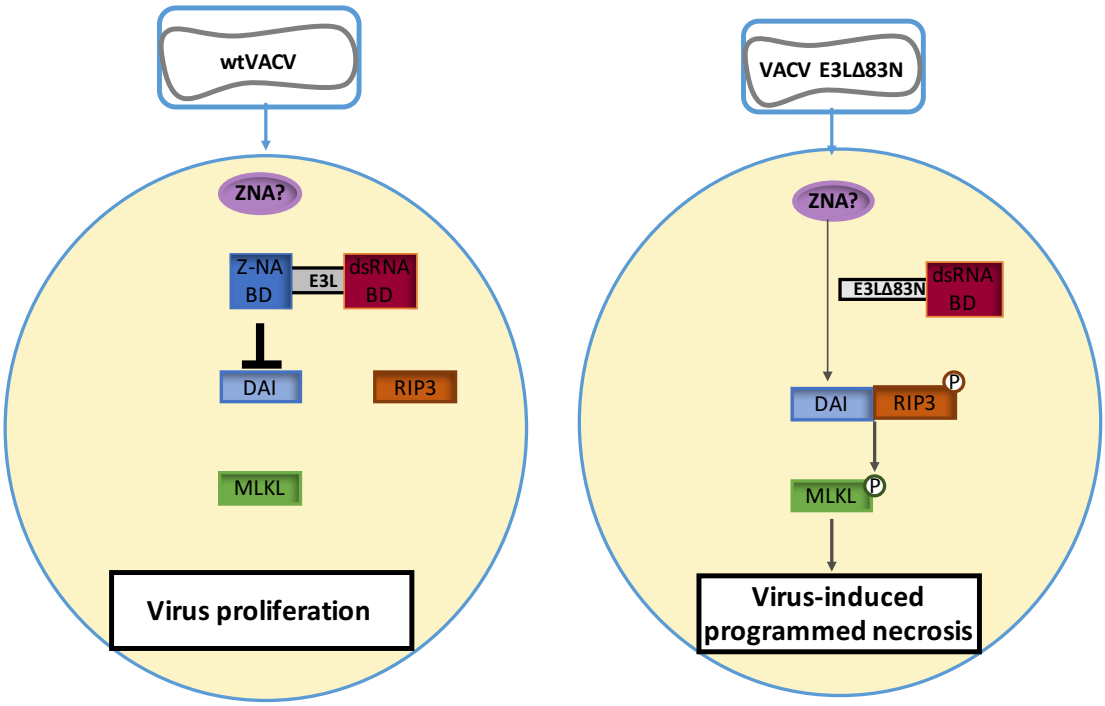

Figure 35. Summary figure. Schematic of the main components of the signaling cascade involved with the alternative form of programmed necrosis is shown for cells infected with either VACV-E3LΔ83N or wt VACV. The VACV-encoded E3 Z-NA-BD functions to prevent the activation of programmed necrosis, utilizing DAI as an adaptor protein for RIP3. In the absence of a functional Z-NA-BD in E3, DAI is believed to function as a PRR and sense Z-NA as a PAMP. In the presence of full length E3 the Z-NA is believed to be sequestered by E3 to prevent detection by DAI.

REFERENCES

1. **Bowie AG, Unterholzner L.** 2008. Viral evasion and subversion of pattern-recognition receptor signalling. Nat Rev Immunol **8:**911-922.

2. **Isaacs A, Lindenmann J.** 1957. Virus interference. I. The interferon. Proc R Soc Lond B Biol Sci **147:**258-267.

3. **Bonjardim CA, Ferreira PC, Kroon EG.** 2009. Interferons: signaling, antiviral and viral evasion. Immunol Lett **122:**1-11.

4. **Alsharifi M, Mullbacher A, Regner M.** 2008. Interferon type I responses in primary and secondary infections. Immunol Cell Biol **86:**239-245.

5. **Samuel CE.** 2001. Antiviral actions of interferons. Clin Microbiol Rev **14:**778-809, table of contents.

6. **Sen GC.** 2001. Viruses and interferons. Annu Rev Microbiol **55:**255-281.

7. **Der SD, Zhou A, Williams BR, Silverman RH.** 1998. Identification of genes differentially regulated by interferon alpha, beta, or gamma using oligonucleotide arrays. Proc Natl Acad Sci U S A **95:**15623-15628.

8. **Takaoka A, Yanai H.** 2006. Interferon signalling network in innate defence. Cell Microbiol **8:**907-922.

9. **Randall RE, Goodbourn S.** 2008. Interferons and viruses: an interplay between induction, signalling, antiviral responses and virus countermeasures. J Gen Virol **89:**1-47.

10. **Sadler AJ, Williams BR.** 2008. Interferon-inducible antiviral effectors. Nat Rev Immunol **8:**559-568.

11. **Akira S, Uematsu S, Takeuchi O.** 2006. Pathogen recognition and innate immunity. Cell **124:**783-801.

12. **Uze G, Lutfalla G, Gresser I.** 1990. Genetic transfer of a functional human interferon alpha receptor into mouse cells: cloning and expression of its cDNA. Cell **60:**225-234.

13. **Novick D, Cohen B, Rubinstein M.** 1994. The human interferon alpha/beta receptor: characterization and molecular cloning. Cell **77:**391-400.

14. **Stark GR.** 2007. How cells respond to interferons revisited: from early history to current complexity. Cytokine Growth Factor Rev **18:**419-423.

15. **Leung S, Qureshi SA, Kerr IM, Darnell JE, Jr., Stark GR.** 1995. Role of STAT2 in the alpha interferon signaling pathway. Mol Cell Biol **15:**1312-1317.

16. **Darnell JE, Jr., Kerr IM, Stark GR.** 1994. Jak-STAT pathways and transcriptional activation in response to IFNs and other extracellular signaling proteins. Science **264:**1415-1421.

17. **Bluyssen AR, Durbin JE, Levy DE.** 1996. ISGF3 gamma p48, a specificity switch for interferon activated transcription factors. Cytokine Growth Factor Rev **7:**11-17.

18. **de Veer MJ, Holko M, Frevel M, Walker E, Der S, Paranjape JM, Silverman RH, Williams BR.** 2001. Functional classification of interferon-stimulated genes identified using microarrays. J Leukoc Biol **69:**912-920.

19. **Best SM.** 2008. Viral subversion of apoptotic enzymes: escape from death row. Annu Rev Microbiol **62:**171-192.

20. **Brierley MM, Fish EN.** 2002. Review: IFN-alpha/beta receptor interactions to biologic outcomes: understanding the circuitry. J Interferon Cytokine Res **22:**835-845.

21. **Wenzel J, Tuting T.** 2008. An IFN-associated cytotoxic cellular immune response against viral, self-, or tumor antigens is a common pathogenetic feature in "interface dermatitis". J Invest Dermatol **128:**2392-2402.

22. **Lamkanfi M, Dixit VM.** 2010. Manipulation of host cell death pathways during microbial infections. Cell Host Microbe **8:**44-54.

23. **Rebouillat D, Hovanessian AG.** 1999. The human 2',5'-oligoadenylate synthetase family: interferon-induced proteins with unique enzymatic properties. J Interferon Cytokine Res **19:**295-308.

24. **Kerr IM, Brown RE, Hovanessian AG.** 1977. Nature of inhibitor of cell-free protein synthesis formed in response to interferon and double-stranded RNA. Nature **268:**540-542.

25. **Cho YS, Challa S, Moquin D, Genga R, Ray TD, Guildford M, Chan FK.** 2009. Phosphorylation-driven assembly of the RIP1-RIP3 complex regulates programmed necrosis and virus-induced inflammation. Cell **137:**1112-1123.

26. **Omoto S, Guo H, Talekar GR, Roback L, Kaiser WJ, Mocarski ES.** 2015. Suppression of RIP3-dependent necroptosis by human cytomegalovirus. J Biol Chem **290:**11635-11648.

27. **Upton JW, Kaiser WJ, Mocarski ES.** 2010. Virus inhibition of RIP3-dependent necrosis. Cell Host Microbe **7:**302-313.

28. **Upton JW, Kaiser WJ, Mocarski ES.** 2008. Cytomegalovirus M45 cell death suppression requires receptor-interacting protein (RIP) homotypic interaction motif (RHIM)-dependent interaction with RIP1. J Biol Chem **283:**16966-16970.

29. **Mocarski ES, Guo H, Kaiser WJ.** 2015. Necroptosis: The Trojan horse in cell autonomous antiviral host defense. Virology **479-480:**160-166.

30. **Duprez L, Wirawan E, Vanden Berghe T, Vandenabeele P.** 2009. Major cell death pathways at a glance. Microbes Infect **11:**1050-1062.

31. **Saelens X, Festjens N, Vande Walle L, van Gurp M, van Loo G, Vandenabeele P.** 2004. Toxic proteins released from mitochondria in cell death. Oncogene **23:**2861-2874.

32. **Bergsbaken T, Fink SL, Cookson BT.** 2009. Pyroptosis: host cell death and inflammation. Nat Rev Microbiol **7:**99-109.

33. **Moriwaki K, Chan FK.** 2013. RIP3: a molecular switch for necrosis and inflammation. Genes Dev **27:**1640-1649.

34. **Micheau O, Tschopp J.** 2003. Induction of TNF receptor I-mediated apoptosis via two sequential signaling complexes. Cell **114:**181-190.

35. **Wu XN, Yang ZH, Wang XK, Zhang Y, Wan H, Song Y, Chen X, Shao J, Han J.** 2014. Distinct roles of RIP1-RIP3 hetero- and RIP3-RIP3 homo-interaction in mediating necroptosis. Cell Death Differ **21:**1709-1720.

36. **Sun L, Wang H, Wang Z, He S, Chen S, Liao D, Wang L, Yan J, Liu W, Lei X, Wang X.** 2012. Mixed lineage kinase domain-like protein mediates necrosis signaling downstream of RIP3 kinase. Cell **148:**213-227.

37. **Wang H, Sun L, Su L, Rizo J, Liu L, Wang LF, Wang FS, Wang X.** 2014. Mixed lineage kinase domain-like protein MLKL causes necrotic membrane disruption upon phosphorylation by RIP3. Mol Cell **54:**133-146.

38. **Su L, Quade B, Wang H, Sun L, Wang X, Rizo J.** 2014. A plug release mechanism for membrane permeation by MLKL. Structure **22:**1489-1500.

39. **Cai Z, Jitkaew S, Zhao J, Chiang HC, Choksi S, Liu J, Ward Y, Wu LG, Liu ZG.** 2014. Plasma membrane translocation of trimerized MLKL protein is required for TNF-induced necroptosis. Nat Cell Biol **16:**55-65.

40. **Dondelinger Y, Declercq W, Montessuit S, Roelandt R, Goncalves A, Bruggeman I, Hulpiau P, Weber K, Sehon CA, Marquis RW, Bertin J, Gough PJ, Savvides S, Martinou JC, Bertrand MJ, Vandenabeele P.** 2014. MLKL compromises plasma membrane integrity by binding to phosphatidylinositol phosphates. Cell Rep **7:**971-981.

41. **Hildebrand JM, Tanzer MC, Lucet IS, Young SN, Spall SK, Sharma P, Pierotti C, Garnier JM, Dobson RC, Webb AI, Tripaydonis A, Babon JJ, Mulcair MD, Scanlon MJ, Alexander WS, Wilks AF, Czabotar PE, Lessene G, Murphy JM, Silke J.** 2014. Activation of the pseudokinase MLKL unleashes the four-helix bundle domain to induce membrane localization and necroptotic cell death. Proc Natl Acad Sci U S A **111:**15072-15077.

42. **Chen X, Li W, Ren J, Huang D, He WT, Song Y, Yang C, Li W, Zheng X, Chen P, Han J.** 2014. Translocation of mixed lineage kinase domain-like protein to plasma membrane leads to necrotic cell death. Cell Res **24:**105-121.

43. **He S, Liang Y, Shao F, Wang X.** 2011. Toll-like receptors activate programmed necrosis in macrophages through a receptor-interacting kinase-3-mediated pathway. Proc Natl Acad Sci U S A **108:**20054-20059.

44. **Kaiser WJ, Sridharan H, Huang C, Mandal P, Upton JW, Gough PJ, Sehon CA, Marquis RW, Bertin J, Mocarski ES.** 2013. Toll-like receptor 3-mediated necrosis via TRIF, RIP3, and MLKL. J Biol Chem **288:**31268-31279.

45. **Meylan E, Burns K, Hofmann K, Blancheteau V, Martinon F, Kelliher M, Tschopp J.** 2004. RIP1 is an essential mediator of Toll-like receptor 3-induced NF-kappa B activation. Nat Immunol **5:**503-507.

46. **Upton JW, Kaiser WJ, Mocarski ES.** 2012. DAI/ZBP1/DLM-1 complexes with RIP3 to mediate virus-induced programmed necrosis that is targeted by murine cytomegalovirus vIRA. Cell Host Microbe **11:**290-297.

47. **Berger AK, Danthi P.** 2013. Reovirus activates a caspase-independent cell death pathway. MBio **4:**e00178-00113.

48. **Guo H, Omoto S, Harris PA, Finger JN, Bertin J, Gough PJ, Kaiser WJ, Mocarski ES.** 2015. Herpes simplex virus suppresses necroptosis in human cells. Cell Host Microbe **17:**243-251.

49. **Robinson N, McComb S, Mulligan R, Dudani R, Krishnan L, Sad S.** 2012. Type I interferon induces necroptosis in macrophages during infection with Salmonella enterica serovar Typhimurium. Nat Immunol **13:**954-962.

50. **Weng D, Marty-Roix R, Ganesan S, Proulx MK, Vladimer GI, Kaiser WJ, Mocarski ES, Pouliot K, Chan FK, Kelliher MA, Harris PA, Bertin J, Gough PJ, Shayakhmetov DM, Goguen JD, Fitzgerald KA, Silverman N, Lien E.** 2014. Caspase-8 and RIP kinases regulate bacteria-induced innate immune responses and cell death. Proc Natl Acad Sci U S A **111:**7391-7396.

51. **Upton JW, Chan FK.** 2014. Staying alive: cell death in antiviral immunity. Mol Cell **54:**273-280.

52. **Kaiser WJ, Upton JW, Mocarski ES.** 2013. Viral modulation of programmed necrosis. Curr Opin Virol **3:**296-306.

53. **Mocarski ES, Upton JW, Kaiser WJ.** 2012. Viral infection and the evolution of caspase 8-regulated apoptotic and necrotic death pathways. Nat Rev Immunol **12:**79-88.

54. **Moss B, Shisler JL.** 2001. Immunology 101 at poxvirus U: immune evasion genes. Semin Immunol **13:**59-66.

55. **Moss B.** 2007. Poxviridade: The viruses and their replication, 5 ed, vol 2.

56. **Reed KD, Melski JW, Graham MB, Regnery RL, Sotir MJ, Wegner MV, Kazmierczak JJ, Stratman EJ, Li Y, Fairley JA, Swain GR, Olson VA, Sargent EK, Kehl SC, Frace MA, Kline R, Foldy SL, Davis JP, Damon IK.** 2004. The detection of monkeypox in humans in the Western Hemisphere. N Engl J Med **350:**342-350.

57. **Upton C, Slack S, Hunter AL, Ehlers A, Roper RL.** 2003. Poxvirus orthologous clusters: toward defining the minimum essential poxvirus genome. J Virol **77:**7590-7600.

58. **Baroudy BM, Venkatesan S, Moss B.** 1982. Incompletely base-paired flip-flop terminal loops link the two DNA strands of the vaccinia virus genome into one uninterrupted polynucleotide chain. Cell **28:**315-324.

59. **Garon CF, Barbosa E, Moss B.** 1978. Visualization of an inverted terminal repetition in vaccinia virus DNA. Proc Natl Acad Sci U S A **75:**4863-4867.

60. **Seet BT, Johnston JB, Brunetti CR, Barrett JW, Everett H, Cameron C, Sypula J, Nazarian SH, Lucas A, McFadden G.** 2003. Poxviruses and immune evasion. Annu Rev Immunol **21:**377-423.

61. **Symons JA, Alcami A, Smith GL.** 1995. Vaccinia virus encodes a soluble type I interferon receptor of novel structure and broad species specificity. Cell **81:**551-560.

62. **Verardi PH, Jones LA, Aziz FH, Ahmad S, Yilma TD.** 2001. Vaccinia virus vectors with an inactivated gamma interferon receptor homolog gene (B8R) are attenuated In vivo without a concomitant reduction in immunogenicity. J Virol **75:**11-18.

63. **Ueda T, Gotoh Y, Shiroshita K, Sakurai T, Kataoka Y.** 1990. [Clinical and histological observation of HBV glomerulonephritis treated with interferon-beta]. Nippon Jinzo Gakkai Shi **32:**1153-1159.

64. **Alcami A, Smith GL.** 2002. The vaccinia virus soluble interferon-gamma receptor is a homodimer. J Gen Virol **83:**545-549.

65. **Perdiguero B, Esteban M.** 2009. The interferon system and vaccinia virus evasion mechanisms. J Interferon Cytokine Res **29:**581-598.

66. **Colamonici OR, Domanski P, Sweitzer SM, Larner A, Buller RM.** 1995. Vaccinia virus B18R gene encodes a type I interferon-binding protein that blocks interferon alpha transmembrane signaling. J Biol Chem **270:**15974-15978.

67. **Smith VP, Bryant NA, Alcami A.** 2000. Ectromelia, vaccinia and cowpox viruses encode secreted interleukin-18-binding proteins. J Gen Virol **81:**1223-1230.

68. **Alcami A, Khanna A, Paul NL, Smith GL.** 1999. Vaccinia virus strains Lister, USSR and Evans express soluble and cell-surface tumour necrosis factor receptors. J Gen Virol **80 (Pt 4):**949-959.

69. **Alcami A, Smith GL.** 1992. A soluble receptor for interleukin-1 beta encoded by vaccinia virus: a novel mechanism of virus modulation of the host response to infection. Cell **71:**153-167.

70. **Beattie E, Denzler KL, Tartaglia J, Perkus ME, Paoletti E, Jacobs BL.** 1995. Reversal of the interferon-sensitive phenotype of a vaccinia virus lacking E3L by expression of the reovirus S4 gene. J Virol **69:**499-505.

71. **Beattie E, Kauffman EB, Martinez H, Perkus ME, Jacobs BL, Paoletti E, Tartaglia J.** 1996. Host-range restriction of vaccinia virus E3L-specific deletion mutants. Virus Genes **12:**89-94.

72. **Beattie E, Paoletti E, Tartaglia J.** 1995. Distinct patterns of IFN sensitivity observed in cells infected with vaccinia K3L- and E3L- mutant viruses. Virology **210:**254-263.

73. **Dobbelstein M, Shenk T.** 1996. Protection against apoptosis by the vaccinia virus SPI-2 (B13R) gene product. J Virol **70:**6479-6485.

74. **Kettle S, Alcami A, Khanna A, Ehret R, Jassoy C, Smith GL.** 1997. Vaccinia virus serpin B13R (SPI-2) inhibits interleukin-1beta-converting enzyme and protects virus-infected cells from TNF- and Fas-mediated apoptosis, but does not prevent IL-1beta-induced fever. J Gen Virol **78 (Pt 3):**677-685.

75. **Legrand FA, Verardi PH, Jones LA, Chan KS, Peng Y, Yilma TD.** 2004. Induction of potent humoral and cell-mediated immune responses by attenuated vaccinia virus vectors with deleted serpin genes. J Virol **78:**2770-2779.

76. **Li M, Beg AA.** 2000. Induction of necrotic-like cell death by tumor necrosis factor alpha and caspase inhibitors: novel mechanism for killing virus-infected cells. J Virol **74:**7470-7477.

77. **Holler N, Zaru R, Micheau O, Thome M, Attinger A, Valitutti S, Bodmer JL, Schneider P, Seed B, Tschopp J.** 2000. Fas triggers an alternative, caspase-8-independent cell death pathway using the kinase RIP as effector molecule. Nat Immunol **1:**489-495.

78. **Chan FK, Shisler J, Bixby JG, Felices M, Zheng L, Appel M, Orenstein J, Moss B, Lenardo MJ.** 2003. A role for tumor necrosis factor receptor-2 and receptor-interacting protein in programmed necrosis and antiviral responses. J Biol Chem **278:**51613-51621.

79. **Arsenio J, Deschambault Y, Cao J.** 2008. Antagonizing activity of vaccinia virus E3L against human interferons in Huh7 cells. Virology **377:**124-132.

80. **Chang HW, Uribe LH, Jacobs BL.** 1995. Rescue of vaccinia virus lacking the E3L gene by mutants of E3L. J Virol **69:**6605-6608.

81. **Brandt TA, Jacobs BL.** 2001. Both carboxy- and amino-terminal domains of the vaccinia virus interferon resistance gene, E3L, are required for pathogenesis in a mouse model. J Virol **75:**850-856.

82. **Lee SB, Esteban M.** 1994. The interferon-induced double-stranded RNA-activated protein kinase induces apoptosis. Virology **199:**491-496.

83. **Ho CK, Shuman S.** 1996. Mutational analysis of the vaccinia virus E3 protein defines amino acid residues involved in E3 binding to double-stranded RNA. J Virol **70:**2611-2614.

84. **Ho CK, Shuman S.** 1996. Physical and functional characterization of the double-stranded RNA binding protein encoded by the vaccinia virus E3 gene. Virology **217:**272-284.

85. **Chang HW, Watson JC, Jacobs BL.** 1992. The E3L gene of vaccinia virus encodes an inhibitor of the interferon-induced, double-stranded RNA-dependent protein kinase. Proc Natl Acad Sci U S A **89:**4825-4829.

86. **St Johnston D, Brown NH, Gall JG, Jantsch M.** 1992. A conserved double-stranded RNA-binding domain. Proc Natl Acad Sci U S A **89:**10979-10983.

87. **Chang HW, Jacobs BL.** 1993. Identification of a conserved motif that is necessary for binding of the vaccinia virus E3L gene products to double-stranded RNA. Virology **194:**537-547.

88. **Yuwen H, Cox JH, Yewdell JW, Bennink JR, Moss B.** 1993. Nuclear localization of a double-stranded RNA-binding protein encoded by the vaccinia virus E3L gene. Virology **195:**732-744.

89. **Watson JC, Chang HW, Jacobs BL.** 1991. Characterization of a vaccinia virus-encoded double-stranded RNA-binding protein that may be involved in inhibition of the double-stranded RNA-dependent protein kinase. Virology **185:**206-216.

90. **Jacobs BL, Langland JO.** 1996. When two strands are better than one: the mediators and modulators of the cellular responses to double-stranded RNA. Virology **219:**339-349.

91. **Kibler KV, Shors T, Perkins KB, Zeman CC, Banaszak MP, Biesterfeldt J, Langland JO, Jacobs BL.** 1997. Double-stranded RNA is a trigger for apoptosis in vaccinia virus-infected cells. J Virol **71:**1992-2003.

92. **Makarova O, Kamberov E, Margolis B.** 2000. Generation of deletion and point mutations with one primer in a single cloning step. Biotechniques **29:**970-972.

93. **Fu Y, Comella N, Tognazzi K, Brown LF, Dvorak HF, Kocher O.** 1999. Cloning of DLM-1, a novel gene that is up-regulated in activated macrophages, using RNA differential display. Gene **240:**157-163.

94. **Poulsen H, Nilsson J, Damgaard CK, Egebjerg J, Kjems J.** 2001. CRM1 mediates the export of ADAR1 through a nuclear export signal within the Z-DNA binding domain. Mol Cell Biol **21:**7862-7871.

95. **Patterson JB, Samuel CE.** 1995. Expression and regulation by interferon of a double-stranded-RNA-specific adenosine deaminase from human cells: evidence for two forms of the deaminase. Mol Cell Biol **15:**5376-5388.

96. **Herbert A, Alfken J, Kim YG, Mian IS, Nishikura K, Rich A.** 1997. A Z-DNA binding domain present in the human editing enzyme, double-stranded RNA adenosine deaminase. Proc Natl Acad Sci U S A **94:**8421-8426.

97. **Berger I, Winston W, Manoharan R, Schwartz T, Alfken J, Kim YG, Lowenhaupt K, Herbert A, Rich A.** 1998. Spectroscopic characterization of a DNA-binding domain, Z alpha, from the editing enzyme, dsRNA adenosine deaminase: evidence for left-handed Z-DNA in the Z alpha-DNA complex. Biochemistry **37:**13313-13321.

98. **Kim YG, Lowenhaupt K, Schwartz T, Rich A.** 1999. The interaction between Z-DNA and the Zab domain of double-stranded RNA adenosine deaminase characterized using fusion nucleases. J Biol Chem **274:**19081-19086.

99. **Kim YG, Lowenhaupt K, Maas S, Herbert A, Schwartz T, Rich A.** 2000. The zab domain of the human RNA editing enzyme ADAR1 recognizes Z-DNA when surrounded by B-DNA. J Biol Chem **275:**26828-26833.

100. **Schwartz T, Lowenhaupt K, Kim YG, Li L, Brown BA, 2nd, Herbert A, Rich A.** 1999. Proteolytic dissection of Zab, the Z-DNA-binding domain of human ADAR1. J Biol Chem **274:**2899-2906.

101. **Kim YG, Kim PS, Herbert A, Rich A.** 1997. Construction of a Z-DNA-specific restriction endonuclease. Proc Natl Acad Sci U S A **94:**12875-12879.

102. **Schwartz T, Behlke J, Lowenhaupt K, Heinemann U, Rich A.** 2001. Structure of the DLM-1-Z-DNA complex reveals a conserved family of Z-DNA-binding proteins. Nat Struct Biol **8:**761-765.

103. **Schwartz T, Rould MA, Lowenhaupt K, Herbert A, Rich A.** 1999. Crystal structure of the Zalpha domain of the human editing enzyme ADAR1 bound to left-handed Z-DNA. Science **284:**1841-1845.

104. **Gajiwala KS, Burley SK.** 2000. Winged helix proteins. Curr Opin Struct Biol **10:**110-116.

105. **Kim YG, Muralinath M, Brandt T, Pearcy M, Hauns K, Lowenhaupt K, Jacobs BL, Rich A.** 2003. A role for Z-DNA binding in vaccinia virus pathogenesis. Proc Natl Acad Sci U S A **100:**6974-6979.

106. **Kim YG, Lowenhaupt K, Oh DB, Kim KK, Rich A.** 2004. Evidence that vaccinia virulence factor E3L binds to Z-DNA in vivo: Implications for development of a therapy for poxvirus infection. Proc Natl Acad Sci U S A **101:**1514-1518.

107. **Bass BL, Nishikura K, Keller W, Seeburg PH, Emeson RB, O'Connell MA, Samuel CE, Herbert A.** 1997. A standardized nomenclature for adenosine deaminases that act on RNA. RNA **3:**947-949.

108. **Takaoka A, Wang Z, Choi MK, Yanai H, Negishi H, Ban T, Lu Y, Miyagishi M, Kodama T, Honda K, Ohba Y, Taniguchi T.** 2007. DAI (DLM-1/ZBP1) is a cytosolic DNA sensor and an activator of innate immune response. Nature **448:**501-505.

109. **Shors ST, Beattie E, Paoletti E, Tartaglia J, Jacobs BL.** 1998. Role of the vaccinia virus E3L and K3L gene products in rescue of VSV and EMCV from the effects of IFN-alpha. J Interferon Cytokine Res **18:**721-729.

110. **Langland JO, Jacobs BL.** 2004. Inhibition of PKR by vaccinia virus: role of the N- and C-terminal domains of E3L. Virology **324:**419-429.

111. **Brandt T, Heck MC, Vijaysri S, Jentarra GM, Cameron JM, Jacobs BL.** 2005. The N-terminal domain of the vaccinia virus E3L-protein is required for neurovirulence, but not induction of a protective immune response. Virology **333:**263-270.

112. **White SD, Jacobs BL.** 2012. The amino terminus of the vaccinia virus E3 protein is necessary to inhibit the interferon response. J Virol **86:**5895-5904.

113. **Borden EC, Sen GC, Uze G, Silverman RH, Ransohoff RM, Foster GR, Stark GR.** 2007. Interferons at age 50: past, current and future impact on biomedicine. Nat Rev Drug Discov **6:**975-990.

114. **Shors T, Kibler KV, Perkins KB, Seidler-Wulff R, Banaszak MP, Jacobs BL.** 1997. Complementation of vaccinia virus deleted of the E3L gene by mutants of E3L. Virology **239:**269-276.

115. **He S, Wang L, Miao L, Wang T, Du F, Zhao L, Wang X.** 2009. Receptor interacting protein kinase-3 determines cellular necrotic response to TNF-alpha. Cell **137:**1100-1111.

116. **Zhang DW, Shao J, Lin J, Zhang N, Lu BJ, Lin SC, Dong MQ, Han J.** 2009. RIP3, an energy metabolism regulator that switches TNF-induced cell death from apoptosis to necrosis. Science **325:**332-336.

117. **Rebsamen M, Heinz LX, Meylan E, Michallet MC, Schroder K, Hofmann K, Vazquez J, Benedict CA, Tschopp J.** 2009. DAI/ZBP1 recruits RIP1 and RIP3 through RIP homotypic interaction motifs to activate NF-kappaB. EMBO Rep **10:**916-922.

118. **Kaiser WJ, Upton JW, Mocarski ES.** 2008. Receptor-interacting protein homotypic interaction motif-dependent control of NF-kappa B activation via the DNA-dependent activator of IFN regulatory factors. J Immunol **181:**6427-6434.

119. **Dey M, Trieselmann B, Locke EG, Lu J, Cao C, Dar AC, Krishnamoorthy T, Dong J, Sicheri F, Dever TE.** 2005. PKR and GCN2 kinases and guanine nucleotide exchange factor eukaryotic translation initiation factor 2B (eIF2B) recognize overlapping surfaces on eIF2alpha. Mol Cell Biol **25:**3063-3075.

120. **Garcia MA, Meurs EF, Esteban M.** 2007. The dsRNA protein kinase PKR: virus and cell control. Biochimie **89:**799-811.

121. **Wang Z, Choi MK, Ban T, Yanai H, Negishi H, Lu Y, Tamura T, Takaoka A, Nishikura K, Taniguchi T.** 2008. Regulation of innate immune responses by DAI (DLM-1/ZBP1) and other DNA-sensing molecules. Proc Natl Acad Sci U S A **105:**5477-5482.

122. **Taghavi N, Samuel CE.** 2013. RNA-dependent protein kinase PKR and the Z-DNA binding orthologue PKZ differ in their capacity to mediate initiation factor eIF2alpha-dependent inhibition of protein synthesis and virus-induced stress granule formation. Virology **443:**48-58.

123. **Ha SC, Kim D, Hwang HY, Rich A, Kim YG, Kim KK.** 2008. The crystal structure of the second Z-DNA binding domain of human DAI (ZBP1) in complex with Z-DNA reveals an unusual binding mode to Z-DNA. Proc Natl Acad Sci U S A **105:**20671-20676.

124. **Ng SK, Weissbach R, Ronson GE, Scadden AD.** 2013. Proteins that contain a functional Z-DNA-binding domain localize to cytoplasmic stress granules. Nucleic Acids Res **41:**9786-9799.

125. **Sridharan H, Upton JW.** 2014. Programmed necrosis in microbial pathogenesis. Trends Microbiol **22:**199-207.

126. **Kahmann JD, Wecking DA, Putter V, Lowenhaupt K, Kim YG, Schmieder P, Oschkinat H, Rich A, Schade M.** 2004. The solution structure of the N-terminal domain of E3L shows a tyrosine conformation that may explain its reduced affinity to Z-DNA in vitro. Proc Natl Acad Sci U S A **101:**2712-2717.

127. **Koo GB, Morgan MJ, Lee DG, Kim WJ, Yoon JH, Koo JS, Kim SI, Kim SJ, Son MK, Hong SS, Levy JM, Pollyea DA, Jordan CT, Yan P, Frankhouser D, Nicolet D, Maharry K, Marcucci G, Choi KS, Cho H, Thorburn A, Kim YS.** 2015. Methylation-dependent loss of RIP3 expression in cancer represses programmed necrosis in response to chemotherapeutics. Cell Res **25:**707-725.